Optimal Vehicle Structural Design for Weight Reduction using Iterative Finite Element Analysis

By

Steven Tebby

A Thesis Submitted in Partial Fulfillment of the Requirements for the Degree of

Master of Applied Science

In

Automotive Engineering

Faculty of Engineering and Applied Science

University of Ontario Institute of Technology

June 2012

© Steven Tebby, 2012

Abstract

The design and analysis of an automotive structure is an important stage of the vehicle design process. The structural characteristics have significant impact on the vehicle performance. During the design process it is necessary to have knowledge about the structural characteristics; however in the preliminary design stages detailed information about the structure is not available. During this period of the design process the structure is often simplified to a representative model that can be analyzed and used as the input for the detailed design process. A vehicle model is developed based on the space frame structures where the frame is the load carrying portion of the structure. Preliminary design analysis is conducted using a static load condition applied to the vehicle as pure bending and pure torsion. The deflections of the vehicle based on these loading conditions are determined using the finite element method which has been implemented in developed software. The structural response, measured as the bending and torsion stiffness, is used to evaluate the structural design. An optimization program is implemented to improve the structural design with the goal of reducing weight while increasing stiffness. Following optimization the model is completed by estimating suitable plate thicknesses using a method of substructure analysis. The output of this process will be an optimized structural model with low weight and high stiffness that is ready for detailed design.

Keywords: Computer Aided Engineering, Finite Element Method, Automotive Structural Design, Simple Structural Beams-Frames (SSB), Multi-Objective

Optimization. Vehicle Stiffness, Torsion Stiffness, Bending Stiffness, Vehicle Weight Reduction, Vehicle Fuel Economy

Acknowledgements

I wish to thank and acknowledge my thesis supervisors, Dr. Ahmad Barari and Dr. Ebrahim Esmailzadeh for their contributions to this thesis work. Their knowledge, insight and encouragement have made this program rewarding and enjoyable.

Financial support of this research from Natural Sciences and Engineering Research Council of Canada is gratefully appreciated.

Finally I wish to acknowledge my family and friends who have supported and encouraged me throughout this program.

Contents

List of Figures

List of Tables

Notations

NVH	Noise, vibration and harshness
FEM	Finite element method
BIW	Body-in-white
SSS	Simple structural surfaces
SSB	Simple structural beams-frames
K_b	Bending stiffness
K_t	Torsion stiffness
W	Structure weight
θ	Angular deflection of structure
δ	Vertical deflection of structure
E	Young’s modulus
G	Shear modulus
ν	Poisson’s ratio
A	Beam element section area
I_z	Beam element moment of inertia
I_y	Beam element moment of inertia
J	Beam element torsion constant
L	Beam element length

Chapter 1

1. Introduction

1.1 Motivation

The design of an automotive structure is an important aspect in the overall vehicle design process. The vehicle structure is important to ensure that the weight of various components and loads applied during vehicle operation are adequately supported without substantial deflection. The structure is also responsible for protecting occupants and payloads during collisions. A vehicle structure must accomplish these two objectives while maintaining a low weight. The weight of the structure has become increasingly important as the fuel efficiency and emissions standards have increased [1]. During the conceptual design stage, when changes to the design are easiest to implement and have lower impact on overall project cost, the weight and structural characteristics are mostly unknown since detailed vehicle information is unavailable at this early stage [2,3]. This lack of knowledge about the design problem can be seen below in Figure 1, while the impact on overall vehicle development cost is illustrated in Figure 2.

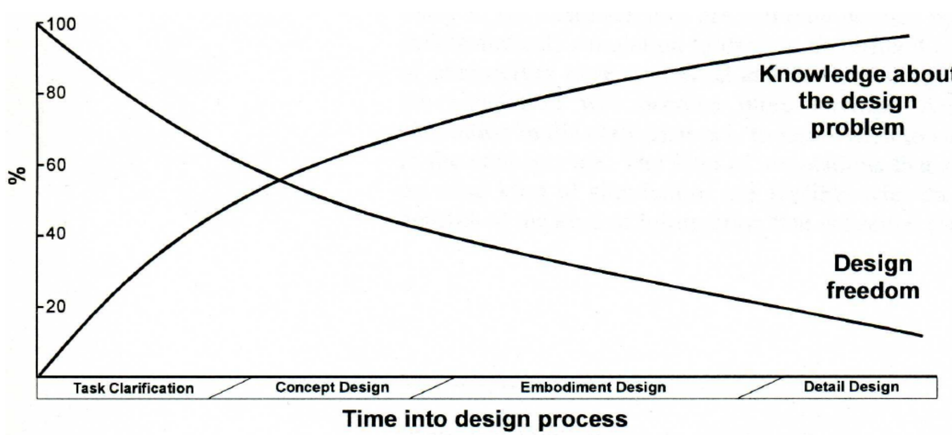

Figure 1: Design information compared during design process [2]

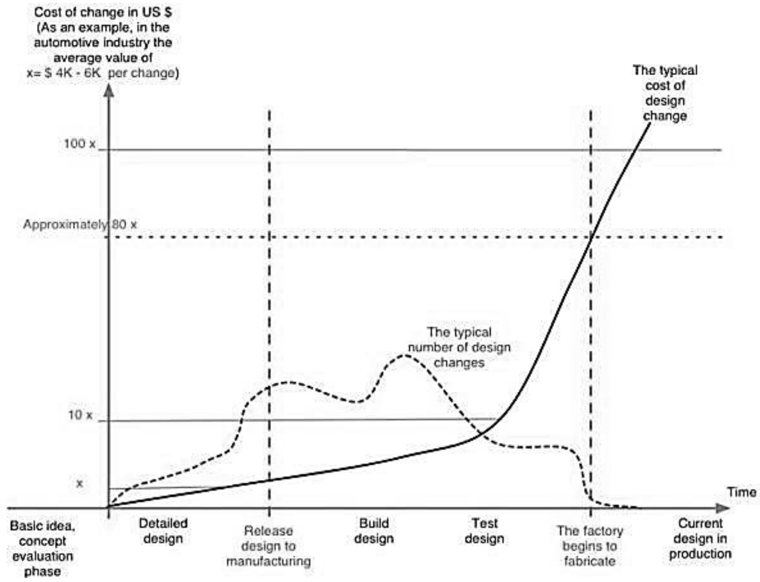

Figure 2: Cost of design changes during design process [3]

However, even with insufficient information, the structural characteristics need to be considered and included in the design process from the outset of the conceptual stage. For the reasons given above the work presented here focuses on the conceptual design stage of an automotive structure.

Ensuring the vehicle structure has sufficient load bearing capabilities, while maintaining a low weight, during the conceptual design stage will improve the overall vehicle design and mean fewer design changes are required during the detailed design process. Several parameters are available for testing the vehicle structural characteristics; however two important parameters are the chassis bending and torsional stiffness's. The stiffness of a vehicle structure has an impact on the overall vehicle performance, as well as the Noise, Vibration and Harshness (NVH) of the vehicle [4,5,6]. Also sufficient stiffness is sought to ensure that the relative displacement of vehicle components is not substantial enough to cause damage to the vehicle. Other structural characteristics for evaluating the design, such as the NVH properties as well as the crashworthiness, are better utilized during the detailed design stage.

The work presented here focuses on the stiffness and weight during the conceptual stage and seeks to develop an optimized preliminary vehicle structure as an input for the detail design activities where every aspect of the vehicle design can be considered.

1.2 Objective

Increasing standards for fuel efficiency and emissions require improvements to the overall vehicle design. As shown in Figure 3 one of the most efficient methods of improving fuel efficiency is by reducing the vehicle weight [7].

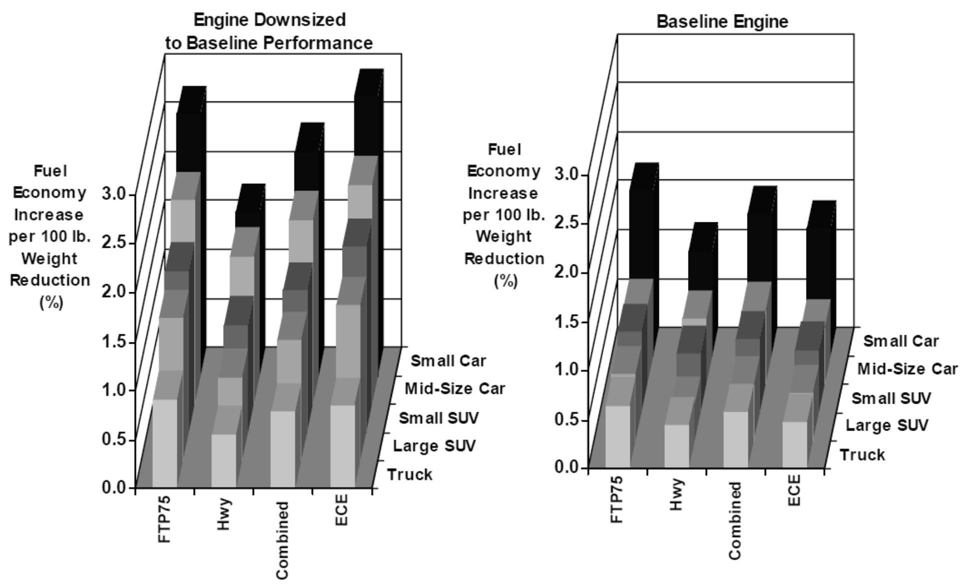

Figure 3: Impact of weight reduction on fuel economy of various vehicles [7]

The x-axis in Figure 3 represents the different standards for estimating vehicle fuel economy. The FTP75 stands for Federal Testing Procedure and is used for determining fuel economy of light duty vehicles in the United States. The highway and combined values are based on the Environmental Protection Agency standard for measuring fuel economy. Finally ECE stands for Economic Commission for Europe and uses the European drive cycle to estimate fuel economy.

A number of methods are available for reducing weight, but the primary focus should be on the vehicle structural design. The vehicle structure, as indicated in Figure 4, comprises the largest individual portion of total weight and therefore has the most to offer in potential weight savings [8].

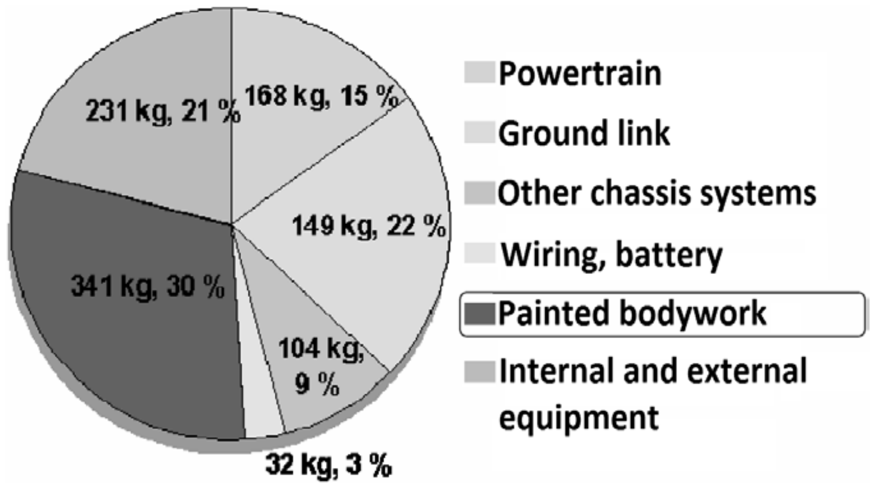

Figure 4: Distribution of vehicle weight [8]

The reduction in structure weight should not however come at the expense of the structural properties. The vehicle structure is responsible for supporting all applied loads and ensuring that the relative movement between components is minimized. For this reason vehicle structural design often requires meeting the potentially conflicting design goal of reducing structural weight while maintaining or improving structural stiffness. The objective of this work is to develop a methodology that can be used to design preliminary structural models with high stiffness and low weight that will be ready for detailed design.

The vehicle structure considered here will be subjected to a multi-objective optimization that seeks to improve the stiffness to weight ratio of a simple sedan car model. The final product of the optimization process will be a low weight structure that features high load carrying capacity. Following this multi-objective optimization a process of substructure analysis is implemented to determine suitable sheet thicknesses for portions of the car where sheets are required such as the floor and roof. The optimized structure, complete with sheet portions, will then be suitable for detailed design activities such as crashworthiness and dynamic analysis.

The presented methodology is intended to be utilized in the conceptual design stage when an approximate model is acceptable. The methodology will be of particular use to structural engineers, production engineers and vehicle system designers as vehicle structures must satisfy a number of roles and is affected by so many parameters. The process that has been developed is implemented in a numerical program (MATLAB) instead of commercially available software, such as NX NASTRAN or Abaqus. The benefits of implementing this process in MATLAB are the simplicity in conducting analysis and availability of existing algorithms for optimization and generating figures. The use of MATLAB also gives access to the internal structure of the program, making it possible to adjust the desired outputs or to develop code for a wider range of analysis. While implementation in MATLAB is the approach chosen here, the presented process and corresponding case study could be readily implemented in other available software. MATLAB is utilized for this work as an alternative to commercial programs and allows for a better understanding of how the developed process works.

The presented design methodology will also have a direct impact on other aspects of the automotive design process, including the powertrain and suspension. Having knowledge of the vehicle structure characteristics early in the design process, which this methodology will provide, allows the process of determining the powertrain requirements and designing the suspension system to begin earlier in the design process than normally possible. The focus on weight reduction will have a significant effect on the powertrain selection as the engine can be downsized from what would be required for a higher weight vehicle and the transmission can be designed based on this engine selection. A downsized engine when combined with the reduced structure weight will greatly increase the fuel economy of the vehicle. With the powertrain selection and design occurring earlier in the design process the engine and transmission testing can also be conducted earlier in the process which will ensure the best possible performance and reliability. Along with the engine and transmission design the suspension design can begin earlier in the vehicle development process since the structural weight and stiffness characteristics are known. Knowledge of the structure stiffness allows the designers and engineers to develop the best suspension geometry and determine suspension parameters (spring stiffness and damping characteristics) that will work in conjunction with the structure stiffness to greatly improve the ride characteristics. Further discussion on the impact the vehicle structure has on vibration is provided below.

1.2.1 Discussion on Objective

As has been mentioned the objective of this work is to introduce a design methodology for developing a lightweight preliminary vehicle structure. A low weight vehicle structure is desirable since weight is a primary factor in fuel efficiency and fuel economy standards are continually increasing. However the stated objectives of a low weight, high stiffness vehicle structure will have an impact on the vibration characteristics of the vehicle. For this reason further discussion regarding how the structure characteristics can impact vehicle vibration is provided here. First changing the structural design will have a direct impact on the structural, or hysteretic, damping. The weight reduction of the vehicle structure will reduce the total material volume present in the structure and since the energy dissipation due to hysteretic damping is related to the material volume the amount of damping will be reduced [9]. Reducing the damping inherent in the structure is undesirable as it can lead to fatigue damage when the vehicle is subjected to excitation and the vehicle suspension must be used to compensate for this reduction in damping [10,11]. Secondly reducing the weight while maintaining or increasing the stiffness of the vehicle structure will increase the natural frequency of the vehicle structure [9]. This increase will move the structure natural frequency away from the suspension natural frequency ensuring the structure dynamic modes do not adversely couple with the suspension dynamic modes and cause excessive vibration [12]. While conducting the optimization the vibration characteristics could be considered if desired by including appropriate penalty values. Also higher structure stiffness is desirable to ensure the suspension is controlling a larger share of the vehicle kinematics and that the suspension geometry is maintained during driving manoeuvres [12]. Finally a high stiffness, especially in torsion is important in a structure as it prevents relative movement from one side to the other which can cause a wheel to lose traction under cornering [12].

1.3 Literature Review

Vehicle structural design and optimization has been the focus of a number of previous works. The following is a review of some of the previously conducted work related to vehicle structural design, analysis and optimization.

The finite element method has been utilized in vehicle structural design for a number of purposes, including design analysis and optimization. The finite element method was applied for stress analysis of a vehicle chassis, as well as a truck chassis with riveted joints [13,14]. Both of these previous works were more preliminary in nature and provided general information that forms part of the foundation of the work here; however existing software is utilized as the analysis being conducted is occurring at a later stage in the design process. Kim et al. used finite element analysis to study the dynamic stress of a vehicle frame [15]. This work again utilizes commercial software to conduct dynamic analysis of the structure which is beyond the scope of the work presented here, but shows the potential of the finite element method as it relates to vehicle structure. Wang et al. applied the finite element method to reinforce the body structure using an optimization process [16]. This work provides further motivation for conducting the research conducted here; however it uses a detailed vehicle structure undergoing optimization in commercial software. Yanhong and Feng used finite element analysis and an optimization process were also applied to the sub-frames of a commercial vehicle [17]. This work provides a good reference related to how an optimization process can be performed on a vehicle structure and as such is relevant to the research being conducted. Kim, Mijar and Arora previously developed a simplified vehicle structure model for the design and optimization of a vehicle based on crashworthiness [18]. The objective of this work was very similar to the focus of the research being presented as a simplified structural model was developed and optimized; however the difference is the focus of the previous work is on crashworthiness instead of static structural characteristics. Beam element structural models have been used in a number of previous works, some of which are described here. The beam model was used to approximate the vehicle panels for implementation in computational methods [19]. This work is a general overview of how the beam model can be utilized in analysis and is a foundation work, but does not contribute specific details to this research. Shiu, Ceglarek and Shi use beam elements to model a vehicle structure has been used to model a sheet metal body assembly for dimensional control [20]. Their work is central to the development of the research being conducted and in it they take an existing vehicle structure, in this case a van, and generate a beam equivalent. Their work does differ from the current research as optimization is not conducted and instead of substructure analysis for sheet metal analysis the sheet components are reduced to an equivalent series of small beams as needed. Mundo et al. previously used a beam structure has been to simplify the vehicle structure model to conduct NVH optimization of a vehicle Body-In-White (BIW) [21]. The work conducted here is similar in nature to the presented research as an optimization process is implemented; however the difference is in the objectives for optimization and the more complex beam sections possible in existing software. While there are differences the work conducted by Mundo et al. is also conducted during the early design stages. Donders et al. used the beam structure has also been combined with a detailed joint model in order to optimize the global body dynamics [22]. This work is an extension of the work conducted by Mundo et al., but is focused on the joint design as part of optimization. The joints in the research presented here are considered rigid; however a method of including joint stiffness components could be included in future research. Lee and Lee used a skeleton vehicle structure for optimization of an aluminum intensive vehicle [23]. The work Lee and Lee developed is a similar process to this research but a complete structural model is subjected to optimization using commercial software. This vehicle model used beam elements in conjunction with sheet elements to represent flat sheets. A method of primitive vehicle structure design using the stick model was an important foundation for the work conducted by Kim and Kim [24]. This work utilizes a simplified structure that has been modelled using beam elements similar to what is being presented here. Kang and Choi also developed a vehicle stick model was for sensitivity analysis to determine the critical structural members [25]. The sensitivity analysis conducted was not considered as part of this research; however it could be used to further improve the understanding of the interaction between beam elements and how the contribute to the overall stiffness. The beam elements found in a vehicle structure have also previously been used as the basis of optimization. Lee, Pine and Jones previously modeled box sections that form a beam element using finite element analysis [26]. This work is not related specifically to automotive structures, but instead to general beam elements and how they withstand torsion. The beams have also been used for the optimization of frame structures with flexible joints by Cameron, Thirunavukarasu and El-Sayed [27]. Their work conducts an optimization process for general frame structures with flexible joints and was used as a foundation for the current research. The main difference is the research conducted here does not consider flexible joints, but they could be included in future extensions of this research. Finally Yoshimura, Nishiwaki and Izui parametrically optimized the beam cross sectional shape using the genetic algorithm [28]. This work optimizes a beam element cross section shape which is similar to the research presented here; however their work is focussed on a single element. The method employed could be used in future work where non-standard section shapes can be determined as part of the optimization.

As part of the optimization program that is used a method of determining the stiffness properties of a vehicle structure was required. Law et al. previously studied the effect of the structure torsion stiffness on vehicle roll stiffness has been previously studied [6]. Their work is not essential for this research, but shows how torsion stiffness can affect vehicle performance and why it is important to have high stiffness. Thompson, Raju and Law have conducted the design of a race car chassis based on torsion stiffness [12]. This work seeks to design a vehicle based on stiffness which is similar in nature to the work presented here; however their optimization is based on element sensitivities and is conducted in commercial software. Finally Thompson, Lampert and Law used an experimental method of estimating the vehicle torsion stiffness [29]. This last work was used to illustrate how the stiffness of a chassis can be calculated based on the presented experimental method.

1.4 Outline

The work presented can be broken down into several sections. The introductory sections explain the motivation for conducting this research and the areas for which it can be applied. Next the definition of the research objectives is stated along with the reasons for choosing these objectives. The final introductory section provides the approach, some background used to develop concepts of this research, as well as the foundation on which it is based.

Following the introductory materials a section that provides background information about the automotive structural design process and different methods of modeling a vehicle structure is presented. After the background about automotive structural design is a discussion about the finite element method and an introduction to the finite elements being used throughout this work. The last background section deals with optimization in general terms and explains the chosen optimization method that is used for the multi-objective optimization process.

After the background section the model geometry is developed and the finite element model introduced. The Simple Structural Beams-Frames (SSB) methodology is introduced by presenting model geometry of a sedan car being optimized, with relevant existing models shown for comparison. From there the geometry of the model is defined based on an existing vehicle structural model with the nodal coordinates for the beam model the result [30]. With the model geometry defined the static analysis is conducted based on assumed component loads and locations. Following the explanation of the static analysis methods of estimating the structural stiffness are introduced. Finally the cross-sectional shape for each beam element is presented with justification for this choice.

Once the model generation using SSB has been explained the specifics about the optimization process are presented. Here the objective functions are introduced and a preliminary analysis is conducted to provide the initial condition. The optimization constraints are described along with the method of penalizing inferior designs during the optimization process. Lastly an optimization flow chart is presented to summarize the overall process.

Following the description of the optimization process is the optimization results. After the optimization results summary a process for validating the optimization results is presented. The validation involves varying individual parameters and measuring the response to show that the set of design parameters that result from optimization are in fact the optimal parameters.

Following the optimization results summary and validation the process of substructure analysis is implemented to estimate the thickness of the sheet components that will complete the structural model. This process breaks the vehicle into a series of substructures consisting of beam elements surrounding a plate element. Each substructure is subjected to an optimization process that will determine the optimum sheet metal thickness to form a completed vehicle structure.

The closing section of the research is conclusions about the process and results. An interpretation and further explanation of what the results indicate and how they can be used is presented. Finally different suggestions for continuation and extension of this work are presented.

The last section of the work is the appendices. These sections contain additional information about previously conducted analysis and optimization of a simpler beam frame structure. Further information regarding some aspects of the developed process is provided, with specific information regarding the implemented penalty functions and the selection of a mesh density for the substructure analysis.

Chapter 2

2. Background

2.1 Automotive Structural Design

The design of a vehicle structure is of fundamental importance to the overall vehicle performance. The vehicle structure plays an important role in the functionality of the vehicle. The structure is responsible for carrying the attached loads, such as the engine, transmission and suspension as well as the passengers and payload. The structure must also offer sufficient impact resistance so as to protect the occupants inside the vehicle. The structural design process is generally a multi-stage procedure that starts with sketches and proceeds to full-size tape drawings before moving on to 3D clay models [30]. As these models and information about the vehicle packaging is made available the coordinates of the structure take shape with information about the packaging of the vehicle. A number of different automotive structure types exist and have seen application in a variety of different vehicles. Some of these structures are highlighted here with brief descriptions. One of the earliest structure types is called the body-on-frame [30]. In this style a body structure featuring the aerodynamic shape is mounted at multiple locations on a rigid frame that supports the drivetrain. The frame is typically a ladder style where a number of cross-members are used to attach the two sides and increase stiffness. An example of this is shown below in Figure 5 [31].

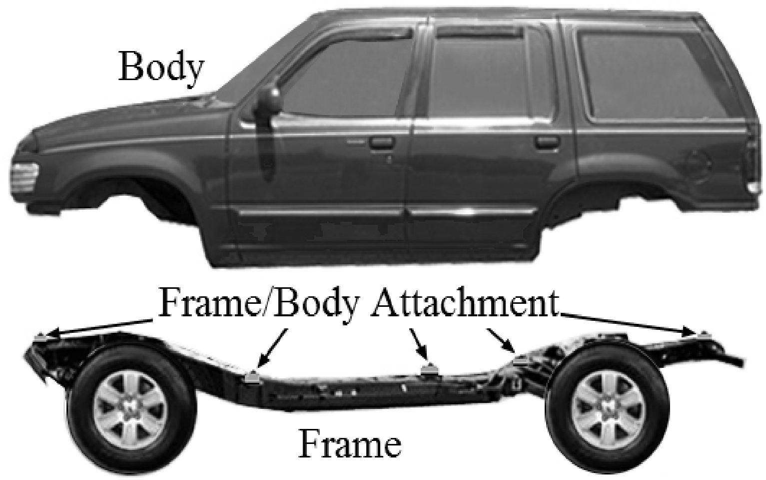

Figure 5: Body-on-frame structure [31]

The primary problem with this structure is the distinct load paths that occur. The body and frame can be considered as springs in parallel, each providing a separate load path, with the amount of load on each portion based on the relative stiffness. For this reason the overall structure stiffness can be reduced if one of these elements has lower stiffness. More modern structures have overcome this by having more integration between body and frame. One such example is the triangulated tube frame, shown below in Figure 6 [30]. This structure type uses a welded tube frame structure to support the applied loads and provide the stiffness. The body is then formed by attaching thin metal panels directly to this frame. This has the effect of lowering the overall weight, while maintaining stiffness. The tube frame structure is commonly found in sports cars.

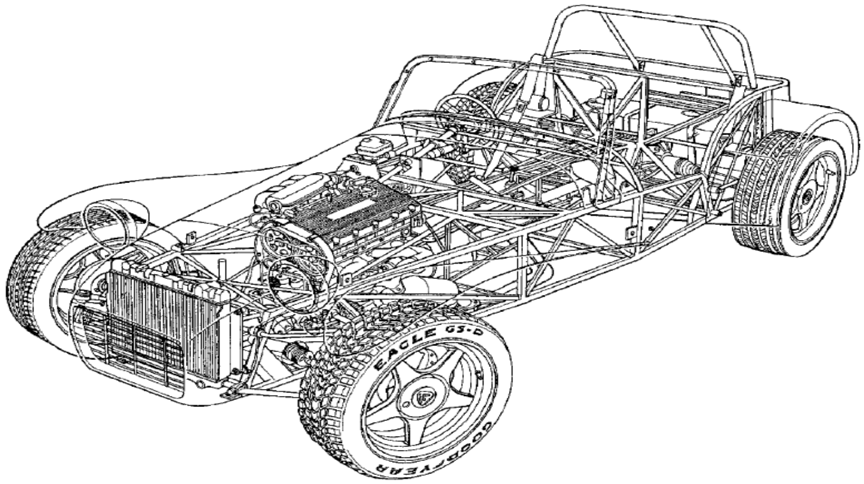

Figure 6: Tube frame structure [30]

This type of structure is generally restricted to low volume sports cars since the tooling costs for manufacture are low, but the complicated and labour intensive manufacturing process makes it prohibitively expensive for mass production. Another modern vehicle structure is shown below in Figure 7. This type of structure is called the punt or platform structure.

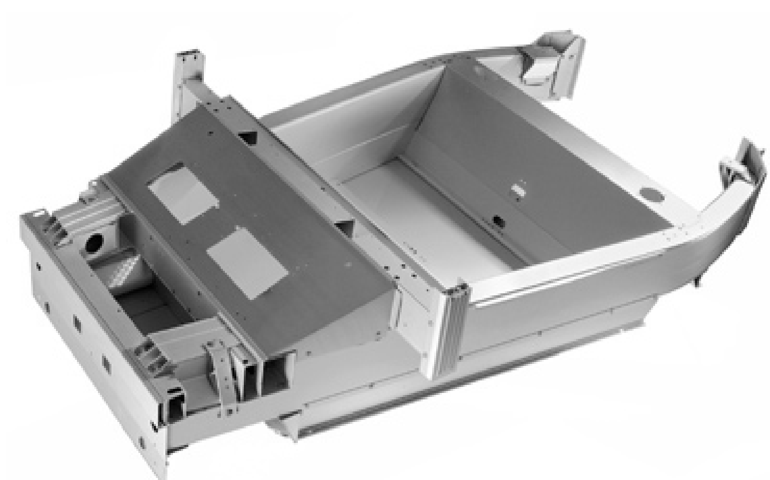

Figure 7: Punt structure[32]

The punt structure features sheet metal construction with closed cross-sections in the floor members [30]. Commonly the upper body is considered as insignificant to the vehicle structure. This type of structure is again commonly used for low production volumes. Next is the perimeter space frame, another example of modern vehicle structure. The space frame is used as the basis for the structural model used throughout the optimization process. An example of the space frame is shown below in Figure 8.

Figure 8: Example of Space Frame [33]

The space frame structure utilizes relatively small tube members built into ring-beams and then joined together at joints or nodes. This structure type can be combined with sheet elements to counteract shear loads that occur. The resulting structure is the most common modern structure type and is called the integral body structure [30]. This body structure, shown below in Figure 9, features pressed sheet metal sub-structures welded together. The structure is suited to mass produced vehicles and the separate chassis is unnecessary as the body is self-supporting.

Figure 9: Typical Integral Structure [30]

The integral body structure, along with all other structure types, is comprised of a number of sub-structures that are assembled together to form the body structure. An exploded view showing this is below in Figure 10.

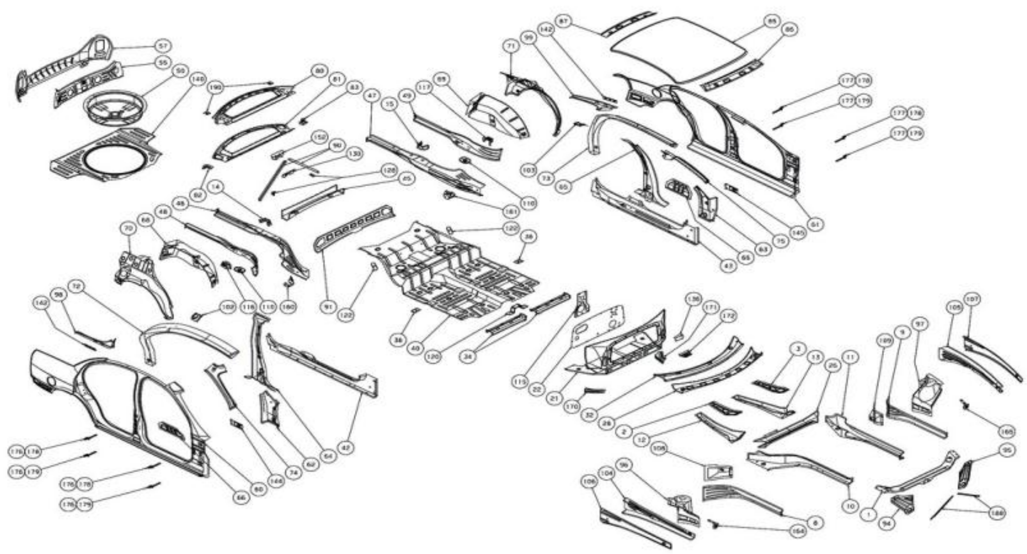

Figure 10: Exploded view of vehicle structure [34]

As can be seen a vehicle structure is comprised of many different components, making it difficult and computationally expensive to perform a complete structural analysis. For this reason it is often necessary to find a method of simplifying the vehicle structure in order that it can be readily analyzed, specifically during the conceptual design stage. The conceptual design stage is an important time during the design process as this is the period when the greatest number of design changes is possible and the costs involved in changing the design are lower when compared with the later stages of the development process, as shown in Figure 1 and Figure 2 [2,3].

One method of representing the vehicle structure uses planar sheets to model the vehicle. This method of simplifying the structure is called the Simple Structural Surface (SSS) method [30]. The SSS method was originally developed to analyze the load path of the vehicle during the concept stage of the design process [30]. While modern vehicles have a large number of complex or curved surfaces the underlying structure or subassemblies can be effectively approximated by planar surfaces. Each plane or surface used in this method is held in a static equilibrium by a series of forces, which are created by the weight of the different components. These loads are transferred from one surface to another through edge loads. It can be determined if the structure has insufficient support to properly react the applied loads. This method of analysis is especially suited to analyzing local structural elements such as cross members or mounts. A sample of a surface is shown below in Figure 11.

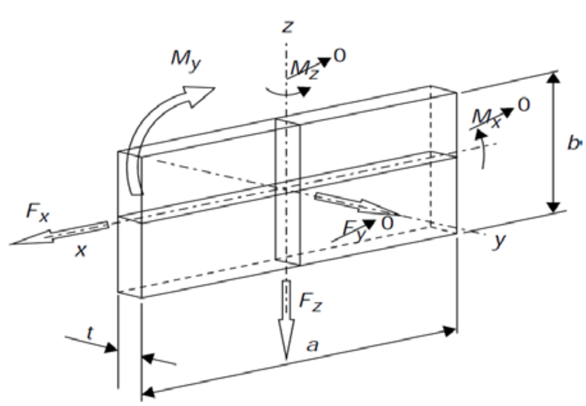

Figure 11: Simple Structural Surface [30]

As can be seen due to the planar nature of the surface only loads (moments or forces) acting in plane can be sufficiently supported. Any out of plane loads that could occur in a vehicle, of which there are multiple, must be reacted by supporting surfaces at the edge. One such example of this is in a floor structure where vertical loads are applied from the firewall structure to the floor. Since these vertical loads are considered out of plane with respect to the floor a supporting surface must be added to the floor to ensure a sufficient load path, this is illustrated in Figure 12, shown below.

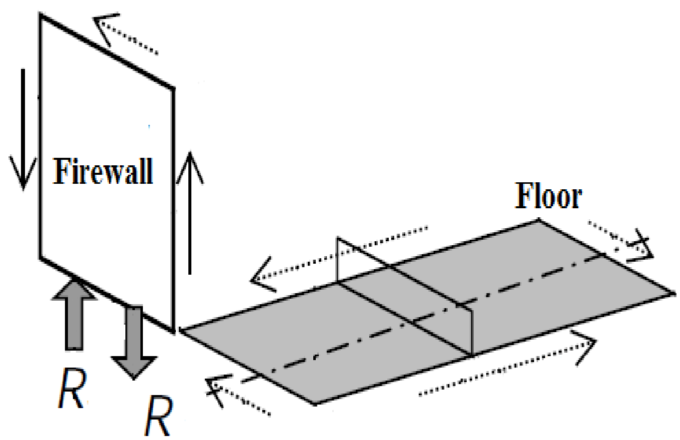

Figure 12: Floor structure with out of plane loads from firewall [30]

As can be seen the vertical loads, R, applied on the firewall are transferred to the floor via the bottom edge. Since the floor structure is inadequate to support this load a vertical structure is applied to the middle of the floor. While the SSS method can be a good indicator of structural performance at an early stage of design there are some limitations [30]. The first is the inability to analyze a redundant structure where multiple load paths exist. In these situations the relative stiffness of each sub-structure will determine each component's share of the applied loads. A typical vehicle structure features multiple redundant structures which limits the effectiveness of this method of structural approximation. Another drawback of the SSS method is the inability to easily determine the structure deflection that occurs for a given loading condition in a straightforward manner. The use of the Finite Element Method (FEM) can be applied in order to determine the deflection of such a vehicle model.

2.2 Finite Element Method

The finite element method is widely used in the automotive industry for a variety of Computer Aided Engineering (CAE) tasks. Background information about this method of analysis and how it can be applied to vehicle structural design is provided here.

The finite element method is a numerical approach to solving problems arising in engineering and physics [35]. Some common problems include structural analysis, heat transfer, fluid flow and mass transport. This method of analysis is utilized where exact analytical solutions are unobtainable due to the complicated nature of the problem. The approach of FEM is to break the problem down into a system of algebraic equations and solving simultaneously. The body is modelled by breaking it down into smaller bodies (finite elements) that are interconnected at points common to two or more bodies, called nodes or nodal points. Equations are generated for each smaller body then combined to obtain the complete solution. The finite element method is applied here for structural analysis where the unknowns are nodal displacements and stresses in each element based on the applied loads. Two approaches are commonly used in finite element analysis. The first is the flexibility or force method where internal forces and compatibility equations are used to determine the unknowns. The second, more commonly used method, is the stiffness or displacement method where the displacements are used as unknowns. The principle of minimum potential energy is also used with the stiffness method. The steps in solving a finite element problem are now described.

1. Discretize and choose element type- the body is divided into an equivalent system of finite elements and the most appropriate element (spring, bar, truss, beam, etc.) is chosen
2. Select displacement function- displacement function in each element is chosen
3. Define strain/displacement and stress/strain relationship- these relations are necessary for deriving equations of each element
4. Derive element stiffness matrix and equations- multiple methods are available for producing an element stiffness matrix that relates applied loads to nodal displacements
5. Assemble element equations to obtain global equations- the element stiffness matrices are combined based on nodal degrees of freedom and boundary conditions are introduced
6. Solve for unknown degrees of freedom- the equation relating applied forces, stiffness and displacements is solved
7. Solve for element stresses and strains- nodal displacements are used to determine stress and strain in each element
8. Interpret results- results are analyzed and revisions to the design can be made based on this information

Two different finite elements are implemented in this work, a summary of both follows.

2.2.1 Beam Element

The element chosen for the modeling of a vehicle structure is the beam element oriented arbitrarily in three dimensions and assembled as a frame structure. The space beam element is derived based on a typical planar beam element, with the local x axis directed along the element length. The beam element utilized here uses Euler-Bernoulli beam theory where shear deformations are neglected. The exclusion of shear deformation is justified where the length of the beam is at least eight times the depth of the section. A cubic shape function is used to describe the bending deflection while linear shape functions are chosen to describe axial and rotational deflections and Galerkin's method is used to derive the stiffness matrix. A space beam element has six degrees of freedom for each node, one translational and one rotational corresponding to each axis. This results in each beam element in the space frame having twelve degrees of freedom. The element stiffness matrix corresponds to these degrees of freedoms and is shown below in Equation 2.1 [35].

$$\{\boldsymbol{K^e}\}=\begin{bmatrix}
\frac{EA}{L} & 0 & 0 & 0 & 0 & 0 & \frac{-EA}{L} & 0 & 0 & 0 & 0 & 0 \\
0 & \frac{12EI_z}{L^3} & 0 & 0 & 0 & \frac{6EI_z}{L^2} & 0 & \frac{-12EI_z}{L^3} & 0 & 0 & 0 & \frac{6EI_z}{L^2} \\
0 & 0 & \frac{12EI_y}{L^3} & 0 & \frac{-6EI_y}{L^2} & 0 & 0 & 0 & \frac{-12EI_y}{L^3} & 0 & \frac{-6EI_y}{L^2} & 0 \\
0 & 0 & 0 & \frac{GJ}{L} & 0 & 0 & 0 & 0 & 0 & \frac{-GJ}{L} & 0 & 0 \\
0 & 0 & \frac{-6EI_y}{L^2} & 0 & \frac{4EI_y}{L} & 0 & 0 & 0 & \frac{6EI_y}{L^2} & 0 & \frac{2EI_y}{L} & 0 \\
0 & \frac{6EI_z}{L^2} & 0 & 0 & 0 & \frac{4EI_z}{L} & 0 & \frac{-6EI_z}{L^2} & 0 & 0 & 0 & \frac{2EI_z}{L} \\
\frac{-EA}{L} & 0 & 0 & 0 & 0 & 0 & \frac{EA}{L} & 0 & 0 & 0 & 0 & 0 \\
0 & \frac{-12EI_z}{L^3} & 0 & 0 & 0 & \frac{-6EI_z}{L^2} & 0 & \frac{12EI_z}{L^3} & 0 & 0 & 0 & \frac{-6EI_z}{L^2} \\
0 & 0 & \frac{-12EI_y}{L^3} & 0 & \frac{6EI_y}{L^2} & 0 & 0 & 0 & \frac{12EI_y}{L^3} & 0 & \frac{12EI_z}{L^3} & 0 \\
0 & 0 & 0 & \frac{-GJ}{L} & 0 & 0 & 0 & 0 & 0 & \frac{GJ}{L} & 0 & 0 \\
0 & 0 & \frac{-6EI_y}{L^2} & 0 & \frac{2EI_y}{L} & 0 & 0 & 0 & \frac{12EI_z}{L^3} & 0 & \frac{4EI_y}{L} & 0 \\
0 & \frac{6EI_z}{L^2} & 0 & 0 & 0 & \frac{2EI_z}{L} & 0 & \frac{-6EI_z}{L^2} & 0 & 0 & 0 & \frac{4EI_z}{L}
\end{bmatrix} \qquad (2.1)$$

In the above equation K is the element stiffness matrix, E the material modulus of elasticity, G the shear modulus, A the element cross section area, I_z the moment of inertia about the element y-axis, I_y the moment of inertia about the element z-axis, J the section torsion constant and L the element length.

The element stiffness matrix is derived in terms of the local coordinate system and before being assembled must be transformed to the global coordinate system using a transformation matrix. The element stiffness matrices for the entire structure are then assembled according to their corresponding degrees of freedom to form the global stiffness matrix. Once the global stiffness matrix has been calculated the loads and boundary conditions can be applied. The method employed to solve this type of problem is analogous to the solution of a spring where the force is related to the displacements by the stiffness matrix, as shown below in Equation 2.2 [35].

$$\{\boldsymbol{F}\} = [\boldsymbol{K}]\{\boldsymbol{d}\} \tag{2.2}$$

In the above equation F represents the vector of global applied loads, K the global stiffness matrix and d the nodal global displacement vector. The force and displacement vectors are of equal length, with one row for each degree of freedom, generalized global force and displacement vectors are shown below with 'n' degrees of freedom [35].

$$\{\boldsymbol{F}\} = \begin{bmatrix} F_{1x} \\ F_{1y} \\ F_{1z} \\ M_{1x} \\ M_{1y} \\ M_{1z} \\ F_{2x} \\ F_{2y} \\ F_{2z} \\ M_{2x} \\ M_{2y} \\ M_{2z} \\ \vdots \\ F_{nx} \\ F_{ny} \\ F_{nz} \\ M_{nx} \\ M_{ny} \\ M_{nz} \end{bmatrix} \qquad \{\boldsymbol{d}\} = \begin{bmatrix} u_1 \\ v_1 \\ w_1 \\ \theta_1 \\ \varphi_1 \\ \psi_1 \\ u_2 \\ v_2 \\ w_2 \\ \theta_2 \\ \varphi_2 \\ \psi_2 \\ \vdots \\ u_n \\ v_n \\ w_n \\ \theta_n \\ \varphi_n \\ \psi_n \end{bmatrix} \tag{2.3}$$

In equation 2.2, shown above, *F* is the global force vector, F_x, F_y and F_z will be the nodal forces along the global x, y and z axes respectively while M_x, M_y and M_z will be the nodal moments about the x, y and z axes respectively. The d vector represents global nodal displacements where *u*, *v* and *w* represents the nodal displacements in the x, y and z axes respectively while θ, φ and ψ represent the nodal rotations about the x, y and z axes respectively. The numerical subscripts represent the node being described ranging from node 1 to node *n*.

Once the nodal displacements have been found post-processing can begin if necessary. Examples of post-processing activities include calculation of nodal element forces as well as element stress values. The post-processing represents the period when the result of design changes can be determined and would be the final step of a finite element analysis.

2.2.2 Plate Element

The second element being utilized, in order to complete the vehicle structure model, is the plate element. The plate finite element has two distinct stiffness matrices that are combined based on the nodal degrees of freedom they correspond to. The first stiffness matrix is related to the in-plane loads, such as tension or shear [35]. The second stiffness matrix is related to the plate bending and its associated rotations. The method of forming each stiffness matrix is similar and is summarized below.

The plate element utilizes a quadrilateral element with four nodes at the corners of the element. A plate element will have two degrees-of-freedom at each node when subjected to in-plane loads, one corresponding two the x-direction and one corresponding to the y-direction. When subjected to a bending load the plate element will have three degrees-of-freedom at each node, one corresponding to vertical displacement and two corresponding to rotation about the x and y axes [35]. The nodal degrees-of-freedom are summarized below.

$$\{\boldsymbol{d_i}\} = \begin{bmatrix} u_i \\ v_i \end{bmatrix} \tag{2.4}$$

$$\{\boldsymbol{d_i}\} = \begin{bmatrix} w_i \\ \theta_{xi} \\ \theta_{yi} \end{bmatrix} \tag{2.5}$$

In the above equations d_i represents the respective displacement vector of the i-th node, u, v and w will be the displacements in the x, y and z directions respectively while θ_x will be rotation about the x axis and θ_y will be rotation about the y-axis. The plate bending element is based on Kirchhoff's plate bending and as such the in-plane and bending analysis of a plate can be performed independently [36]. The plate stiffness matrix is based on an isoparametric formulation where the x and y coordinates have been transferred to the s and t coordinate system with values ranging from -1 to 1 and is shown below in Figure 13 [35].

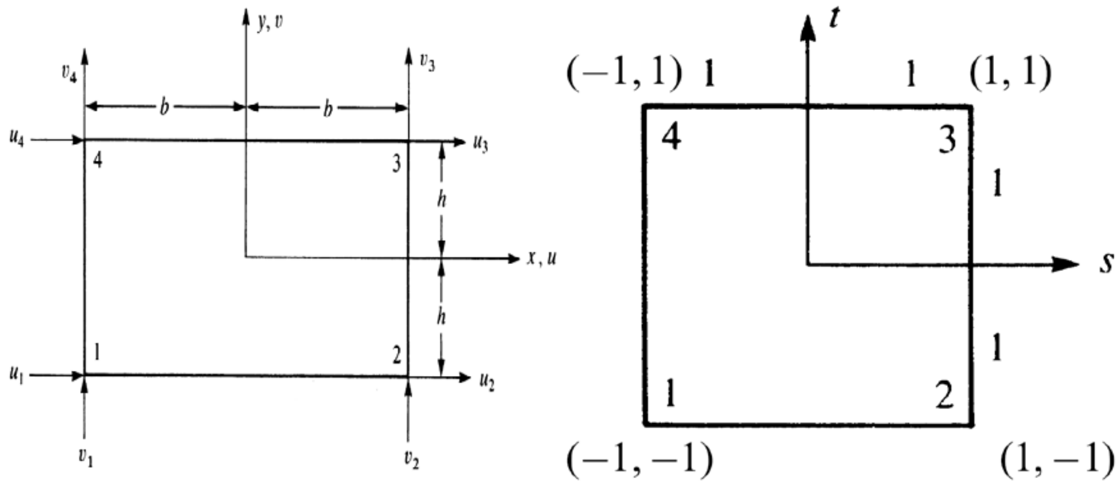

Figure 13: Coordinate System Transfer to Isoparametric System [35]

The stiffness matrix for the in-plane loads is shown below [35].

$$[\boldsymbol{k}] = \int_{-1}^{1}\int_{-1}^{1}[\boldsymbol{B}]^T[\boldsymbol{D}][\boldsymbol{B}]h|\boldsymbol{J}|dsdt \tag{2.6}$$

The transformation of coordinate systems results in complicated expressions within the integral so the stiffness matrix is often calculated numerically. In the above equation the plate thickness is represented by *h*. The *B* matrix in the above equation is developed based on element shape functions, *J* is the Jacobian of those shape functions and the *D* matrix represents the material properties and can be calculated as follows [35].

$$[\boldsymbol{D}] = \frac{E}{1-\nu^2}\begin{bmatrix} 1 & \nu & 0 \\ \nu & 1 & 0 \\ 0 & 0 & \frac{1-\nu}{2} \end{bmatrix} \tag{2.7}$$

In the above equation *E* is the modulus of elasticity and *v* is Poisson's ratio. The integration of Equation 2.6 is typically done numerically using two point Gauss quadrature [35]. The bending stiffness matrix is found using the following equation.

$$[\boldsymbol{k}] = \int_{-1}^{1}\int_{-1}^{1}[\boldsymbol{B}]^T[\boldsymbol{D}][\boldsymbol{B}]|\boldsymbol{J}|dsdt \tag{2.8}$$

In the above equation *B* represents the gradient matrix that was developed based on the shape functions, *J* is again the Jacobian of the shape functions and *D* represents the rigidity matrix which is calculated using the following equation [35].

$$[\boldsymbol{D}] = \frac{Et^3}{12(1-\nu^2)}\begin{bmatrix} 1 & \nu & 0 \\ \nu & 1 & 0 \\ 0 & 0 & \frac{1-\nu}{2} \end{bmatrix} \tag{2.8}$$

In the above equation *E* is once again the modulus of elasticity, ν is Poisson's ratio and *t* represents the plate thickness.

2.3 Optimization

Optimization is one of the oldest fields in mathematics and has found modern application in a variety of scientific and engineering disciplines [37]. The goal of optimization is to seek the maximum or minimum of an objective function [38]. A number of algorithms are available to perform optimization, but they all start with the definition of the optimization problem. Optimization seeks to minimize or maximize performance criterion derived based on a number of parameters. The basic optimization problem can be defined as follows:

$$\text{minimize } F = f(x_1, x_2, x_3, \dots\ x_n) \tag{2.9}$$

In the above equation *F* represents the objective function to be minimized and x_1 to x_n represents parameters that are varied through the optimization process. Optimization algorithms will vary the independent parameters in order to achieve the desired goal. A typical optimization process is a multi-step procedure and is summarized below.

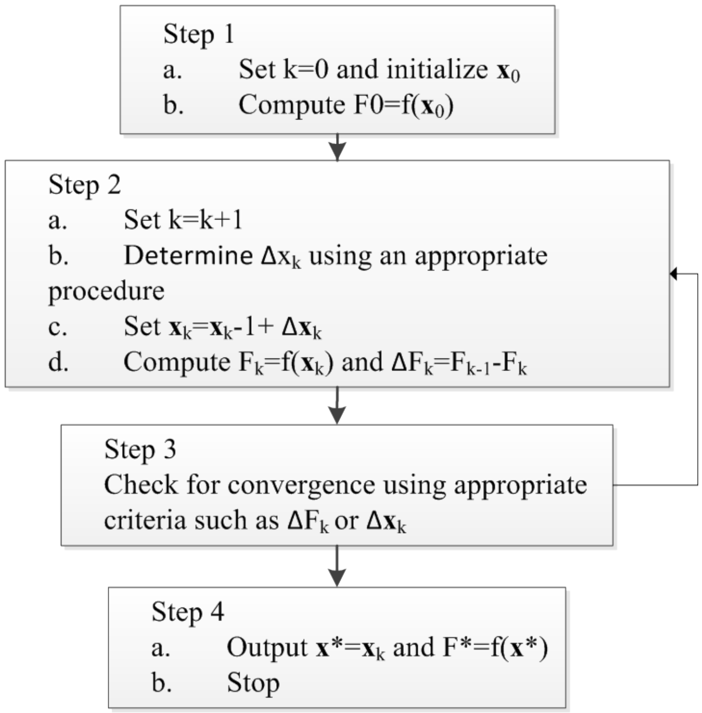

Figure 14: Typical optimization process [38]

The initial estimate for **x** is based on knowledge of the problem, but often an arbitrary selection is necessary. The check for convergence can be completed in a number of ways, depending on the problem and optimization method being used. Convergence is checked by comparing the current output function with the previous output function, if the difference between these values is less than a specified target or tolerance value then convergence has been achieved. This is illustrated using Equation 2.10 shown below.

$$|\Delta F_k| = |F_k - F_{k-1}| < \epsilon_F \tag{2.10}$$

In the above equation ΔF_k is the change in objective function, F_k is the current objective function value, F_{k-1} is the previous iteration's objective function value and ε_F is the tolerance or target value used for the convergence.

Finally many optimization problems require constraints on the design problem that must be solved before the optimization can be considered complete. The constraint equations are summarized below.

$$\text{subject to:}\quad \begin{matrix} \text{minimize } f(\boldsymbol{x}) \text{ with } \mathrm{x} \in E^n \\ a_i(\boldsymbol{x}) = 0 \; for \; i = 1, 2, \dots p \\ c_j(\boldsymbol{x}) \geq 0 for \; j = 1, 2, \dots q \end{matrix} \tag{2.11}$$

In the above equation *x* is the variables to be adjusted through optimization, *f* is the optimization objective function, a_i represents the constraint equality equation and c_j represents the constraint inequality equations and *i* and *j* represent the number of constraint equations.

Constrained optimization problems are generally more difficult to solve than unconstrained optimization. Recent developments have focused on reformulating constrained optimization problems as unconstrained optimization. A number of optimization programs are available for the problem of being solved in this work, but the goal attainment method was selected for the optimization of the vehicle structural design.

The goal attainment method was selected as it is capable of minimizing a multi-objective optimization problem [39]. The problem can be set-up as follows:

$$\text{minimize x}, \gamma \text{ such that } \begin{cases} F(\boldsymbol{x}) - weight \cdot \gamma \leq goal \\ c(\boldsymbol{x}) \leq 0 \\ ceq(\boldsymbol{x}) = 0 \\ A \cdot \boldsymbol{x} \leq b \\ Aeq \cdot \boldsymbol{x} = beq \\ \boldsymbol{lb_i} \leq \boldsymbol{x_i} \leq \boldsymbol{ub_i} \end{cases} \tag{2.12}$$

The goal of this method is to reduce the objective functions defined by *F* below a set of goals defined for each objective. The vector ***x*** defines the input parameters that are varied during each iteration starting at an initial condition. The inequalities, represented by *c* and *A*, along with the equalities represented by c_{eq} and A_{eq} are used to apply constraints to the problem if necessary but can be neglected resulting in an unconstrained optimization process. Finally the vectors ***lb*** and ***ub*** define the lower bound and upper bound values respectively for the input parameters defined in ***x*,** the subscript *i* is an index used to show that the bounds are not uniform for each entry of the input parameters. The variable γ is a slack variable used as a dummy argument to minimize the objectives defined in F simultaneously. The goal attainment method will attempt to reduce the objective functions below their defined goals, however the goals are not always initially known. The weight vector is used to define the priority for minimization with the result being that the objective function given a higher weighting will likely be overachieved, potentially at the expense of other objective functions. The goal attainment method can be represented geometrically, in general terms with a single objective function, as shown below in Figure 15 [40].

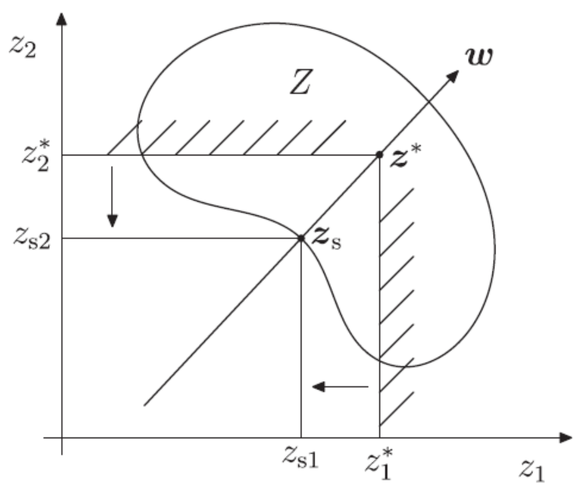

Figure 15: Geometric representation of goal attainment [40]

In the above image Z represents the Pareto front, z_1 and z_2 are the objective function values, z_i^* represents the objectives of the current iteration, z_{si} represents the objective function goals of the goal attainment algorithm and *w* represents the weight factor for each objective value.

One advantage of using the goal attainment method is that a number of other algorithms can be included in order to improve the robustness of the method [41,42,43,44,45]. Specifically goal attainment can be posed as a nonlinear programming problem and algorithms for sequential quadratic programming (SQP) can be used. The use of SQP allows for modifications to the line search and Hessian to be made. With the line search method an exact merit function is used and when the merit function shows improvement the line search is terminated. A modified Hessian is also used because of the nature of the goal attainment problem. While the goal attainment method is fairly robust, especially with the additional algorithms from nonlinear programming, the major limitation is that the method may only give a local solution. This limitation implies that the optimization process may need to be repeated to determine whether the results are a global optimum or one of many possible solutions.

The goal attainment method is selected as it has been previously used successfully to optimize a simplified vehicle structure [46]. The knowledge gained from that process has been applied here which resulted in a simplified implementation of the revised structural model. Also the goal attainment method is utilized in place of other algorithms because it allows for the input of an initial condition which can be used as the preliminary values that the optimization penalty functions are based on. The penalty function implementation is made easier by having an initial condition and including the penalty functions is desirable to drive the optimization to convergence.

Chapter 3

3. Method of Simple Structural Beams-Frames

3.1 Model Geometry

The geometry of the structure being considered is based on general parameters of a typical sedan car. The developed methodology is implemented and presented utilizing a general case study, the dimensions of which are based on typical vehicle sizes and a previously analyzed structure. Representative structures that were used as the foundation for the developed case study structure are shown below.

Figure 16: Sedan Body-in-White [46]

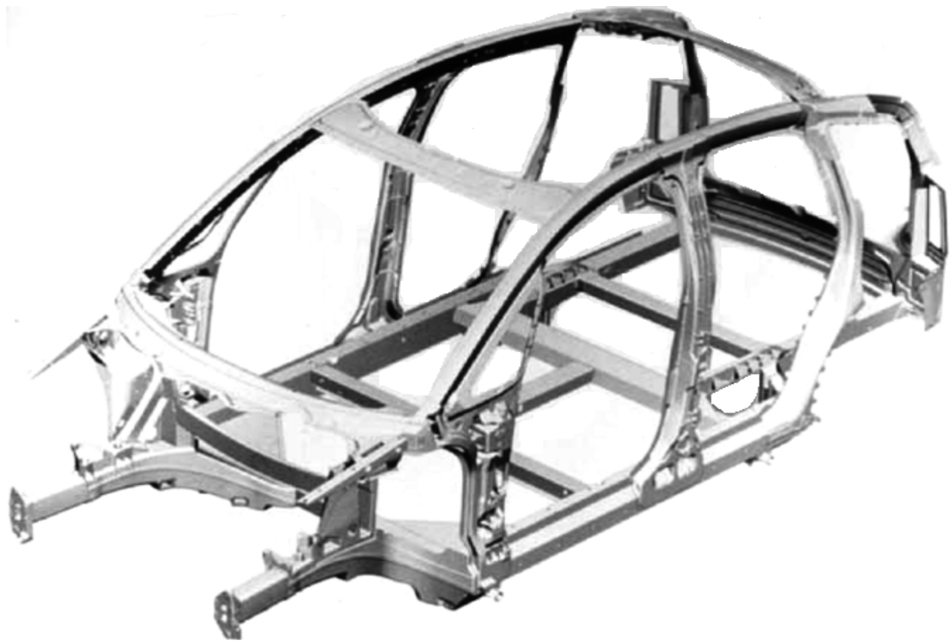

Figure 17: Space Frame [30]

As can be seen both the Body-In-White and the space frame are lacking sheet elements in some areas. The space frame shown in Figure 17 specifically is missing sheet elements for both the floor and roof. Since they are not included in certain existing vehicle designs it can be assumed that the SSB representation of a structure is adequate for supporting the vehicle components as well as provide a sufficient path for loading conditions that can occur. The vehicle dimensions are also based on previous work, but have been adjusted slightly to account for some of the curvature commonly found in automotive structures. The vehicle being used to provide geometric properties has been previously analyzed using the SSS method and is shown below in Figure 18 [30].

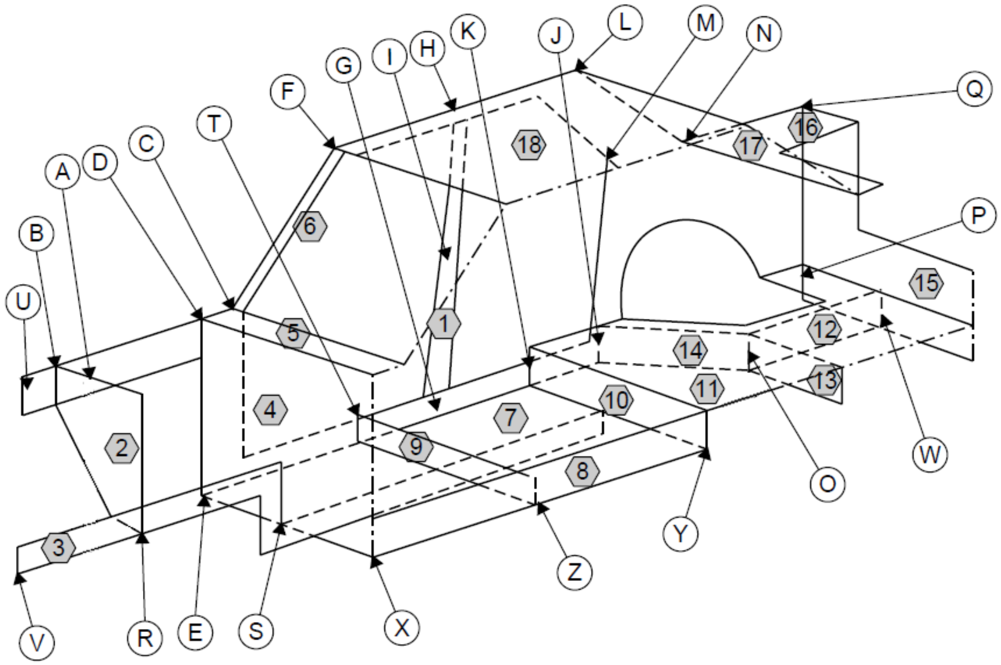

Figure 18: Geometry of SSS model [30]

The dimensions of the structure shown above can be seen below in Table 1.

Node	Description	x (mm)	y (mm)	z (mm)
A	Top of front suspension strut	900	560	800
B	Front fender longitudinal outboard of strut	900	750	800
C	Lower corner of windshield A-pillar	1450	750	800
D	Fender longitudinal to cowl	1350	750	800
E	Base of A-pillar/sill (rocker)	1450	750	170
F	Upper corner of windshield/cantrail	2050	750	1350
G	Base of B-pillar/sill (rocker)	2350	750	170
H	Top of B-pillar/cantrail	2550	750	1350
I	Middle of B-pillar	2450	750	760
J	C-pillar/sill (rocker)	3200	750	170
K	Floor crossbar (rear seat)/sill	2800	750	170
L	Upper corner of backlight/cantrail	3300	750	1350
M	Middle of C-pillar/front of parcel tray	3500	750	900
N	Rear corner of parcel tray/lower corner backlight	3850	750	900
O	Rear suspension spring mounting	3500	450	400
P	Rear lower corner of boot (trunk)	4400	750	400
Q	Rear upper corner of boot (trunk)	4400	750	900
R	Engine rail below A	900	500	400
S	Engine rail/dash panel	1350	500	170
T	Cross-beam (front seats)/sill	2000	750	170
U	Front end of upper fender rail	350	750	800
V	Front end of engine rail	0	500	420
W	Rear end of rear longitudinal rail	4400	450	400
X	Centre tunnel/dash	1350	0	170
Y	Centre tunnel/rear seat cross-beam	2800	0	170
Z	Front seat cross-beam/centre tunnel	2000	0	170

Table 1: Dimensions of SSS model [30]

The dimensions above give the location of each nodal position in absolute coordinates, where the position is measured in millimetres. The longitudinal (x) axis is measured from the front edge of the engine rail (node V in Figure 18), the lateral (y) axis is measured from the centreline of the vehicle model and the vertical (z) axis is measured from the bottom of the lower part of the engine rail (labelled 3 in Figure 18). This information along with the space frame shown in Figure 17 is used as the foundation of the beam frame model utilized throughout this process. The nodal locations have been adjusted to better reflect the space frame vehicle and to account for the curvature that cannot be present in the SSS method. The geometry with labelled nodes is shown below in Figure 19.

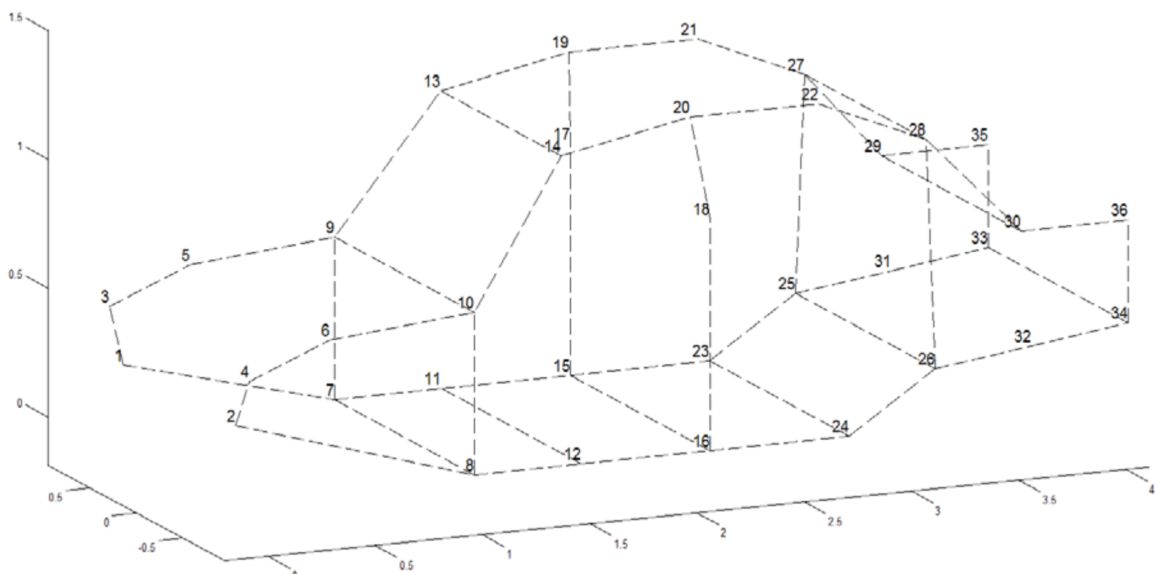

Figure 19: Developed beam frame model

The geometry of the beam frame model is summarized below in Table 2.

Node	x (m)	y (m)	z (m)
1	0	0.6	0.25
2	0	-0.6	0.25
3	0	0.75	0.45
4	0	-0.75	0.45
5	0.375	0.75	0.58
6	0.375	-0.75	0.58
7	1.05	0.75	0
8	1.05	-0.75	0
9	1.05	0.75	0.63
10	1.05	-0.75	0.63
11	1.55	0.75	0
12	1.55	-0.75	0
13	1.5	0.65	1.18
14	1.5	-0.65	1.18
15	2.15	0.75	0
16	2.15	-0.75	0
17	2.15	0.75	0.9
18	2.15	-0.75	0.9
19	2.1	0.65	1.28
20	2.1	-0.65	1.28
21	2.7	0.65	1.28
22	2.7	-0.650	1.28
23	2.8	0.75	0
24	2.8	-0.75	0
25	3.2	0.75	0.23
26	3.2	-0.75	0.23
27	3.2	0.65	1.1
28	3.2	-0.65	1.1
29	3.6	0.75	0.73
30	3.6	-0.75	0.73
31	3.65	0.75	0.28
32	3.65	-0.75	0.28
33	4.1	0.75	0.33
34	4.1	-0.75	0.33
35	4.1	0.75	0.73
36	4.1	-0.75	0.73

Table 2: Geometry of developed beam frame

The coordinates described above define the absolute coordinates of the nodes. The nodal locations are measured in metres and the vehicle coordinate system is oriented in the same manner as before. The x-axis is oriented along the length of the vehicle's centreline from front to rear. The y-axis is oriented in the lateral dimension from left to right and the z-axis is oriented vertically upward.

3.1.1 Finite Element Model

The beam elements are then determined by connecting two nodes, this is shown below in Figure 20.

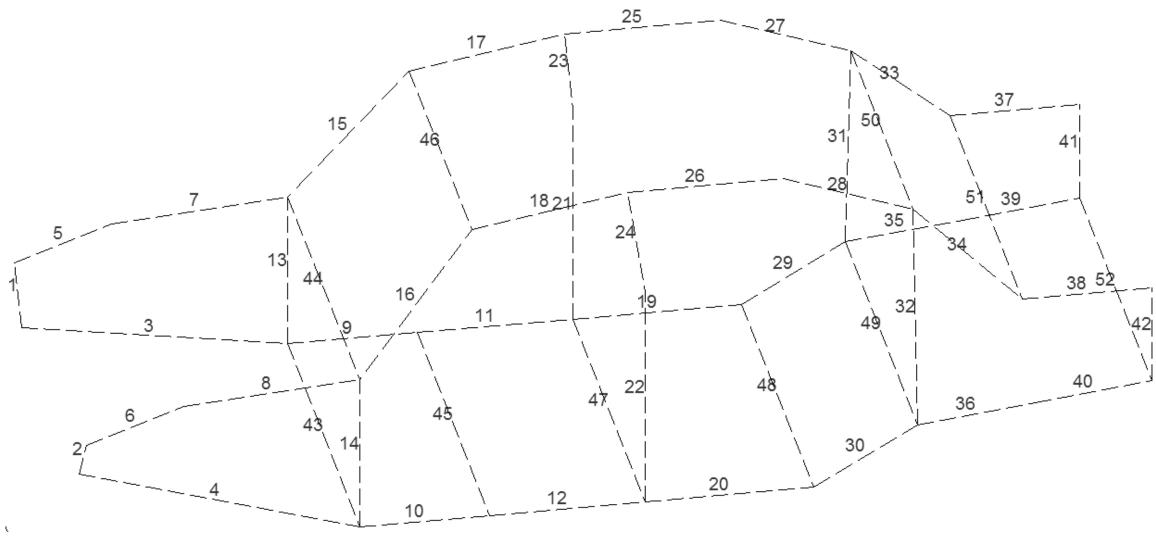

Figure 20: Beam elements of vehicle

The beam elements of the vehicle structure, shown in Figure 20, represent the finite element model of the vehicle structure. The finite element model features fifty-two total elements with thirty-six nodes. A node occurs at every point where multiple elements intersect. It should be noted that one important aspect of vehicle structure finite element modeling is the joint (node) stiffness values. The joint stiffness in a vehicle structure has a significant impact on the overall structural stiffness. Generally a joint will be a semi-rigid connection that will have individual stiffness values based on the joining process and cross-section properties of the elements that are connected at the joint [47]. Individual joint stiffness's can be accounted for when using a commercial software, however the inclusion of joint stiffness greatly increases the computation power required and time to perform analysis, as well as a greater complexity in the program itself. For this reason the joint design is better conducted following the cross-section design, but early in the structural design process. The model considered here uses a rigid joint connection which will reduce the accuracy and result in a stiffness value that is artificially higher.

3.2 Static Analysis

The vehicle is analyzed based on a static loading condition with fixed values for component loads. A summary of these loads and their longitudinal position is shown below in Table 3 [30].

Component	Load (N)	Position (mm)
Front Bumper	200	0
Powertrain	3000	525
Front Passenger	2000	1850
Rear Passenger	2500	2475
Fuel Tank	500	3000
Luggage	950	3650
Rear Bumper	300	4100
Exhaust	350	2150

Table 3: Component loads being applied [30]

The component loads being applied to the structure will be combined with the structure weight to determine the force applied at the front axle. The structure weight is calculated by considering a uniform material of known density along with individual element cross sectional areas and their lengths. The area and length of each element give the volume which, when combined with density will give the mass of each element. The values for each element are then added together and multiplied by gravity to determine the weight.

The location of the centre of gravity of the vehicle structure is required in order to determine the force applied to the front axle. It can be assumed that the component loads are applied through the vehicle structure centre of gravity. The structure centre of gravity is located 2230mm from the front of the vehicle along the vehicle centreline. The force on the front axle can then be found by taking a moment about the rear suspension. This is better illustrated using the diagram shown below in Figure 21.

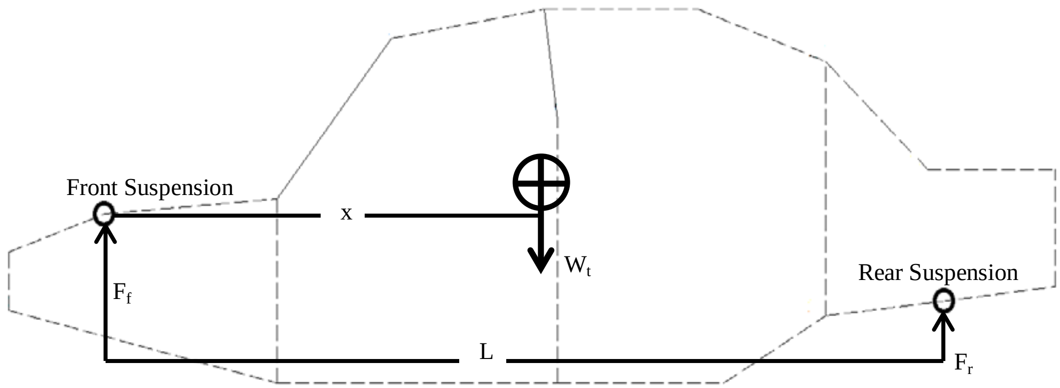

Figure 21: Vehicle diagram with suspension reaction forces

The force on the front axle is then found using Equation 3.1, shown below. It should be noted that the calculated axle force will be divided by two in order to determine the nodal force applied during the finite element analysis.

$$F_f = \frac{W_t(L-x)}{L} \quad (3.1)$$

In the above equation the force on the front axle is represented by F_f, the total applied weight by W_t, the wheelbase by L and the location of the centroid by x. The nodal force that is calculated based on the front axle load represents a static loading condition of a vehicle resting on level ground. This result would be comparable to using a set of scales at each wheel location and measuring the weight. The rear axle weight is not considered in the static loading condition as those locations are fixed and do not contribute to the deflection of the structure. Once the nodal force for the front suspension has been calculated the vehicle structure can be analyzed in order to determine the nodal deflections. The next step in the process is using the static loading condition to perform an initial analysis in order to determine the starting point for the multi-objective optimization.

3.3 Initial Parameter Estimation

This section will explain the process of determining suitable cross-section shapes as well as the dimensions that result in the desired maximum deflection values. The shape of each element will be kept uniform throughout the structure and the result of the initial estimate will make every element have equal cross-sectional dimensions. Before conducting the initial design analysis a method of estimating the bending and torsion stiffness values, as well as an explanation of what each value represents in a vehicle is presented.

3.3.1 Estimation of Bending Stiffness

A pure bending load is developed in a vehicle structure when the vehicle's front wheels strike a bump simultaneously, as shown in Figure 22 [30]. This simultaneous impact results in equal forces being applied vertically upward on the front of the structure.

Figure 22: Vehicle striking a bump [30]

The bending condition is simulated in a finite element solver by applying vertical forces of equal magnitude at the nodal positions representing the front suspension, as indicated in Figure 23.

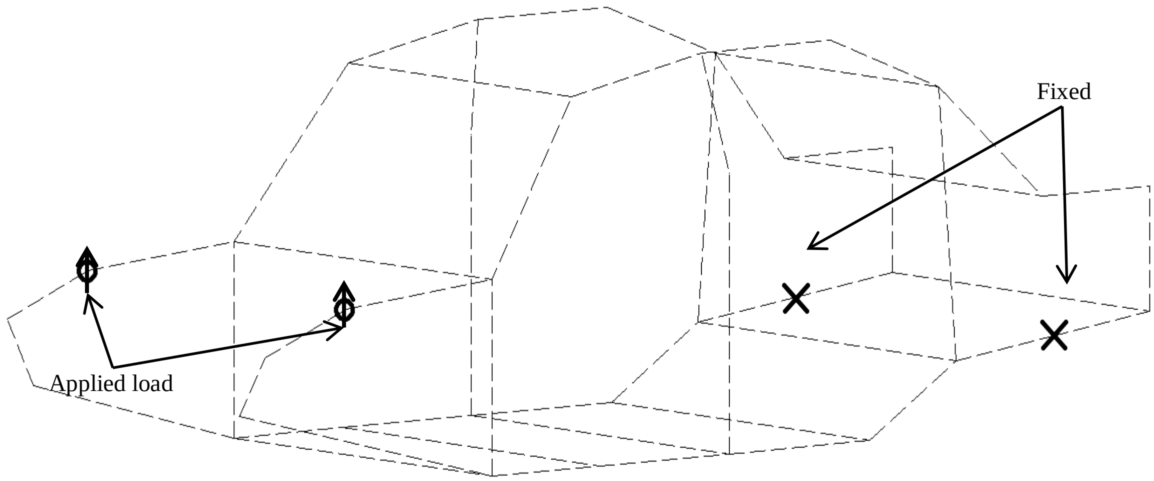

Figure 23: Bending load of vehicle finite element model

The result of applying this type of load is shown below in Figure 24.

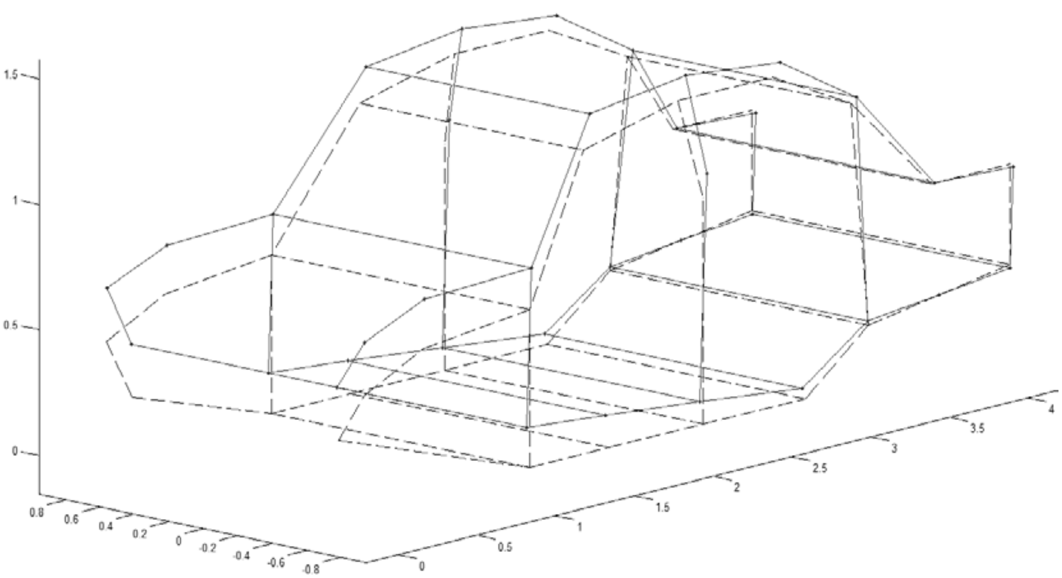

Figure 24: Deflection result of bending load

As can be seen the bending loads produce a primarily vertical deflection at each node. It should be noted that the results shown above are exaggerated so that the deflected structure, shown with solid lines, is more clearly visible. The bending stiffness of the structure will be the structural resistance to an applied bending load and can be calculated using Equation 3.2.

$$K_b = \frac{F}{\delta} \tag{3.2}$$

In the above equation K_b represents the bending stiffness, F the combined force at the front suspension and δ the vertical deflection at the front of the vehicle. The force being applied is considered to be the combined load since the sum of the forces is responsible for the resultant deflection. The deflection is measured at the front of the vehicle as this represents the greatest magnitude of vertical deflection. The deflection values for each side of the vehicle are averaged to produce the value used in calculating the stiffness even though they should be equal.

3.3.2 Estimation of Torsion Stiffness

A pure bending load is developed in a vehicle structure when one of the vehicle's front wheels strikes a bump, as shown in Figure 25 [30]. When the wheel strikes the bump a torque is generated due to the weight transfer from one side to the other.

Figure 25: Vehicle striking a bump [30]

The bending condition is simulated in a finite element solver by applying vertical forces of equal magnitude at the nodal positions representing the front suspension, as indicated in Figure 26.

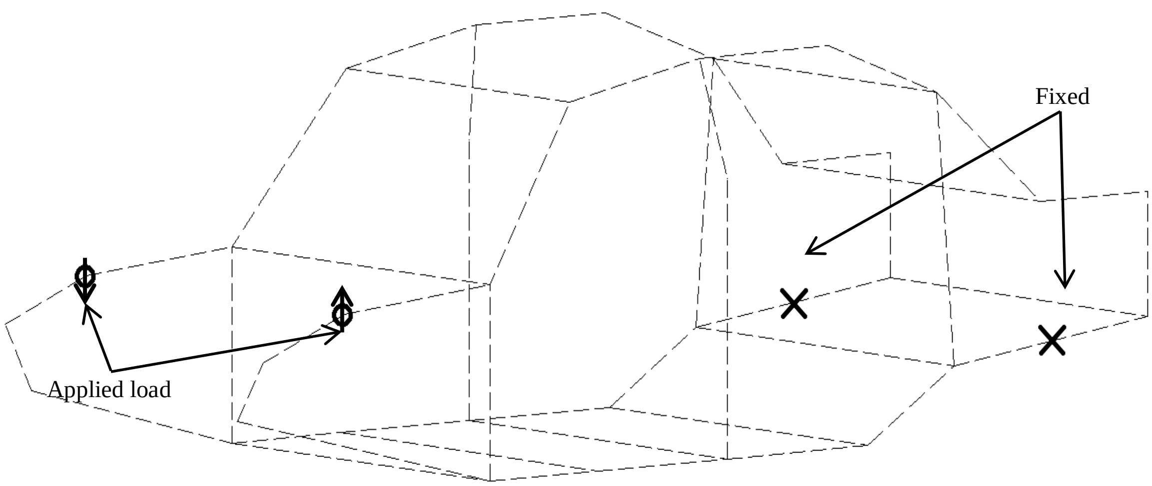

Figure 26: Torsion load of vehicle finite element model

The result of applying this type of load is shown below in Figure 27.

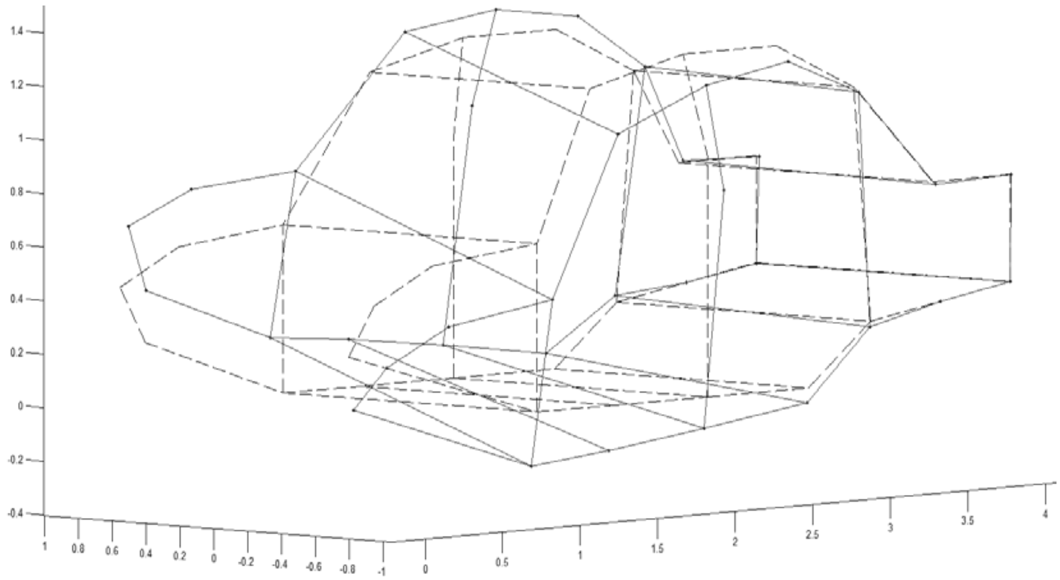

Figure 27: Deflection result of torsion load

As can be seen the torsion loads produce a combination of deflections at each node, but the main deflection is in the vertical direction. It should be noted that the results shown above are exaggerated so that the deflected structure, shown with solid lines, is more clearly visible. The torsion stiffness of the structure will be the structural resistance to an applied torsion load and can be calculated using Equation 3.3.

$$K_t = \frac{T}{\theta} = \frac{FB}{\theta_d + \theta_p} \tag{3.3}$$

In the above equation K_t represents the torsion stiffness, *F* represents the force applied at one wheel, *B* the track width of the vehicle and θ the angular deflection. The torque being applied can be considered the sum of the nodal forces on the front suspension multiplied by the distance to the vehicle centreline. The forces are added together as they both act in the same direction about the vehicle x-axis. The angular deflections can be calculated using Equation 3.4 and Equation 3.5, with‘d’ representing the driver side and ‘*p*’ the passenger side.

$$\theta_d = \tan^{-1}\left(\frac{\delta_d}{B/2}\right) \tag{3.4}$$

$$\theta_p = \tan^{-1}\left(\frac{\delta_p}{B/2}\right) \tag{3.5}$$

In the above equation δ represents the vertical deflection at the corresponding node. The deflection is measured at the front of the vehicle as this represents the greatest magnitude of vertical deflection. The deflection values for each side of the vehicle are averaged to produce the value used in calculating the stiffness even though they should be equal.

3.3.3 Cross-Section Selection

Prior to determining the initial size of the beam elements a suitable shape and material must be selected. The material chosen will be uniform for the vehicle structure as the focus is on section size optimization. Previous work has been done to optimize the vehicle structure material distribution [48]. The material distribution of typical vehicle structures is shown below in Figure 28 [49,50].

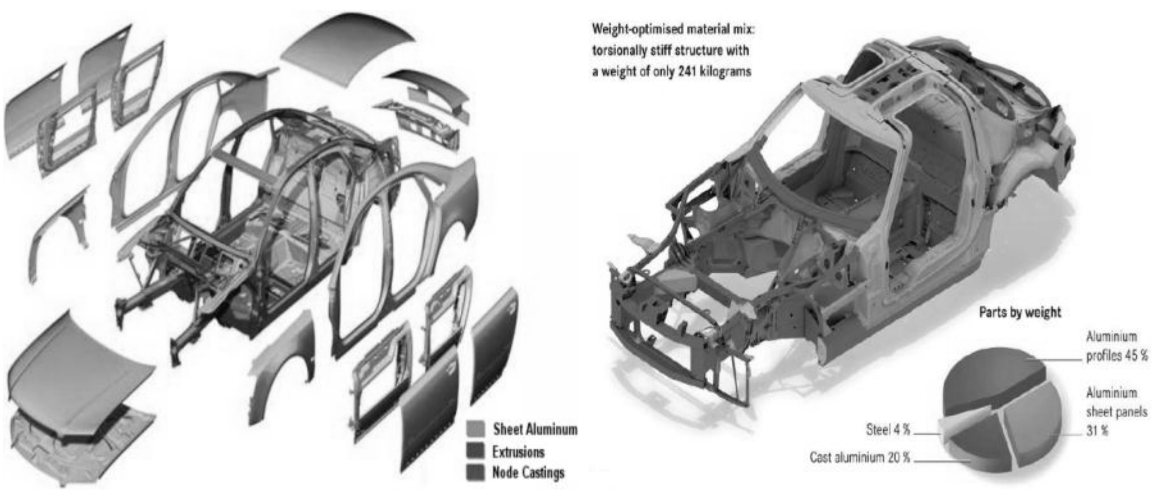

Figure 28: Materials distribution of typical vehicle structures [49,50]

The material chosen is standard steel, commonly found in existing automotive structures. The material properties for the steel are listed below in Table 4 [51].

Material Property	Value
Young's Modulus, E	206GPa
Shear Modulus, G	79.85GPa
Poisson's Ratio	0.29
Density	7850kg/m^3

Table 4: Steel material properties [51]

A number of cross-sections are available to be used for the beam elements of the vehicle structure. These include open and closed sections as well as hollow or solid sections. The best shape will be efficient for a general loading condition. An efficient cross-section is one that minimizes deflection for a given section area [52].

While the loads being applied in this work are primarily vertical, lateral loading occurs in a vehicle structure when the vehicle is cornering [30]. Generally an I-beam will be the most efficient shape for bending; however this is only true if the load is applied perpendicular to the flange as shown in Figure 29.

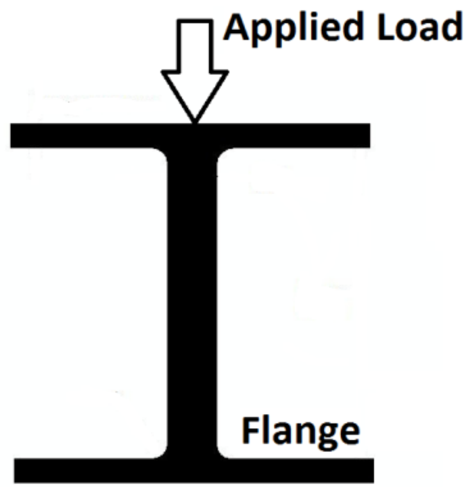

Figure 29: I-beam with vertical load

Since the loading condition of a vehicle will vary and it cannot be assumed that the applied load on a beam element will always be in the vertical direction an I-beam is not the ideal choice. The best choice will have equal stiffness values whether the loads are vertical or lateral, as shown in Figure 30.

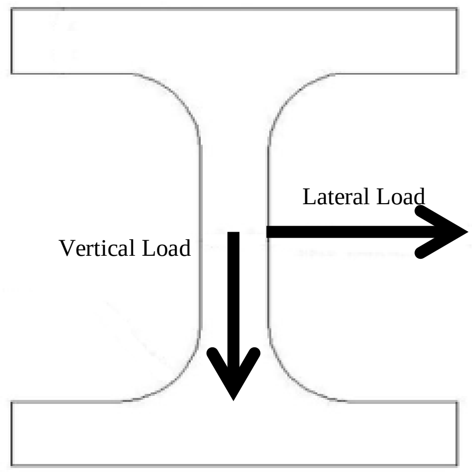

Figure 30: Two dimensional bending

Since the primary deflections are the result of bending a square cross-section is selected because for a given area it is more efficient than a circle [52]. Finally the cross-section will be hollow since it will offer greater weight savings and still be sufficiently stiff when compared to a solid cross section of equal area [52]. The selection of a square cross-section offers other advantages not related to the loading condition. Flat surfaces are easier to drill into and weld together making vehicle assembly simpler. Also a hollow cross-section will offer protection for components, such as wiring and tubing that runs along the length of the vehicle. Lastly since the cross-section is closed there is limited space for water or snow to accumulate and cause corrosion.

With a suitable cross-section shape chosen the next step is to determine the element sizes that will provide the initial condition for the optimization process. This step is done in an iterative process. Initially an outer size and wall thickness are chosen for the elements, the section shape is shown below in Figure 31.

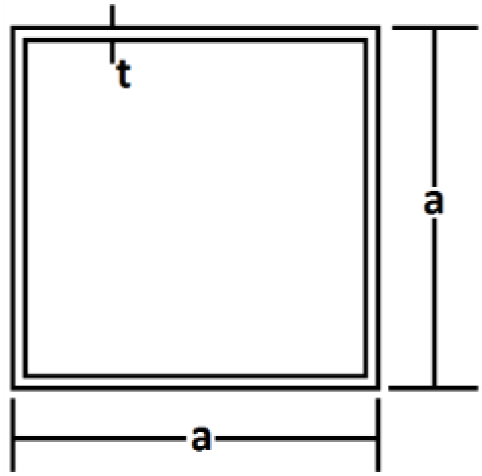

Figure 31: Beam cross section parameters

For the preliminary sizing uniform values are chosen resulting in every beam element having the same section geometry. The optimization process will vary these parameters on an individual basis. The objective of the preliminary analysis is to determine a uniform set of values, such that the maximum deflection will be smaller than a target value. This can be seen in Equation 3.6 shown below.

$$\text{Determine } \{a_1, t_1, a_2, t_2, a_3, t_3, \ldots a_n, t_n\} \text{ such that } \delta_{max} \leq \delta_{target} \qquad (3.6)$$

In the above equation 'a' is the length of the section side, 't' the wall thickness and the subscript denotes the element number. The δ represents the objective functions. Generally an acceptable maximum deflection would be 3.5mm as this will ensure all elements remain in the elastic domain [53]. However, this amount of deflection may result in section sizes that are over constrained from the initial stage so a larger deflection is chosen as the target. The value selected was 15mm with the assumption that this leaves room for the optimization to further reduce the maximum deflections. The deflection value will be based on the bending condition as this load produces the greatest maximum deflection due to both forces acting in the same direction. A starting side length of 50mm was chosen with a thickness of 1mm. The wall thickness was then increased in increments of 1mm until the target deflection was achieved. As the side length was kept constant there will be a point where the thickness causes an infeasible section. When an infeasible section is achieved the side length is increased to accommodate a wider range of thickness values. The load applied was calculated based on the structure weight so increasing the thickness resulted in an increased load. It was found that at a certain point the increase in load was not counteracted by a sufficient increase in stiffness. When this point was reached the iterative process was halted as the deflections would then begin to increase. In order to ensure the best possible initial condition and reduce the time required for optimization this process was repeated based on the results of the initial analysis. The results of the entire process are shown below in Table 5.

	Initial		Final		
Test	Side Length (mm)	Thickness (mm)	Thickness (mm)	Weight (N)	Max Deflection (mm)
1	50	1	14	6068	54.6
2	55	1	15	7224	40.3
3	60	1	15	8127	30.7
4	65	1	16	9439	24
5	70	1	16	10403	19.2
6	75	1	16	11366	15.7
7	80	1	16	12895	13

Table 5: Results of preliminary size estimation

As can be seen the best test was number seven with a final side length of 80mm and a thickness of 16mm. Based on the results of this process the initial condition for the optimization process has been established. The next step will be to perform the multi-objective optimization in order to reduce the weight while maintaining the vehicle stiffness.

3.4 Alternative Approach to Parameter Selection

It should be noted that previous analysis and optimization has been conducted on a simplified vehicle structure that featured beam elements with circular sections. Also the selection of the initial condition for optimization was conducted in a different manner. The initial condition for this simplified structure was chosen based on a data generation and filtering process. The data was experimentally generated by varying the element radiuses one at a time and monitoring the results. A large number of trials conducted and following the data generation process a series of filters were applied to determine the initial condition. One filter was based on the structure weight and the second was based on the stiffness being considered. In this process only one aspect of stiffness (bending or torsion) was considered. Further details about this process can be found in Appendix I and Appendix II.

Chapter 4

4. Multi-Objective Optimization

This section will provide the necessary information regarding the optimization procedure. As mentioned previously a goal attainment method is implemented for optimizing the vehicle structural design. This method was chosen as it is a robust method of performing multi-objective optimization. The goal of the optimization process will be to find the set of parameters that minimize the objective functions to a specified goal. Initially it is not known if the goal will be attained, so an attainment factor is used to determine how the goals should be adjusted. The first step of the optimization is determining an appropriate initial condition, which has been described above. As previously stated symmetry is implemented to reduce the number of design parameters available for optimization. Based on the image shown below, elements that are mirrored about the longitudinal (x) axis of the vehicle will have the same dimensions and are defined as unique elements. While having every individual element available for optimization could result in an improved design, the increase in computation time is unnecessary.

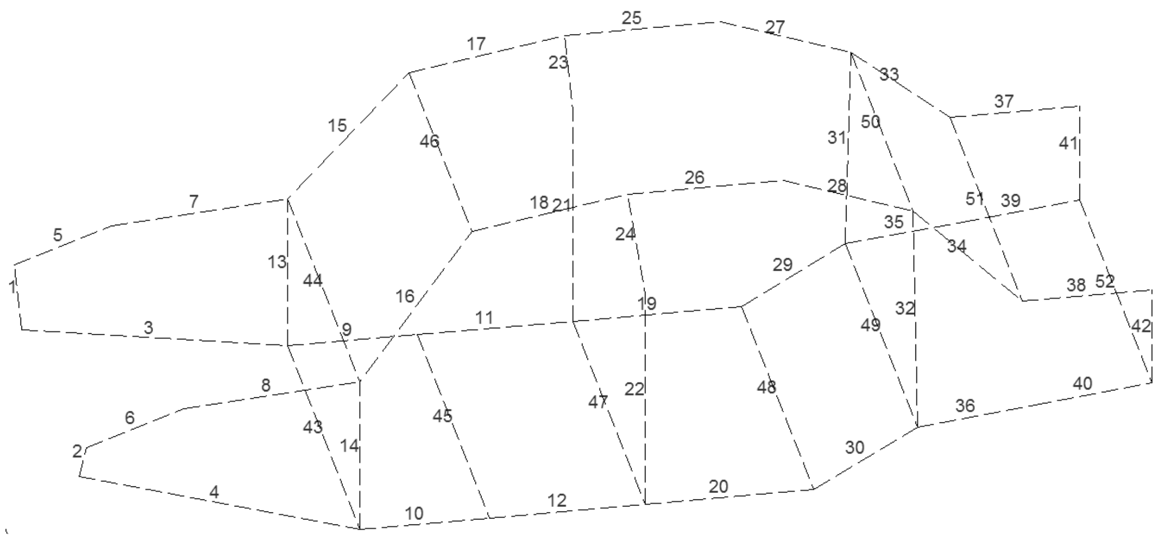

Figure 32: Beam element vehicle model

The list of unique elements is shown below in Table 6 with the element numbers based on Figure 32 included.

	Elements		Elements		Elements		Elements
Unique Element 1	1-2	Unique Element 9	17-18	Unique Element 17	33-34	Unique Element 25	46
Unique Element 2	3-4	Unique Element 10	19-20	Unique Element 18	35-36	Unique Element 26	47
Unique Element 3	5-6	Unique Element 11	21-22	Unique Element 19	37-38	Unique Element 27	48
Unique Element 4	7-8	Unique Element 12	23-24	Unique Element 20	39-40	Unique Element 28	49
Unique Element 5	9-10	Unique Element 13	25-26	Unique Element 21	41-42	Unique Element 29	50
Unique Element 6	11-12	Unique Element 14	27-28	Unique Element 22	43	Unique Element 30	51
Unique Element 7	13-14	Unique Element 15	29-30	Unique Element 23	44	Unique Element 31	52
Unique Element 8	15-16	Unique Element 16	31-32	Unique Element 24	45		

Table 6: List of unique elements

A design sensitivity analysis using the finite difference method was conducted to ensure that elements in mirrored positions will have the same effect on the structure. The inclusion of plates later in the process will not affect the symmetry since the thickness is uniform throughout each plate component. The sensitivity analysis also gave insight into the effect each element has on the total vehicle stiffness.

4.1 Optimization Objectives

The multi-objective optimization process utilizes two objective functions, defined below.

$$\text{minimize}\left(Obj_1 = \frac{W}{K_b}\right) \tag{4.1}$$

$$\text{minimize}\left(Obj_2 = \frac{W}{K_t}\right) \tag{4.2}$$

In the above objective function equations *Obj* stands for objective, *W* is the structure weight, K_b the bending stiffness and K_t the torsion stiffness. Prior to performing the optimization process the initial objective functions were calculated using the uniform values determined previously. The initial values for the optimization are shown below in Table 7.

Structure Weight, W (N)	12567.91
Bending Stiffness, K_b (N/m)	738024.9
Torsion Stiffness, K_t (Nm/rad)	1511743
Objective 1, W/K_b (m)	0.0170291
Objective 2, W/K_t (rad/m)	0.0083135

Table 7: Initial design parameters

The initial objective functions will be used as the basis for improvement and the optimization process will be used to reduce these values.

4.2 Optimization Constraints

While the goal attainment optimization program used here is considered unconstrained there are other constraints to be considered due to the nature of the problem. Since the optimization is being used to solve a problem that has geometric properties a restriction on the element thickness values is implemented. Prior to the calculation of the objective functions the thickness is checked to ensure the values being used are not greater than or equal to half the side length. If the thickness of a particular element is larger than half the side length then the thickness is replaced by a value equal to one-tenth the side length. This process is better explained using the image shown in Figure 33.

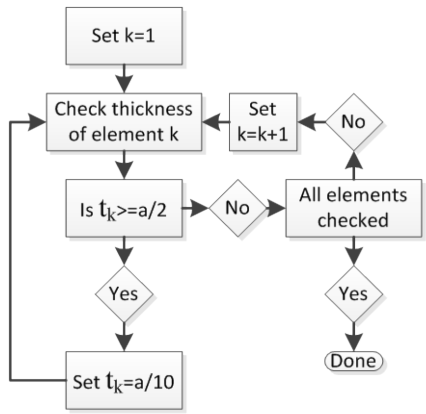

Figure 33: Element thickness check

The use of the thickness check ensures that the element cross-section dimensions that result from the optimization process are physically possible and will not have negative areas. The wall thickness, noted as t_k in the above diagram, is checked against the side length, noted as a in the above diagram, to ensure that the total thickness is not equal to the side length. In the event that the total thickness is equal to the side length it is divided by ten to reduce the thickness by an order of magnitude. The check on element thickness is important however it is not the only area of concern for the optimization.

4.2.1 Structural Stress Consideration

One of the primary concerns when performing the optimization is the stress generated in each element due to the applied loads. It is desirable to have all elements remain in the elastic range so that any deflection that does occur will be recovered when the load is removed. One method of doing this would be to calculate the element stress values for each iteration and perform a check similar to that of the thickness. This check however adds an unnecessary layer of complexity to a program that was implemented largely for the simplicity of it. Due to the nature of the loading condition applied to the vehicle structure the bending stress will be a primary concern. Bending stress calculations require extra equations as the stress will vary depending on the location within the cross section, with the maximum and minimum values occurring at the outer edges. Similarly the torsion stress will vary with the location on the cross section with the maximum again occurring at the outer edge, but since the sections are not circular the calculation is more complex. An alternative approach is to ensure the maximum deflection of the vehicle remains below a specific value. If the total deflection, which can be considered as the sum of the local element deflections, remains below this specified value then the stress will remain in the elastic range. For this purpose a maximum global deflection of 15mm was selected and the location of measurement is considered as the front of the vehicle. The location of measurement was selected as the front of the vehicle and not the location of the applied force since the deflection will continue to increase toward the front of the vehicle. This is analogous to having a cantilevered beam with a force applied at an intermediate point along the length of the beam. The selected deflection value is the same as that selected for the initial condition and is measured based on the bending stiffness.

4.2.2 Penalty Functions

The focus of the optimization process is to increase the structure stiffness and reduce the structure weight. However these goals are conflicting as increasing stiffness generally requires increasing an elements section dimensions which will in turn increase the weight. A series of penalty functions were implemented to improve the optimization results and reduce convergence time. The goal of the penalties is to artificially increase the objective function values that do not satisfy the stated minimization goals for a given iteration of design parameters. The implementation of the penalty functions is illustrated in Figure 34.

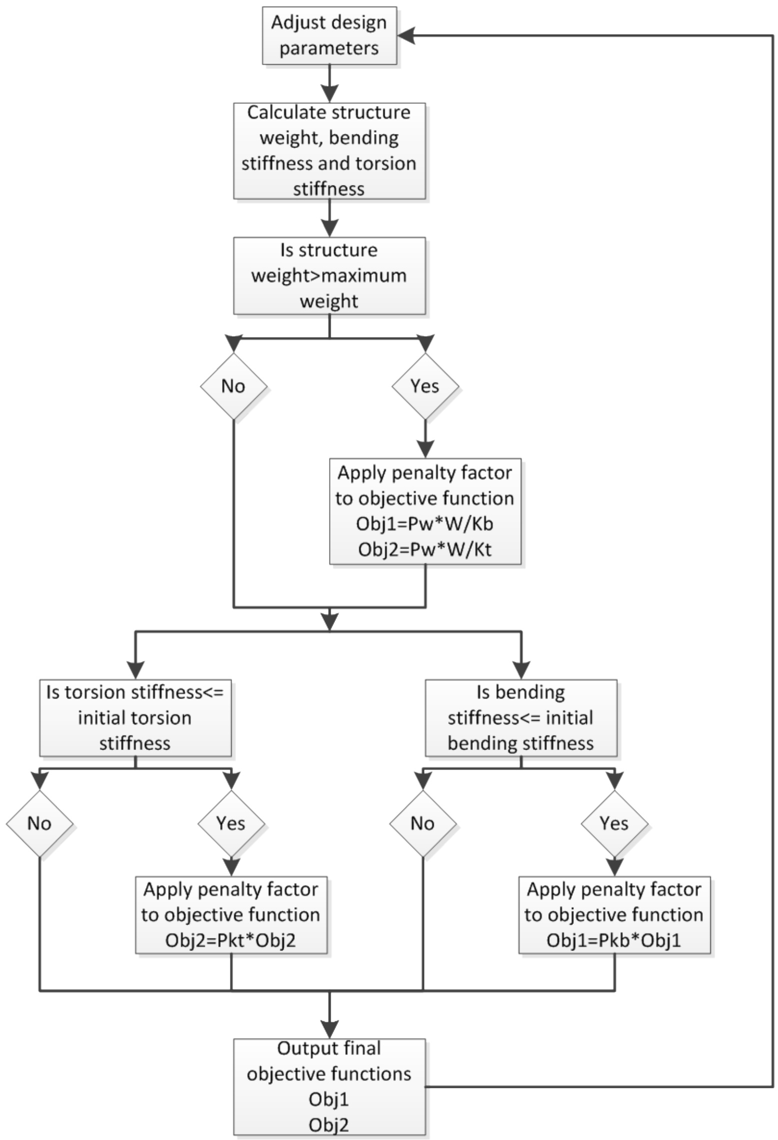

Figure 34: Penalty application flow chart

The use of penalty values P_w, P_{kt} and P_{kb} will affect the objective function by increasing them should any of the criteria not be satisfied. For the case of structural weight the penalty to the objective functions is applied for both the bending and torsion case simultaneously since the weight of a given iteration will be the same and the objective function must be increased equally. If either of the stiffness values is smaller than the corresponding initial value the penalty is applied. For cases where the weight and stiffness do not meet the requirements the penalties are combined. The penalties are applied using a differential scheme where the penalty value will be the relative difference multiplied by a scaling factor. These penalty values are summarized below.

$$P_w = \alpha \left(\frac{W_k - W_{max}}{W_{max}}\right) \tag{4.3}$$

$$P_{k_t} = \alpha \left(\frac{K_{t_k} - K_{t_{initial}}}{K_{t_{initial}}}\right) \tag{4.4}$$

$$P_{k_b} = \alpha \left(\frac{K_{b_k} - K_{b_{initial}}}{K_{b_{initial}}}\right) \tag{4.5}$$

In the above equations *P* represents the penalty value, *α* the scaling factor, *W* the weight and *K* the stiffness. The subscripts *t* and *b* correspond to torsion and bending respectively while the *k* subscript represents the value of the current iteration. The implementation of penalty functions is designed to increase a given iteration's objective functions to reduce the effectiveness of that set of design parameters in achieving the stated objectives. The scaling factor is constant for each penalty value in order to ensure each objective is equally weighted when the optimization is being performed as the weight reduction is as important as maintaining stiffness. The reason for implementing the penalty functions is to drive the optimization algorithm in the desired direction. The use of penalty functions has been established previously, primarily in constrained optimization problems [54,55,56]. Further discussion and verification of the use of penalty functions as well as selection of the scaling factor is presented in Appendix V.

4.3 Optimization Process

The goal attainment program that was chosen to simultaneously optimize the vehicle structure was implemented using the built-in MATLAB function. The use of the built-in function simplifies the optimization process allowing the focus to be placed on interpreting the results and improving the overall process. The built-in function requires a set of initial design parameters that have already been chosen as well as a function that determines the objective functions to be minimized. The function that is developed uses the design parameters of the current iteration to calculate the structure weight as well as the torsion and bending stiffness. The objective functions are then calculated with penalties applied when applicable. The process continues until a stopping criterion is met such as optimization convergence or the maximum number of iterations being reached. The overall optimization process is illustrated below in Figure 35.

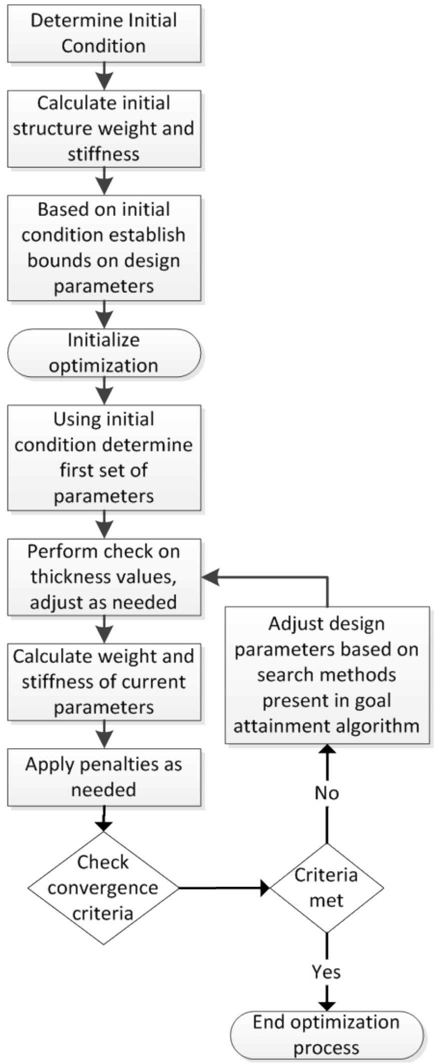

Figure 35: Optimization process

The initial conditions that suited the problem were a side length of 80mm and a uniform thickness of 17mm. The bounds on the design parameters also needed to be established. These values represent the possible variation in side length and wall thickness. A variation of 10% from the initial side length was allowed for the optimization process while the thickness was allowed a 50% variation from the initial value. A summary of the possible dimensions is shown below in Table 8.

Dimension	Minimum (mm)	Initial (mm)	Maximum (mm)
Side Length	72	80	88
Thickness	8	16	24

Table 8: Allowable section dimensions

The goals and weight for the objective functions also need to be determined. Initially it is not known whether the goals can be attained so a very small target value is selected and once the optimization has been completed the attainment factor can be analyzed to determine more suitable goals if needed. Goals of 1×10^{-15} for both objective function ratios were chosen, however this ratio between weight and stiffness is very small and may not be feasible. This value will ensure that the objective ratios are minimized as much as possible given the optimization parameters. The weights are used to balance the focus of optimization and since the goal is to optimize both stiffness parameters simultaneously equal weighting was chosen, with a specific value of one used.

The last step of the optimization is the convergence/stopping criteria. These are used to determine when the optimization is completed. The convergence criteria is the preferred end as this signifies that the optimization has been able to satisfactorily optimize the structural design, however to avoid the potential for an infinite loop a stopping criteria is implemented. The stopping criterion is based on the number of function evaluations and iterations however it is not initially known how many iterations will be required for convergence.

The function is evaluated a number of times for each iteration in the process. For this reason the maximum iterations will be different from the maximum function evaluations. The number of function evaluations per iteration depends on different factors, the main one is the method used to calculate the gradient. For this optimization process a central difference scheme was chosen as it will be more accurate. Using the central difference scheme approximately 127 function evaluations are performed for every iteration. The tolerance values represent the convergence criteria. The parameter tolerance represents the variation in design parameters between the current iteration and previous iteration. If the difference between any two corresponding values is less than this tolerance the optimization process stops. The function tolerance represents the variation in objective functions. If the difference between the objectives of the current iteration and previous iteration are smaller than the specified tolerance the optimization process stops.

Chapter 5

5. Optimization Results

The non-linear optimization process has been explained above; this section will summarize the results of the optimization process. The control parameters of the optimization are detailed below in Table 9.

Parameter	Value
Max Iterations	500
Max Function Evaluations	20000
Design Parameter Tolerance	$1x10^{-5}$
Function Tolerance	$1x10^{-15}$
Constraint Tolerance	$1x10^{-15}$
Goals	$1x10^{-15}$
Weight, [Obj_1 Obj_2]	[1 1]
Scale Factor	100

Table 9: Optimization parameters of optimization

The results of this optimization program are shown below in Table 10.

Parameter	Value	% Improvement
Weight (N)	8702.851	-30.7534
Bending Stiffness (N/m)	767037.3	3.931089
Torsion Stiffness (Nm/rad)	1671002	10.53479
Objective 1 (m)	0.0113461	-33.3726
Objective 2 (rad/m)	0.0052082	-37.3531
Attainment Factor	0.0052	

Table 10: Results of optimization process

As can be seen a substantial reduction in weight was achieved while both stiffness values were increased slightly. The optimization attainment factor indicates that the objectives were under attained, however given the optimization parameters that were used the optimization achieved convergence. This indicates that the stated goals were unrealistic and should be adjusted for a future optimization process.

5.1 Results Summary

The results of the optimization are summarized in the following figures. The side lengths of each unique element are shown below in Figure 36.

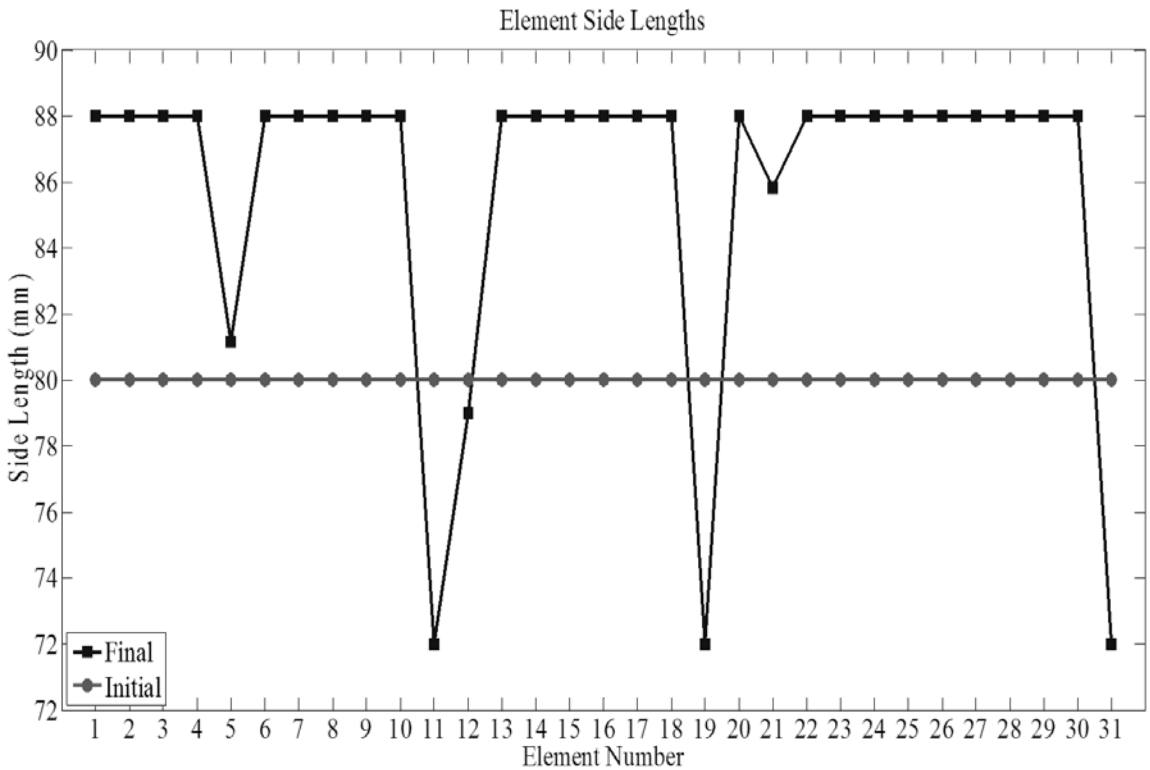

Figure 36: Side lengths during optimization

As can be seen the side lengths have had a substantial change from the initial condition with those elements that are not as structurally important having a reduction in size. The element thickness values are shown below in Figure 37.

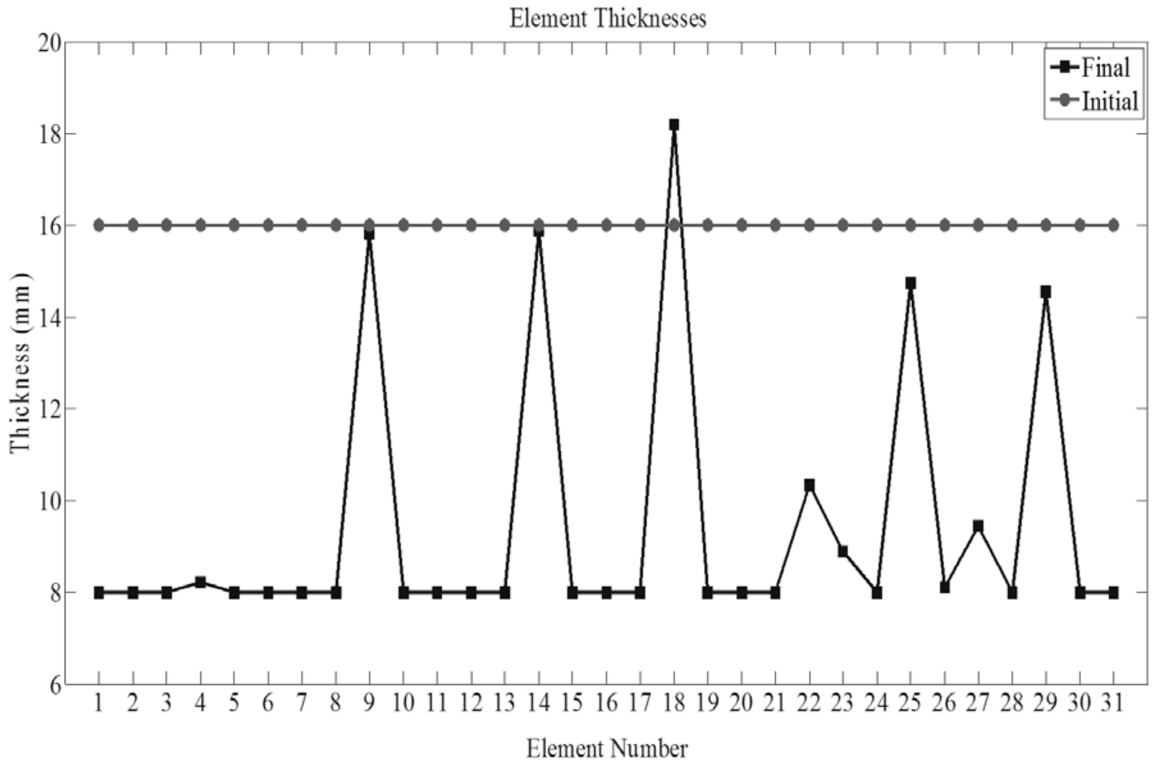

Figure 37: Thickness during optimization

Unlike the section side lengths the thicknesses were reduced in comparison to the initial design instead of increased; however the thickness of those elements that had the greatest contribution to stiffness were increased. Generally the elements that are more critical to stiffness have thicker sides. The results of the side length and thickness are an extension of basic solid mechanics. For a given bending load the amount of deflection can be reduced by increasing the distance from the neutral axis to the majority of the mass. This implies creating a larger section with decreased wall thickness will actually be stiffer than a smaller section with thicker walls. The beam section sizes can be better illustrated by displaying them graphically as shown below in Figure 38 and Figure 39. In these images the section side length is placed below the value for the section thickness.

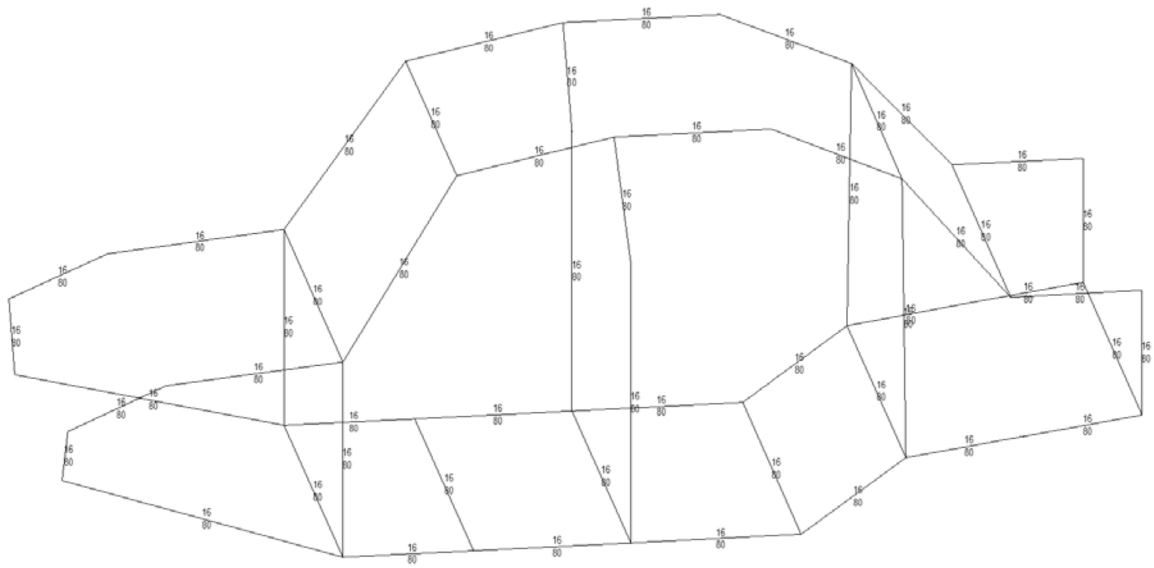

Figure 38: Initial vehicle structure with section sizes

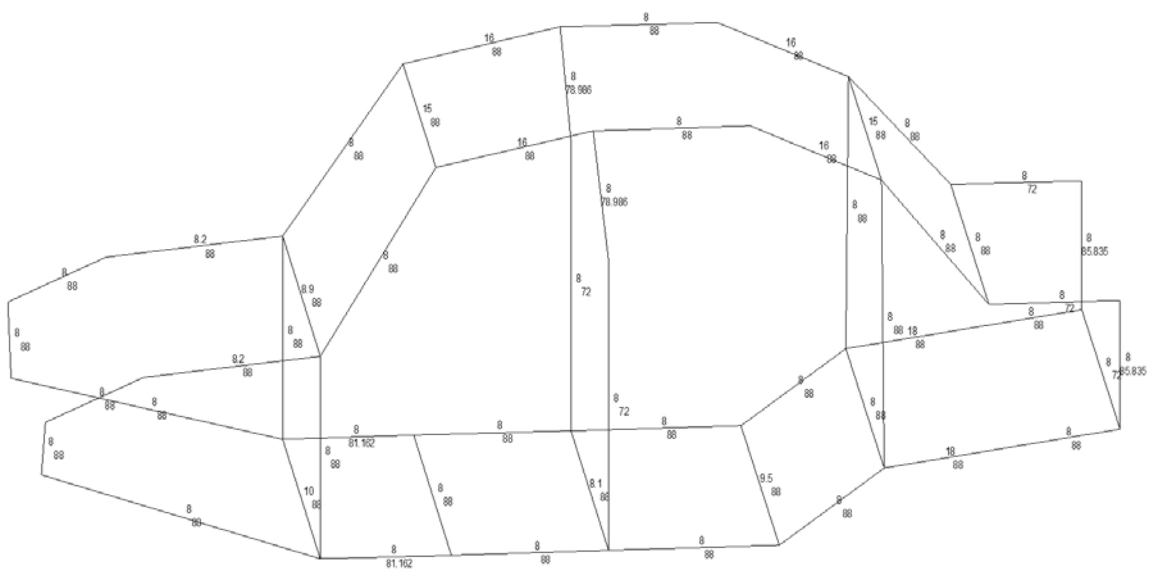

Figure 39: Optimized vehicle structure with section sizes

In order to judge the success of the optimization process the objective function values that were calculated for each iteration are illustrated below.

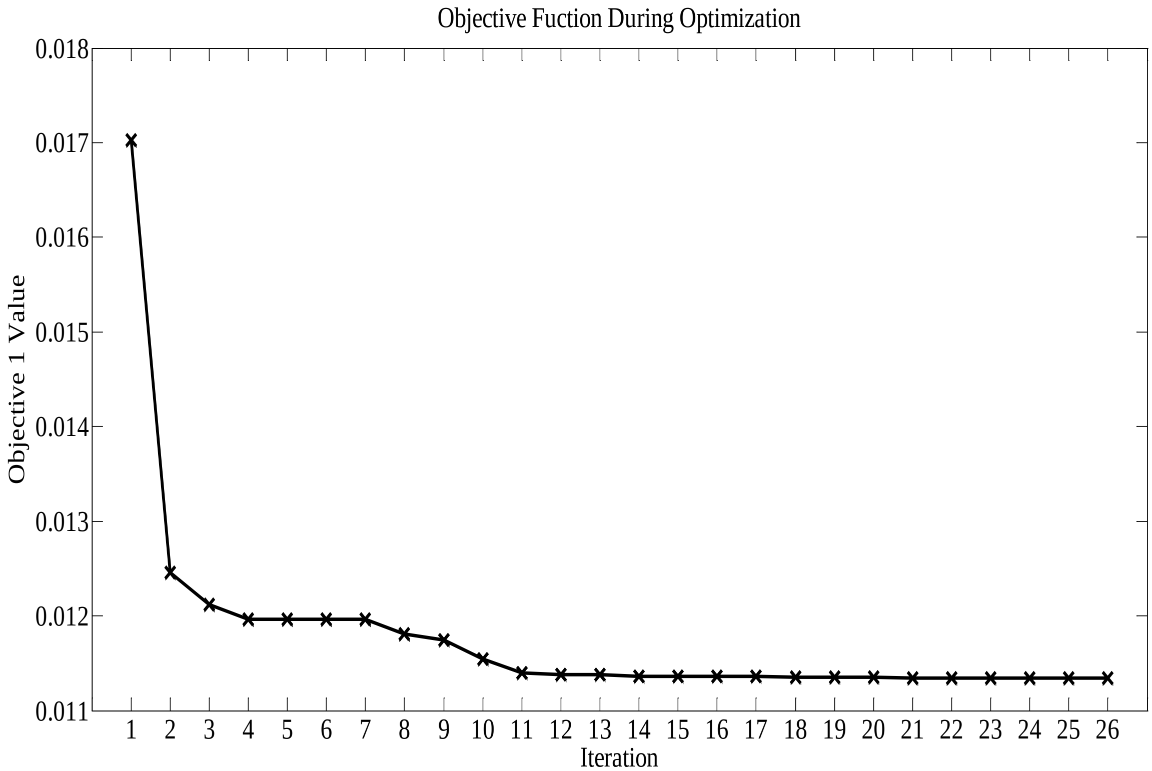

Figure 40: Objective one values during optimization

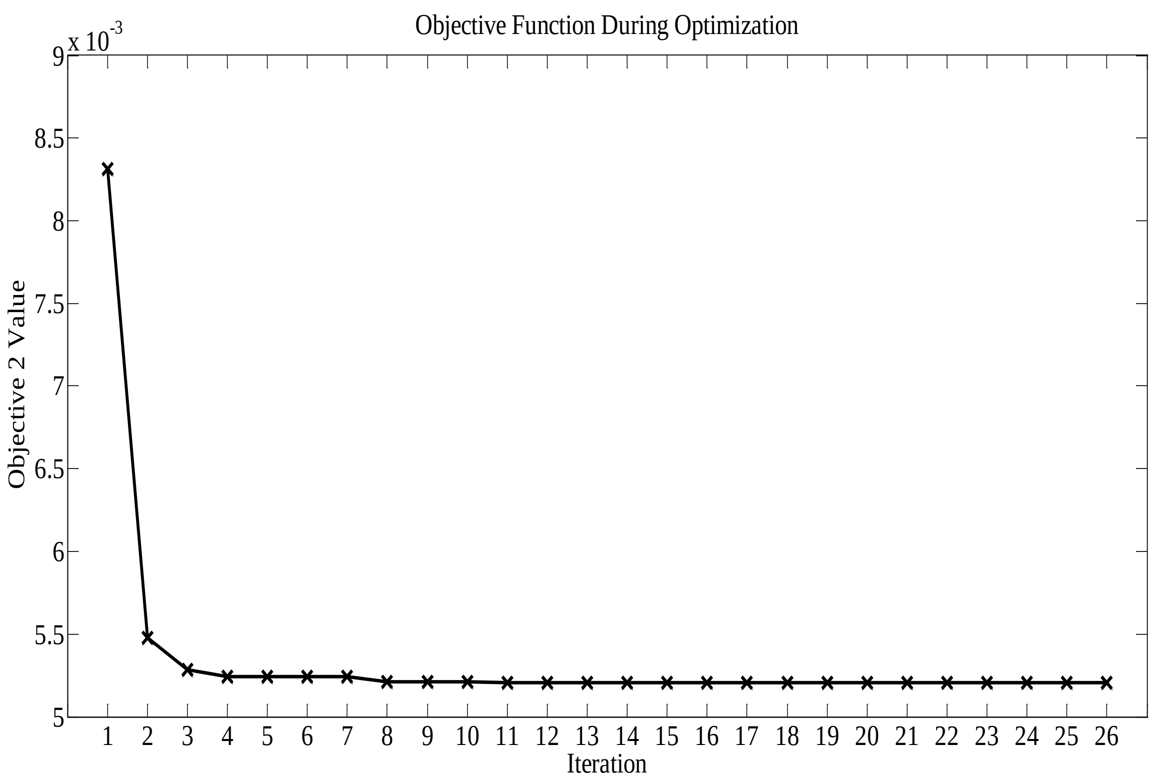

Figure 41: Objective two values during optimization

As can be seen the objective functions were both reduced as a result of the optimization process. The reduction in the objective function relating to bending (Objective 1) was larger because the bending stiffness had a more substantial increase compared to the increase in torsion stiffness. It should also be noted that the values for Objective 2, as shown in Figure 41, converged in fewer iterations than the values for Objective 1. Finally in order to show the relationship between the two objectives they are both plotted on the same graph, as illustrated below in Figure 42.

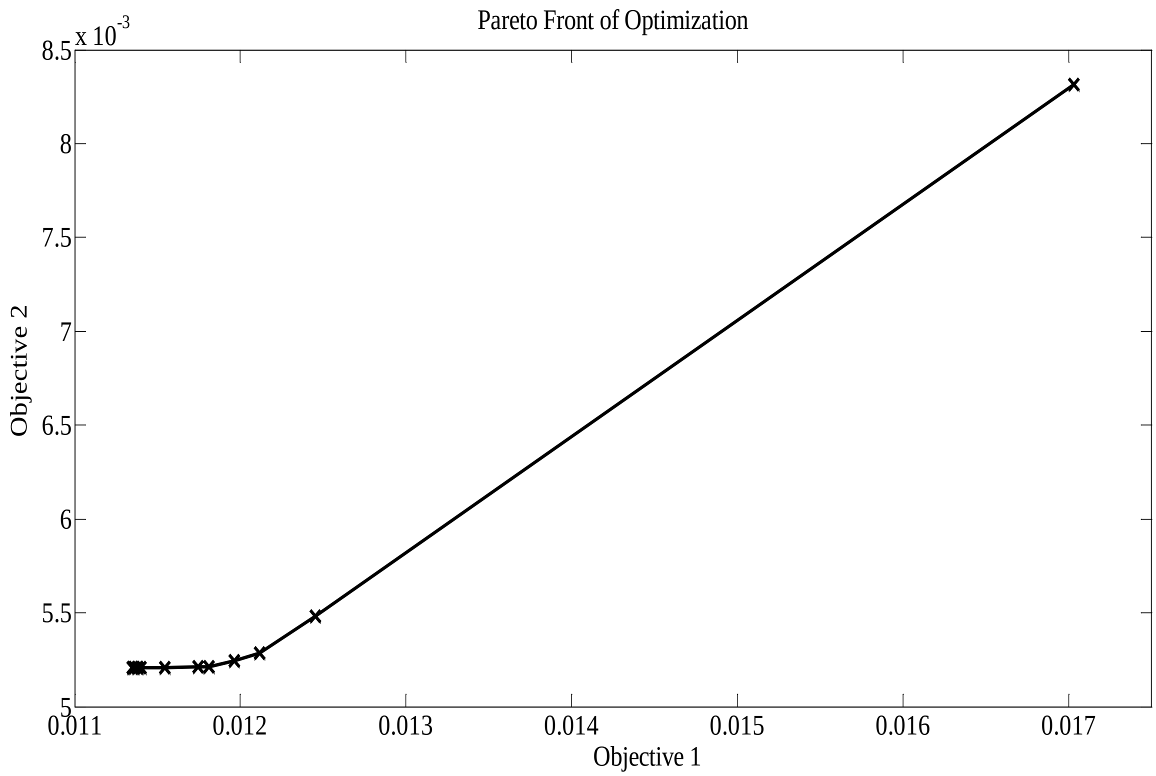

Figure 42: Pareto front of optimization process

In the above figure the left most point represents the optimized values as it is the minimization of both objective functions. The linearity of the graph is due to Objective 2 settling on a constant value quicker than Objective 1, so Objective 2 is a constant value while Objective 1 reduces resulting in a linear portion.

The optimization process achieved the stated goal of reducing the structure weight while maintaining and actually increasing the stiffness. However, the results of the optimization need to be validated to ensure this represents the optimal point.

5.2 Results Validation

The process of validating the optimization results that were obtained involves varying an individual element's section dimensions and checking the corresponding changes in structural properties. The process of varying an element design slightly from optimal should result in a design with larger objective functions, as larger objective functions signify inferior designs. The use of the goal attainment algorithm may produce local solutions only, so all values that are being tested will fall within the specified set. The optimum result obtained here may represent one of many solutions that could exist. The objective of the validation is to ensure that the optimization produced a true optimum design, even if it is only in a specific range. The validation process will vary the side length and thickness of different elements, but ensure that the adjusted dimensions are still within the specified range. This will provide a fair test of the optimization since testing side dimensions beyond the defined limits will require a new optimization program as these values exist outside the allotted solution space. The validation process involves choosing random unique elements as defined in Table 6 and adjusting them based on the results. Element pairs are chosen in order to be consistent with the assumption that mirrored elements will have the same impact on stiffness. Dimensions that lie on the upper bound are reduced while those on the lower bound are increased. The adjustment value was kept constant in magnitude across all tests. The adjustment for the side length was chosen to be 10mm and the adjustment for thickness was chosen to be 3mm. A summary of the results are shown below in Table 11.

Test	Elements	Adjustment	Objective 1 (m)	Objective 2 (rad/m)	% Change Objective 1	% Change Objective 2
1	1, 2	Increase side length and thickness	0.011407725	0.005226645	0.543491735	0.354907164
2	7, 8	Decrease side length, increase thickness	0.011409576	0.005272006	0.559802208	1.225862414
3	13, 14	Decrease side length, increase thickness	0.01140413	0.005242284	0.511803856	0.655178875
4	21, 22	Decrease side length, increase thickness	0.011462458	0.00523974	1.025882922	0.606333141
5	29, 30	Decrease side length, increase thickness	0.011524821	0.005246991	1.575531995	0.745567617
6	47	Increase side length and thickness	0.01154087	0.005165671	1.71697829	-0.815837331
7	37, 38	Decrease side length, increase thickness	0.011668229	0.005226722	2.839476923	0.356392283
8	50	Decrease side length, increase thickness	0.011341908	0.005369879	-0.036594526	3.10508597
9	49	Increase side length and thickness	0.011540605	0.005229042	1.714642008	0.400940106
10	52	Increase side length and thickness	0.01151117	0.005263328	1.45521448	1.059245015
11	3, 4	Decrease side length, thickness unchanged	0.011291243	0.00524716	-0.483135894	0.748811574
12	15, 16	Decrease side length, thickness unchanged	0.011358746	0.005243652	0.111804634	0.68146149
13	19, 20	Decrease side length, thickness unchanged	0.011348354	0.005258322	0.020216539	0.963118815
14	44	Decrease side length, thickness unchanged	0.011291509	0.0052847	-0.480795227	1.469607598
15	48	Increase side length, thickness unchanged	0.011404088	0.005131373	0.511438757	-1.47437236
16	29, 30	Side length unchanged, decrease thickness	0.011532966	0.005209983	1.647320654	0.034984223
17	35, 36	Side length unchanged, decrease thickness	0.01159483	0.005213233	2.192564186	0.097390128
18	39, 40	Side length unchanged, decrease thickness	0.012417342	0.005187284	9.44188336	-0.400848732
19	3, 4	Side length unchanged, increase thickness	0.011520823	0.00525311	1.540297929	0.863060877
20	15, 16	Side length unchanged, increase thickness	0.011436372	0.005235485	0.795970867	0.524633463

Table 11: Results of optimization validation

As can be seen adjusting a design parameter for an individual element increases one or both of the objective functions. An increase in the objective function represents an inferior design in comparison with the optimized structure. It should be noted that there were some scenarios where an objective function was reduced, but the other objective function was increased for that trial and so the design can still be considered inferior.

5.3 Comparison with Commercial Software

As has been stated previously, the objective of this work is to develop an optimized preliminary vehicle structure that provides the best starting point of a more detailed process. The preliminary structural model can be realized using the developed software utilized here; however detailed design activities will require more comprehensive tools. These more comprehensive tools as are typically found in a commercially available program that is capable of performing dynamic analysis such as vibration and crash testing. For this reason the structure that was modeled using the developed software has been created in commercial software so the results of the two programs can be compared. The program chosen to perform the analysis was NX-Nastran. The geometry of the vehicle model was kept constant and a total of four tests were performed. The initial section sizes were tested for both bending and torsion then the optimized sections were tested for both bending and torsion. The finite element model is shown, as it would appear in a commercial solver, in Figure 43.

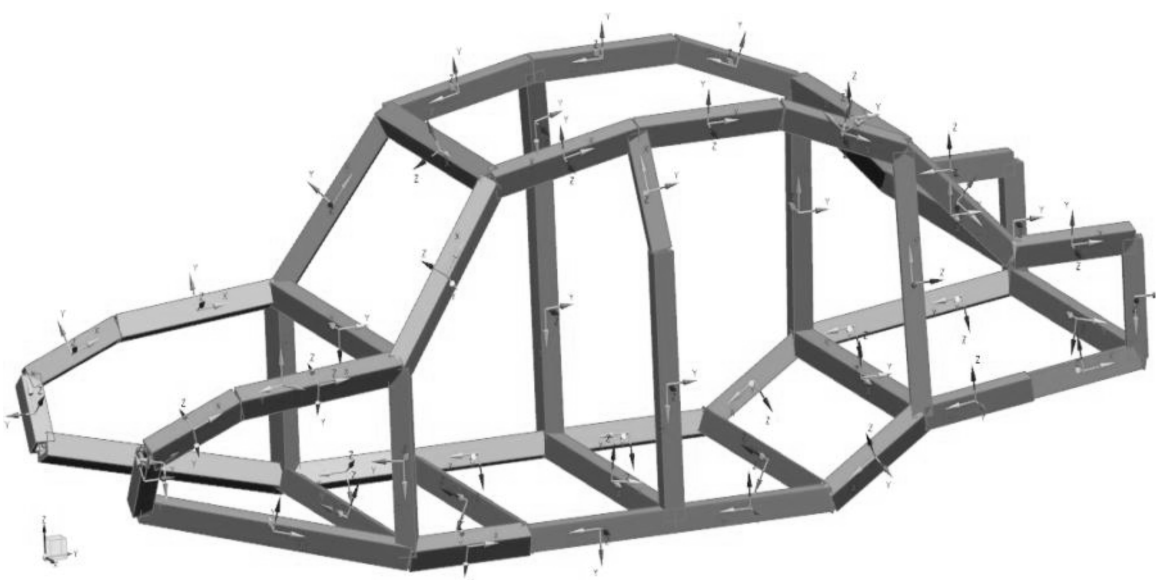

Figure 43: Initial vehicle finite element model from commercial solver

The results of each of the four trials are summarized below in Table 12.

	MATLAB		Nx-Nastran		% Difference	
	Initial	Optimized	Initial	Optimized	Initial	Optimized
Maximum Bending Deflection (mm)	13.2	10.5	13.68	10.9	3.51	3.67
Bending Stiffness (N/m)	738024	767037	710036	730445	3.94	5.01
Maximum Torsion Displacement (mm)	1.8	1.4	1.813	1.394	0.717	0.43
Torsion Stiffness (Nm/rad)	1511743	1671002	1506823	1621103	0.309	3.08

Table 12: Comparison of MATLAB and NX-Nastran results

As can be seen there is some difference between the commercial and the developed program results, however the differences are within the allowable error that is inherent in the utilized finite element algorithms. Further detail regarding the validation of the FEA program that has been developed is provided in Appendix IV.

5.4 Results Analysis

Based on the above validation and optimization results the process was successful. Given the allowed variation in design parameters and the initial condition the resulting optimized results represent the best possible design for the stated goals. The optimization process works by redistributing the material and increases the section sizes that are most critical to the stiffness. The first step is increasing the section side length as this will provide the greatest increase in stiffness. The second step is adjusting the section thicknesses with those sections that are more essential to increasing stiffness having a larger thickness. The overall result of the optimization is a preliminary structure that has had a substantial weight reduction with an increase in stiffness. The sections that have had the greatest increases in size are located closer to the fixed constraint which will greatly increase the stiffness. The stated objectives were achieved and the process can continue by determining suitable plate thicknesses.

Chapter 6

6. Modified SSS Method

6.1 Substructure Analysis

With the beam elements of the vehicle structural model optimized the process of determining suitable plate thicknesses can begin. To relate the work presented here with previous methods of automotive structural analysis this process has been named the modified SSS method as the process involves thin plates. Unlike the SSS method however the plate/beam combination are not reduce to a single plate, but are instead analyzed as a combination. The process begins with dividing the vehicle structure into a series of substructures, with each substructure composing of a series of beams that border the plate component in the middle. A substructure is illustrated below in Figure 44.

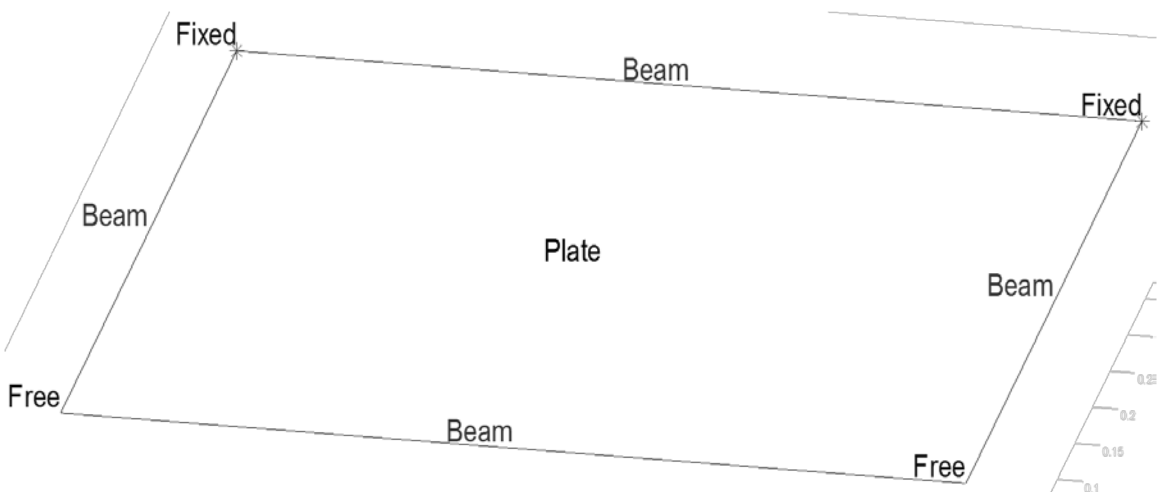

Figure 44: Beam/plate substructure

The different vehicle substructures are shown below in Figure 45.

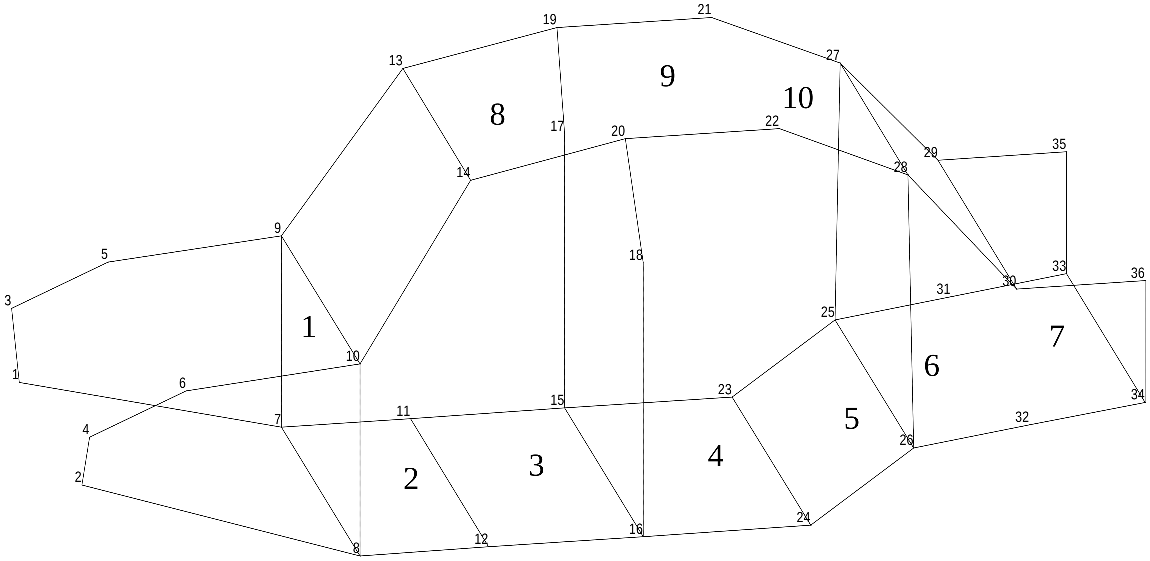

Figure 45: Vehicle substructures

The substructures are more clearly defined below in Table 13.

Plate Number	Bounded By Elements			
1	13	14	43	44
2	9	10	43	45
3	11	12	45	47
4	19	20	47	48
5	29	30	48	49
6	35	36	49	
7	39	40		52
8	17	18	46	
9	25	26		
10	27	28		50

Table 13: Vehicle substructures

Empty entries in the above table represent a missing beam element from the substructure. In these situations the optimization assigns null values for the section properties and the algorithm continues with the optimization.

6.2 Plate Optimization

The plate thickness is calculated by utilizing an optimization process for each substructure. The optimization uses the same goal attainment algorithm used for the beam structure as a multi-objective optimization is still required. The objective of using the optimization is to maintain the structure weight and stiffness that resulted from the optimization while including the plate components in the structure. The optimization parameters are kept the same as before, however the optimization has a known goal in the initial substructure weight. Substructure analysis is used to break the vehicle model into smaller structures so that they can be analyzed and optimized within the numerical software. The substructure will utilize beam elements around the plate component while the sheet will use the plate element that was described previously. Each beam element in the substructure is allowed a ten percent reduction in each section dimension. The optimization will be able to slightly reduce the beam dimensions to account for the plate structure, with the addition of the plate counteracting any increase in deflection. The plate thickness is uniform for each substructure and can vary as indicated below.

	Thickness (mm)	Thickness (gauge)
Minimum	0.60706	24
Maximum	6.07314	1

Table 14: Range of plate thicknesses

The thickness values shown above in Table 14 have a large amount of allowed variation in order to represent all possible standard thicknesses. It is expected that a typical thickness would be in the 24-18 gauge as these values are typically found in automotive structures [57].

The substructures are loaded in a manner similar to a cantilevered beam with the portion of the substructure that is towards the rear of the vehicle fixed. The loads are applied at the free end and are determined based on the internal loads that result from a bending and torsion analysis of the optimized beam structure. The load condition of a typical substructure is shown below in Figure 46.

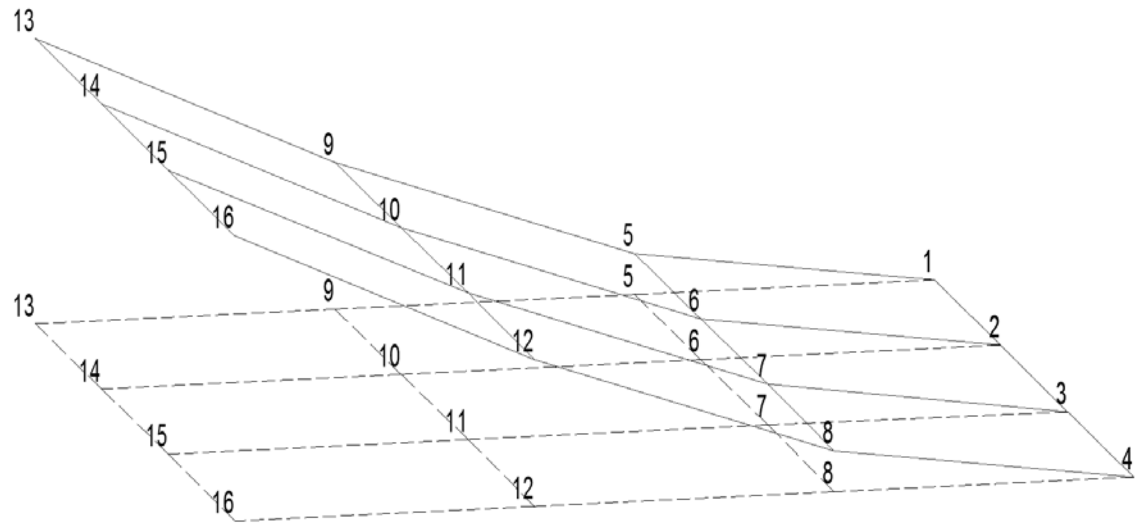

Figure 46: Plate/beam substructure

As can be seen the loads are applied to the free end at nodes 13 and 16. The other end (nodes 1-4) is fixed. The plate has nine elements arranged in a three by three pattern. Dividing the plate into smaller elements requires splitting each beam element into three elements. This mesh condition was chosen as it provided higher accuracy than a single element, with a faster computation time than using a larger number of elements. Further information regarding this selection is shown in Appendix V.

6.3 Substructure Optimization Results

The substructure weights that result from this optimization process are shown below.

Substructure	Initial Weight (N)	Final Weight (N)	% Change
1	934.0776811	934.9528168	0.093689826
2	836.004276	836.6834023	0.081234792
3	831.3175387	832.1346962	0.098296675
4	899.8936079	900.7972153	0.100412687
5	808.6046517	808.8590387	0.031459997
6	661.5415193	662.1530043	0.092433358
7	413.997696	414.6089011	0.147634893
8	864.3126006	865.0189541	0.08172431
9	236.570112	237.2765498	0.298616682
10	793.341567	793.4837977	0.017928054

Table 15: Weight change of substructures

As can be seen there is a slight weight increase in each substructure, however this change in comparison with the total structure weight is insignificant. The final beam element dimensions are shown below in Figure 47 and Figure 48.

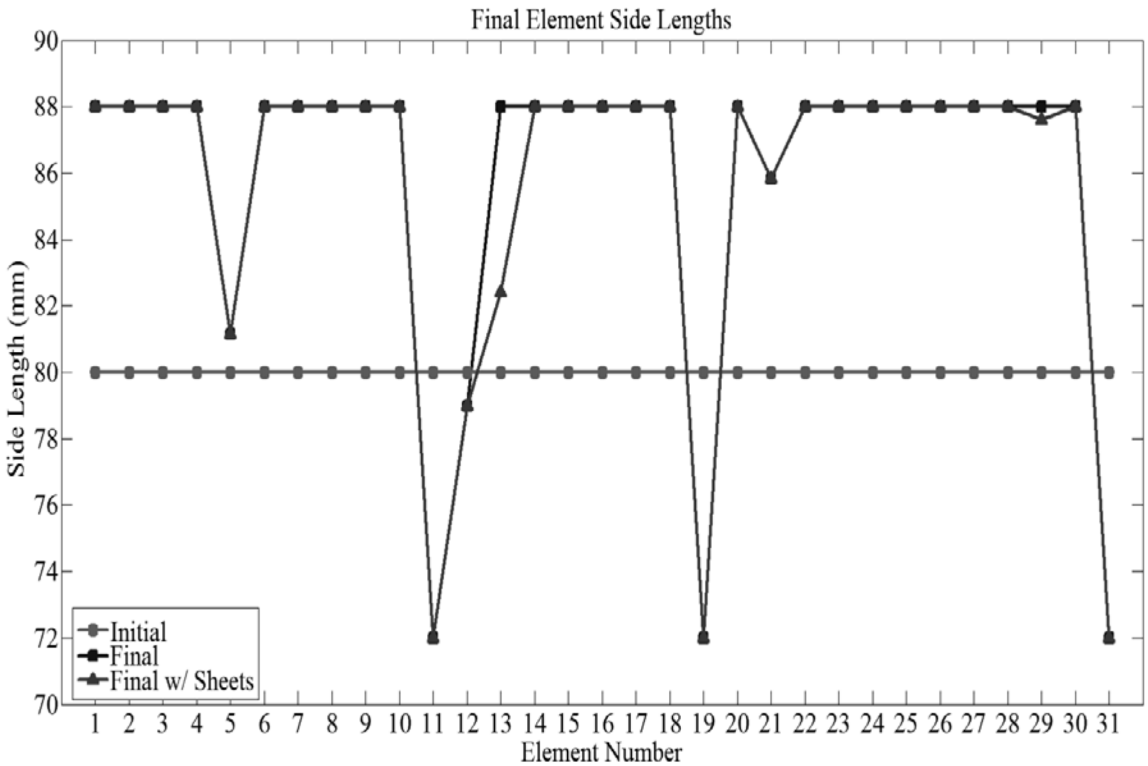

Figure 47: Final element side lengths

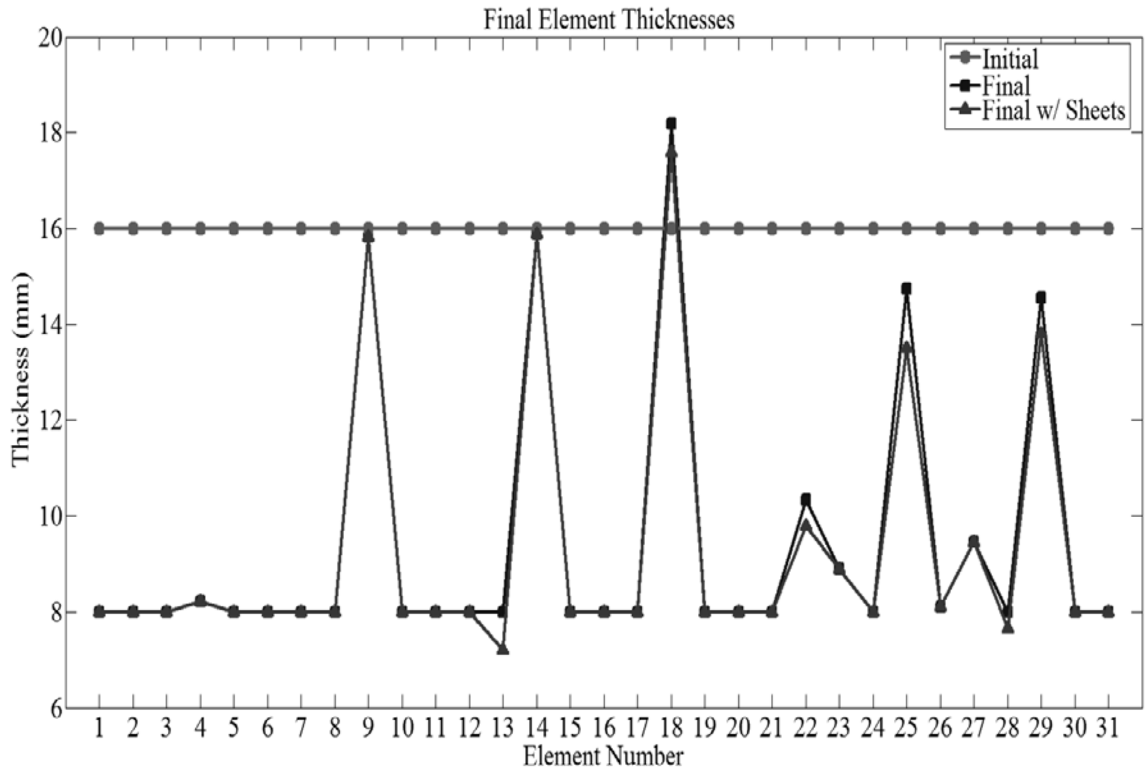

Figure 48: Final structure thicknesses

The plate thicknesses that resulted from the optimization process are summarized below.

Plate	Thickness (mm)
1	0.620752946
2	0.60706
3	0.608724024
4	0.621295302
5	0.60706
6	0.60706
7	0.60706
8	0.60706
9	0.60706
10	0.60706

Table 16: Plate thicknesses

The final step will be transferring the information of the final vehicle structure, including the newly added plate elements, to the commercial software as though it were about to undergo a detailed design process. The finite element model is shown below.

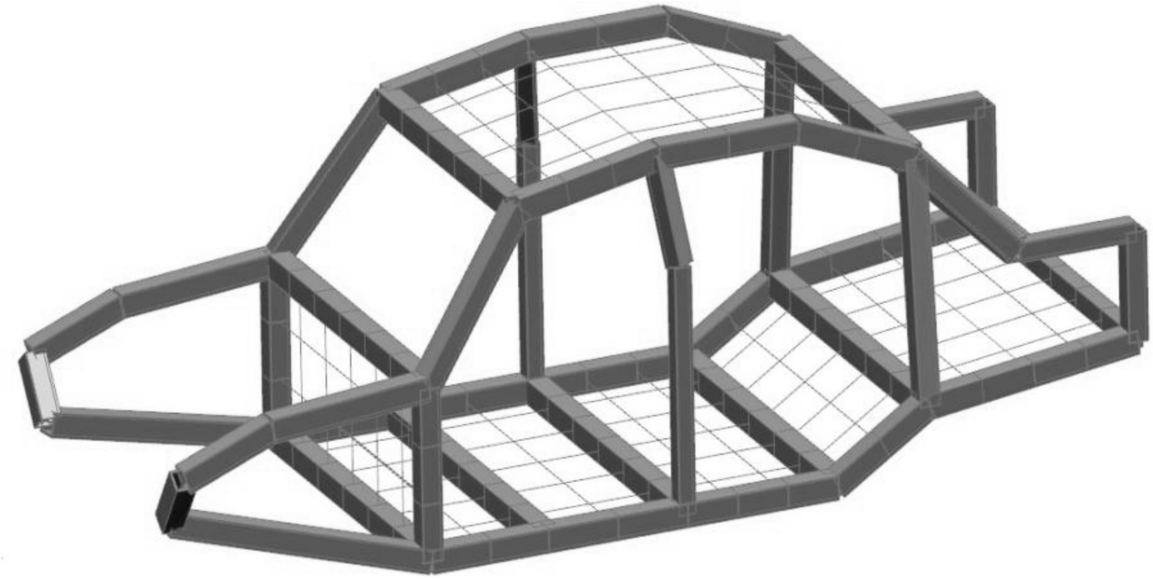

Figure 49: Final vehicle structural model

As can be seen the final structural model features a combination of beams and plates, with the beams the primary structural component. The structure was then analyzed using the commercial program once again to ensure that the structural characteristics were maintained while the weight was not increased with the addition of the plates. The results of the analysis are summarized below in Table 17.

	Final Model	Final Model w/ Plates
Bending Displacement (mm)	10.94	10.92
Torsion Displacement (mm)	1.394	0.5049
Weight (N)	8709.7	9086.5

Table 17: Final structural model characteristics

As can be seen there is a slight increase in the weight, however this is expected given the limited amount of beam section reduction that was available. The addition of the plates also increases the stiffness, particularly the torsion stiffness. The structural model that has been developed is now suitable for the detailed design process. The deformed model due to the applied loads is shown below in Figure 50 and in Figure 51.

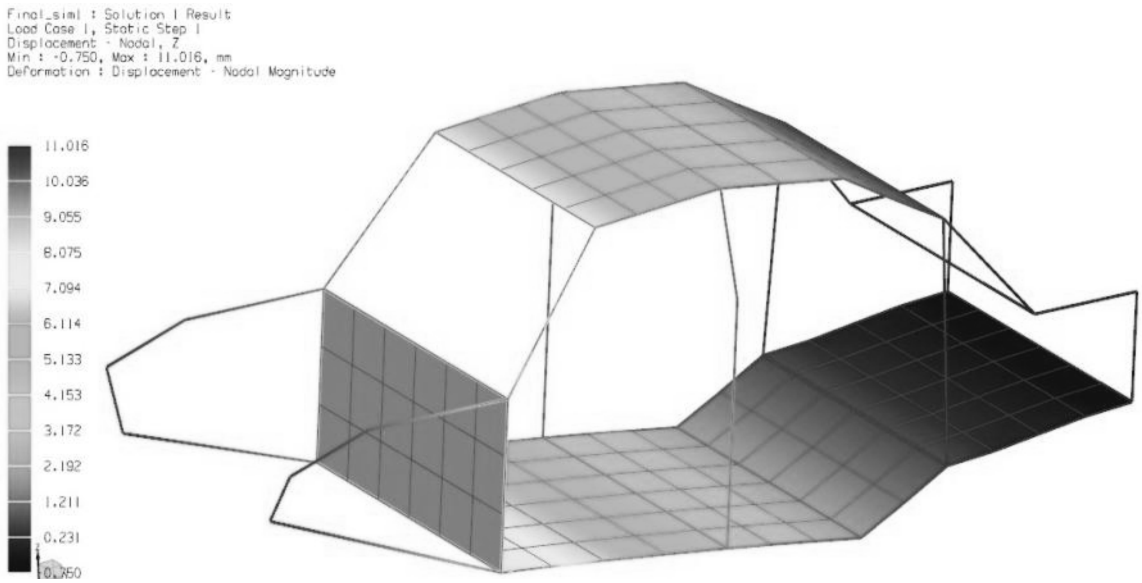

Figure 50: Final model under bending load

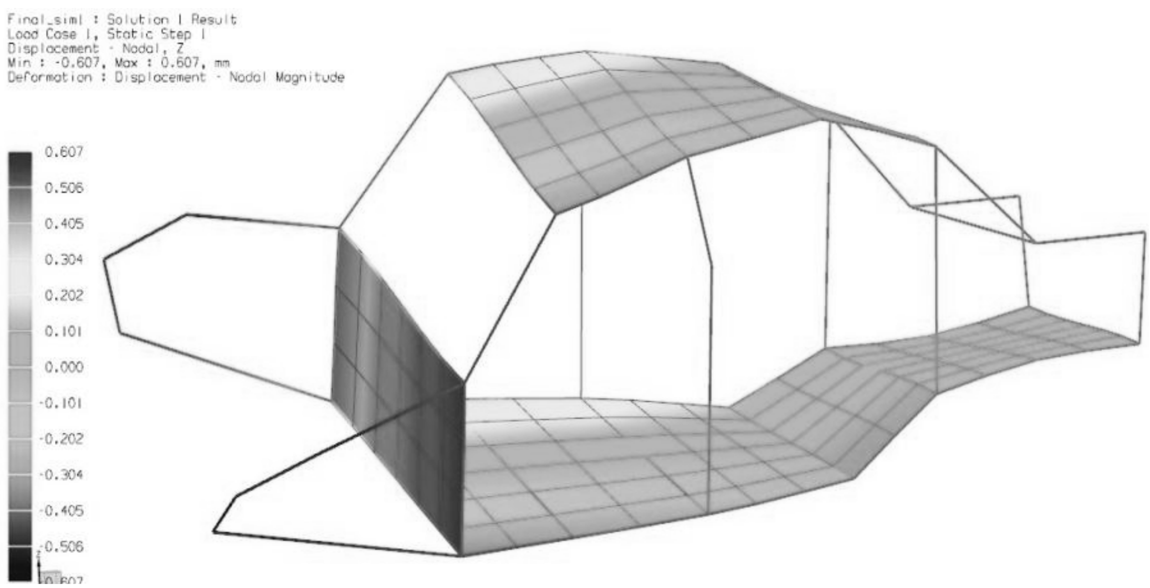

Figure 51: Final model under torsion load

Chapter 7

7. Conclusion and Future Work

7.1 Conclusion

In conclusion the goal of developing an optimized preliminary vehicle structural model was successful. The process began with using beam elements to develop the vehicle geometry. An initial design is developed using uniform square beam section dimensions. The loads applied are static and based on assumed component loads and the structure weight. They are applied at the front of the vehicle as a suspension load while the rear suspension is held fixed during the process. After the initial structural characteristics and weight are determined an optimization process is implemented. The initial characteristics are used as the baseline for the optimization, with the objective being to minimize the weight to stiffness ratio. Two stiffness values are used, bending and torsion, and as a result the optimization process is a multi-objective optimization. The section side lengths and thickness are used as design parameters for the optimization process. The result of the optimization was a structural model that had a significant reduction in weight and slight increases in torsion and bending stiffness. The next stage of the process was to determine suitable plate thicknesses to form the complete structural model.

The estimation of plate thicknesses was conducted using substructure analysis and optimization. The vehicle structure was divided into a number of substructures with each substructure featuring four optimized beam elements bordering a single plate component. To determine the thickness of the plates another optimization process was implemented.

The objective of optimization was to maintain the original substructure weight, but with the plate component included. In order to accommodate the plate component the beam elements were allowed a reduction in section size with the assumption that the inclusion of the plate component will provide additional stiffness to counteract the applied loads. Following the analysis of all substructures the structural model was then checked using commercial software, as would be done prior to detailed design, to ensure the structure stiffness and weight were maintained following the addition of plate components. The final structural model will then be ready for detailed design activities.

The use of a numerical finite element method and optimization allowed the structure analysis to be conducted quickly which is desirable in the early stage of the design process when rapid iterations allow for a shorter design time. Following the development of the preliminary model the square beam element section properties can be transferred to an existing section library.

The results of the substructure optimization process are thinner plates than may be required in the final structural design; however the detailed design process will perform a wider array of analysis which may result in thicker plates being required. The results presented here represent the optimal design for a static loading condition.

7.1.1 Discussion on Fuel Economy

As has been mentioned earlier in this work the optimization of an automotive structure can produce substantial increases in the vehicle fuel economy. A sample estimate of the potential increase in fuel economy is presented here using an existing sedan vehicle. The vehicle used for this calculation is described below in Table 18 [58,59].

2007 Mazda 6 Sedan	
Engine	2.3L, 4 Cylinder
Transmission	5-speed Automatic
EPA Combined Fuel Economy (MPG)	23
Curb Weight (lbs)	3091

Table 18: Vehicle information [58,59]

To perform the calculation it is assumed the curb weight has been reduced by the same amount as the optimized vehicle structure used in this work and as a result the reduction in weight will be considered as 30.7%. Using this value as a percent of weight reduction the total amount of weight removed is found to be 948.94lbs. Using the correlation shown in Figure 3 this reduction in weight will increase the fuel economy by 4.74% which is a revised combined fuel economy of 24.1MPG. It should be noted that the increase in fuel economy presented here is based on the baseline engine shown in Figure 3, but if the engine is considered as part of a comprehensive design process the downsized engine can be used instead. Based on the data shown in Figure 3 the increase in fuel economy for a weight reduction of 948.94lbs will be 16.13% which corresponds to a combined fuel economy of 26.71MPG.

7.2 Future Work

Automotive structural design is a complex task with a number of different aspects. The work presented here is just one of those aspects and continuation of this work would incorporate other aspects into a wider optimized design process. One of the main improvements to the process would be incorporating a beam section shape optimization. The shape optimization could be built off existing work that utilizes general parametric section and optimizes the shape based on the loading conditions being considered [28]. Along with shape optimization a program of materials optimization could also be incorporated. A wider range of materials, such as reinforced polymers and lightweight alloys, are now available for automotive structural design and incorporating these can offer further improvements.

The second improvement would be within the finite element program that was developed. Currently the plate thickness must be estimated using substructure analysis as combining different elements is a difficult task within the numerical finite element program. Future work would incorporate the plate elements as part of the vehicle structure optimization process. Another improvement to the finite element program would be making it more general so that changes to the geometry are simpler to implement. This would be advantageous as it would save time when adding or removing elements which may be required based on an initial analysis or optimization process. Adding extra elements could be used to increase the global stiffness, or reduce deflections in a localized area and removing elements may be useful to further reduce the weight if the structure is over constrained.

Another extension of this work would be in the analysis of the structure, specifically NVH characteristics, dynamic performance and crashworthiness. The noise and vibration of a vehicle structure is an important characteristic and while increasing the structure stiffness can mitigate these effects it is beneficial to have an understanding of the vibration characteristics of a structure. It is also beneficial to know how the vehicle structure reacts during driving manoeuvres such as accelerating or cornering. Lastly a method to analyze the crashworthiness of the vehicle structure could be developed. Of course this aspect of the design process often requires highly detailed structure models to produce accurate reliable results.

Finally the process presented here could be applied to an existing structural design. The use of this process on an existing structural design would remove some of the assumptions or generalizations that were required to complete this work without a predecessor model. The use of an existing structure would narrow the range of section sizes available as knowledge about the manufacturing constraints would be available. Lastly the initial condition of the optimization would feature beam elements with fluctuation in the sections sizes instead of the uniform sizes used here. The use of varied initial section sizes could allow for greater improvement from the optimization as the allowed section sizes would be based on existing design knowledge.

References

[1] J. K. Shin, K. H. Lee, S. I. Song, and G. J. Park, "Automotive door design with the ULSAB concept using structural optimization," Case Study 10.1007/s00158-002-0189-z, 2002.

[2] W. Zeiler, P. Savanovic, and E. Quanjel, "Design decision support for the conceptual phase of the design process," in *International Association of Societies of Design Research*, Hong Kong, 2007.

[3] P. G. Ranky. (2005, September) Manufacturing Systems Syllabus.

[4] A. Crocombe, E. Sampe, and A. Somiotti, "Chassis torsional stiffness: analysis of the influence on vehicle dynamics," in *SAE 2010 World Congress & Exhibition*, 2010.

[5] A. R. George and W. B. Riley, "Design, analysis and testing of a formula SAE car chassis," in *SAE Motorsports Engineering Conference and Exhibition*, 2002.

[6] E. H. Law, S. Raju, P. H. Soni, and L. L. Thompson, "The effects of chassis flexibility on roll stiffness of a winston cup car," in *Motorsports Engineering Conference Proceedings*, 1998.

[7] A. Casadei and R. Broda, "Impact of vehicle weight reduction on fuel economy for various vehicle architectures," The Aluminim Association, 2008.

[8] G. Maeder, "Lightweight vehicle design: contribution to fuel savings," Renault, 2000.

[9] S. S. Rao, *Mechanical Vibrations*, 4th ed. Singapore: Pearson Prentice Hall, 2004.

[10] F. Kagnici, "Vibration induced fatigue assessment in vehicle development process," *World Academy of Science, Engineering and Technology*, no. 64, pp. 88-93, April 2012.

[11] D. P. Taylor, "Buildings: design for damping," Taylor Devices, Inc., North Tonowanda, Presentation 1999.

[12] L. L. Thompson, S. Raju, and E. H. Law, "Design of a winston cup chassis for torsional stiffness," in *Motorsports Engineering Conference Proceedings*, Dearborn, 1998.

[13] S. S. Sane, G. Jadhav, and H. Anandaraj, "Stress analyis of a light commercial vehicle chassis by FEM," Piaggio Vehicles Private Limited,.

[14] C. Karaoglu and N. S. Kuralay, "Stress analyis of a truck with riveted joints," *Finite Elements in Analysis and Design*, vol. 38, pp. 1115-1130, October 2001.

[15] G. H. Kim, K. Z. Cho, I. B. Chyun, and G. S. Choi, "Dynamic stress analysis of vehicle frame using a nonlinear finite element method," *KSME International Journal*, vol. 17, no. 10, pp. 1450-1457, July 2003.

[16] L. Wang, P. K. Basu, and J. P. Leiva, "Automobile body reinforcement by finite element optimization," *Finite Elements in Analysis and Design*, vol. 40, pp. 879-893, April 2003.

[17] C. Yanhong and Z. Feng, "The finite element analysis and the optimization design of

the Yj3128-type dump truck's sub-frames based on ANSYS," *Procedia Earth and Planetary Science*, vol. 2, pp. 133-138, 2011.

[18] C. H. Kim, A. R. Mijar, and J. S. Arora, "Development of simplified models for design and optimziation of automotive structures for crashworthiness," *Structural Multidiscplineary Optimization*, vol. 22, pp. 307-321, November 2001.

[19] J. Happian-Smith, Ed., *An Introduction to Modern Vehicle Design*. England: Butterworth-Heinemann, 2002.

[20] B. W. Shiu, D. Ceglarek, and J. Shi, "Flexible beam-based modeling of sheet metal assembly for dimensional control," *Transactions of NAMRI/SME*, pp. 49-54, 1997.

[21] D. Mundo et al., "Simplified modeling of joints and beam-like structures for BIW optimization in a concept phase of the vehicle design process," *Finite Elements in Analysis and Design*, vol. 45, pp. 456-462, February 2009.

[22] S. Donders et al., "A reduced beam and joint concept modeling approach to optimize global vehicle body dynamics," *Finite Elements in Analysis and Design*, vol. 45, pp. 439-455, February 2009.

[23] D. C. Lee and J. I. Lee, "A structural optimization design of an aluminum-intensive vehicle," *Proceedings of the Institution of Mechanical Engineers*, vol. 217, pp. 771-779, May 2003.

[24] C. W. Kim and J. H. Kim, "A method of primitive structural design by stick model," *SAE Technical Paper*, pp. 533-541, 1991.

[25] S. J. Kang and J. H. Choi, "Design sensitivity analysis of body structure using skeleton model," *SAE Technical Paper*, November 1991.

[26] N. M. K. Lee, T. Pine, and T. B. Jones, "Automotive box section design under torsion," *Proceedings of the Institution of Mechanical Engineers*, vol. 214, pp. 347-485, August 1999.

[27] T. M. Cameron, A. C. Thirunavukarasu, and M. E.M. El-Sayed, "Optimization of frame structures with flexible joints," *Structural and Multidiscpliary Optimization*, vol. 19, pp. 204-213, January 2000.

[28] M. Yoshimura, S. Nishiwaki, and K. Izui, "A multiple cross-sectional shape optimization method for automotive body frames," *Journal of Mechanical Design*, vol. 127, pp. 49-57, January 2005.

[29] L. L. Thompson, J. K. Lampert, and E. H. Law, "Design of a twist fixture to measure the torsional stiffness of a winston cup chassis," in *Motorsports Engineering Conference Proceedings*, Dearborn, 1998.

[30] J. C. Brown, S. T. Serpento, and A. J. Robertson, *Motor Vehicle Structures Concepts and Fundamentals*. Woburn, United States of America: Reed Elsevier, 2002.

[31] Ford Explorer and Sport Trac Frame/Body Cushions.

[32] E. Grabianowski. How Stuff Works. [Online]. http://auto.howstuffworks.com/lotus-elise3.htm

[33] GRECAV Automotive. GRECAV Safety. [Online]. http://www.grecav.it/images/pagine/SICUREZZA/Frame.jpg

[34] ULSAB. (2012, March) flickr.

[Online]. http://www.flickr.com/photos/worldautosteel825/7024676553/in/set-72157629689513391

[35] D. L. Logan, *A First Course in the Finite Element Method*, 4th ed. United States of America: Thomsen, 2007.

[36] J. N. Reddy, *Theory and analysis of elastic plates and shells*, 2nd ed. Boca Raton, United States of America: CRC Press, 2007.

[37] K. Lange, *Optimization*. Los Angeles, United States of America: Springer Verlag, 2004.

[38] A. Antoniou and W.S. Lu, *Practical Optimization Algorithms and Engineering Applications*. New York, United States of America: Springer Science+Business Media, 2007.

[39] F. W. Gembecki, "Vector optimization for control with performance and parameter sensitivity indices," Case Western Reserve University, Cleveland, Ph.D. Dissertation 1974.

[40] J. Dobes, J. Michal, V. Panko, and L. Pospisil, "Reliable procedure for electrical characterization of MOS-based devices," *Solid-State Electronics*, vol. 54, pp. 1173-1184, June 2010.

[41] R. K. Brayton, S. W. Director, G. D. Hachtel, and L. Vidigal, "A new algorithm for statistical circuit design based on quasi-Newton methods and function splitting," *IEEE Transactions on Circuits and Systems*, vol. 26, pp. 784-794, September 1979.

[42] P. J. Fleming and A. P. Pashkevich, "Computer aided control system design using a multi-objective optimisation approach," in *Control Conference*, Cambridge, 1985, pp. 174-179.

[43] A. C.W. Grace, "Computer-aided control system design using optimization techniques," University of Wales, Gwynedd, Ph.D. Dissertation 1989.

[44] S. P. Han, "A globally convergent method for nonlinear programming," *Journal of Optimization Theory and Applications*, vol. 22, no. 3, pp. 297-309, July 1977.

[45] M. J.D. Powell, "A fast algorithm for nonlinearly constrained optimization calculations," *Numerical Analysis*, vol. 630, pp. 144-157, 1978.

[46] S. Tebby, A. Barari, and E. Esmailzadeh, "Multi-Objective Optimization of Vehicle Structure under Various loading Condition Using Simple Structural Beam Frame Approach ," in *Proceedings of the 2012 CSME CONGRESS*, Winnipeg, 2012.

[47] P.l Du Bois et al., *Vehicle Crashworthiness and Occupant Protection*, Priya Prasad and Jamel E. Belwafa, Eds. Southfield, United States of America: American Iron and Steel Institute, 2004.

[48] R. Chi and J. Wang, "Impact of joint on car body stiffness at concept design stage," in *Conference on Consumer Electronics, Communications and Networks*, 2011, pp. 406-409.

[49] L. Berger, M. Lesemann, C. Sahr, S. Hart, and R. Taylor, "SuperLIGHT-CAR the multi-material car body," in *LS-DYNA Conference*, 2009.

[50] H. H. Braess and U. W. Seiffert, *Handbook of Automotive Engineering*. United States of America: SAE International, 1005.

[51] M. Smith. (2010, October) Boron Extrication. [Online]. http://boronextrication.com/tag/mercede-benz/

[52] R. C. Hibbeler, *Mechanics of Materials*, 8th ed. United States of America: Pearson Prentice Hall, 2010.

[53] Indian Institute of Technology. Solid Mechanics. [Online]. http://www.iitg.ernet.in/scifac/qip/public_html/cd_cell/chapters/CD-Cell.pdf

[54] Queensland Transport. (1992) Code of Practice Light Vehicle Reductions. [Online]. http://www.tmr.qld.gov.au/~/media/2d5a8c4c-62c6-4535-9d22-410360e6523e/codeofpracticelightvehiclesreductionspart8.pdf

[55] A. M. Rubinov, X. Q. Yang, and B. M. Glover, "Extended Lagrange and penalty functions in optimization," *Journal of Optimization Theory and Applications*, vol. 111, no. 2, pp. 381-405, November 2001.

[56] B. W. Kort and D. P. Bertsekas, "A new penalty function method for constrained minimization ," in *Symposium on Adaptive Processes*, 1972, pp. 162-166.

[57] J. A. Snyman, N. Stander, and W. J. Roux, "A dynamic penaltyfunctionmethod for the solution of structural optimization problems," *Applied Mathematical Modelling*, vol. 18, no. 8, pp. 453-460, August 1994.

[58] American Iron and Steel Institute Consortium, "Ultralight Steel Auto Body," American Iron and Steel Institute, Washington, 1998.

[59] (2013, January) EPA Fuel Economy.

[60] (2013, January) Edmunds.

Appendix I- SSB Optimization for Bending Stiffness using Circular Elements

Proceedings of the ASME 2012 International Design Engineering Technical Conferences &
Computers and Information in Engineering Conference
IDETC/CIE 2012
August 12-15, 2012, Chicago, IL, USA
DETC 2012-71288

Analysis and Optimization of Automotive Structure's Bending Stiffness Using Beam Elements

Steven Tebby
Faculty of Engineering and Applied Science, University of Ontario Institute of Technology, Oshawa, ON, Canada
Steven.Tebby@uoit.ca

Ahmad Barari
Faculty of Engineering and Applied Science, University of Ontario Institute of Technology, Oshawa ON, Canada
Ahmad.Barari@uoit.ca

Ebrahim Esmailzadeh
Faculty of Engineering and Applied Science, University of Ontario Institute of Technology, Oshawa, ON, Canada
ezadeh@uoit.ca

ABSTRACT

Optimum design of vehicle's structure is an important task in its development. The structure of a vehicle plays complex interactions with the other vehicle components and has significant impact on the performance of the vehicle. Structural design is usually completed by a complex iterative process. The design changes at late design stages effect many other parameters in the design of vehicle. Therefore, it is highly valuable for designers to employ simple but effective analyses at the early design stages. One method of analysis is using Simple Structural Surfaces. This method utilizes planar sheets to model the vehicle structure and allows the determination of the forces in each sheet. The major drawback of this method is its inability to easily determine deflections in a structure. To overcome this drawback a method that uses beam elements to represent the vehicle structure has been developed. This method uses a numerical finite element method and is able to determine unknown deflections and reaction forces as well as the internal loading on each member. This method can also be readily adapted to allow for parametric optimization for bending stiffness. The parameters associated with each beam element are the length, orientation and the beam characteristics of beams' cross-sectional area and moment of inertia. An automated process is developed that manipulates some of these parameters to develop a structure that will have the greatest bending stiffness.

INTRODUCTION

The design of an automotive structure is critical to the overall performance of a vehicle. The structure of the vehicle is important to ensure it can satisfactorily carry the applied loads that occur [1]. The structure of a vehicle interacts with all other vehicle sub-components and has a complex influence one their functionality. Due to the structural design complexity, design process is traditionally conducted by trial and error and is subject to numerous changes even in the latest stages of the design process. However, some of the changes in the design of structure may cause significant re-design of the other vehicle components and this may become very costly. Typically, it is much more desired to maximize design changes during the early design stages and particularly before the detailed design activities [2]. However, employing a very comprehensive and detailed process of analyses at the conceptual design stage, when there is a greater range of design choices still available, may become very time consuming and computationally expensive. Therefore, it is very valuable for designers to employ simple but effective analyses at the early design stages.

One of the most important criteria in automotive structural design is structural stiffness. The chassis stiffness, both in bending and torsion, has significant impacts on the ride and comfort characteristics as well as the overall dynamic vehicle performance [3-5]. For this reason the stiffness values are used as design parameters to be optimized. Increasing the structural stiffness is highly critical in enhancing the vehicle's performance. However, due to economic constraints increasing the vehicle stiffness by increasing the structural weight is not recommended. An optimized solution is desired that maximizes structural stiffness while keeping the structural weight as low as possible.

Being able to efficiently analyze the body structure during the conceptual design stages is important to determining the performance characteristics. A primary method used to analyze the structure is the method of Simple Structural Surfaces (SSS) [1], [6]. This method utilizes planar sheets to model the body structure. The SSS method can be used to determine the load-paths present in a body structure, but is unable to analyze an indeterminate static loading condition. Alternatively, the method utilized in this work, uses beam-frame elements to represent the structure as an equivalent space frame. The approach of using beam elements has the advantage of being able to determine displacements due to these forces by using the Finite Element Method (FEM). The use of the beam-frame finite element model can be used for basic analysis of a vehicle structure and as an initial estimate of some important vehicle parameters such as bending and torsion stiffness as well as some vibration characteristics. Using analogy of names, this method is referred to in this paper as the Simple Structural Beam (SSB) method. This paper presents an approach to optimize design parameters of a SSB model to optimize the bending stiffness of a conceptual model. The optimization of the model will improve the stiffness to weight ratio compared with an initial model that has been used in previous analysis.

An SSS model has been previously analyzed using commercial finite element software [6]. A diagram of this geometry is shown below in Fig. 1. The deflection results that were produced using this model are shown in Fig. 2.

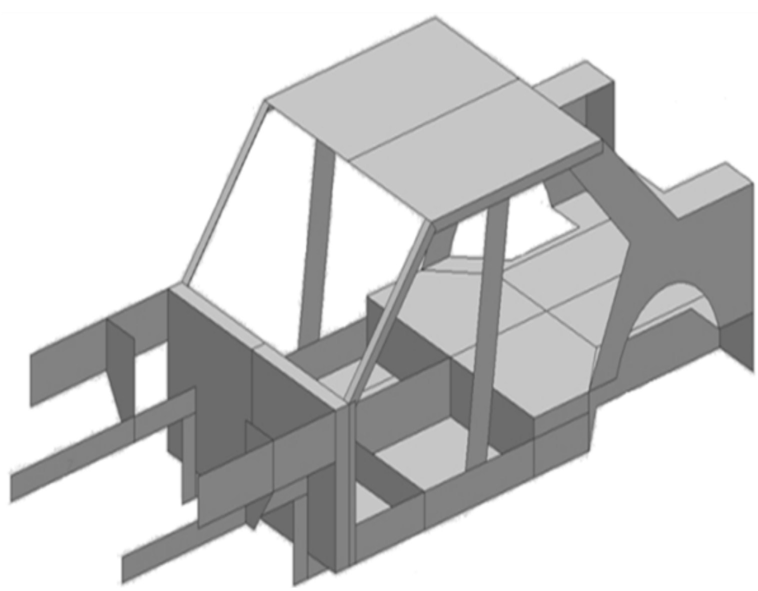

FIG. 1: SSS MODEL [6]

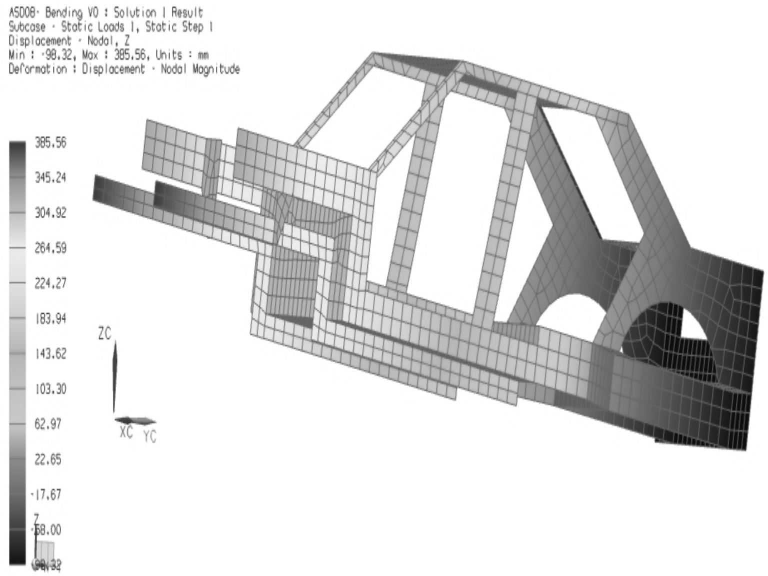

FIG. 2: DEFLECTION OF SSS MODEL [6]

BACKGROUND

Both SSS and SSB methods can be used to determine forces that are present throughout the structure and assist with preliminary design decisions. A brief explanation of both of these analysis methods is presented here as background information. Another important aspect of this structural analysis is the utilized finite element method that is also briefly presented here.

The Simple Structural Surface method uses planar surfaces to model a structure. It was developed initially to analyze the load path of a vehicle [1]. The surfaces are able to react in plane loads only and transfer the forces from one surface to another via edge shear loads. The original intent of this method is to analyze the structure and determine a suitable load path. This method of analysis has a few limitations which restrict the benefits however as an initial estimation before the development of improved techniques it is sufficient. One of the major limitations of this method is that it cannot analyze structures with redundancy without utilizing the finite element method. Redundancy occurs regularly in automotive vehicles. This requires that the structure to be statically determinant throughout. This may not be able to fully represent the structure and simplifications may be required. The second major limitation is this method does not have the capacity to determine deflections that will occur due to different loading conditions. This disadvantage prevents the method from significantly contributing to the design process since it doesn't allow an initial analytical estimation of some important design parameters such as stiffness. Overall the SSS method is only of interest as part of early automotive structural design and has been replaced by improved models that allow for a greater range of analysis such as the SSB method presented here.

In order to overcome some of the limitations of the SSS method the SSB method is employed in this work. A beam-frame uses beam elements to model the structure of the vehicle [7-9]. An example of simple beam frame model is shown in Fig. 3. The beam frame model was developed primarily because it can be easily implemented in the FEM. This method allows the determination of the deflection of the vehicle based on applied loading conditions. Once the deflections have been found, it is possible to determine bending stiffness of the chassis. This method neglects the sheet components that occur in a structure however where necessary an extra beam element is implemented in the model to account for missing sheets [10]. The beam frame model also has the added flexibility of allowing for optimization of the design by improving the cross-section type and dimensions [11]. Finally the beam element model allows for the determination of the vibration characteristics [12].

More complete models have been developed that utilize plate and shell elements to more accurately model the vehicle structure [10]. However, their application may become too computationally expensive for an optimization process when there are many design variables. This is typically the case during the early stages of the design process. It is more appropriate to use a simplified conceptual model during the early optimization process to roughly select values for majority of the structural design parameters and then use the more accurate models for a few more important parameters and the final tuning during detail design. The SSB method presented here is a trade-off between accuracy and time, and is sufficient for the purposes of preliminary design estimation of majority of the design parameters.

The finite element solver developed for the SSB method uses typical beam elements with linear shape functions and Galerkin's Method is used for deriving the beam element equations [13]. The method divides the structure into nodes and beams (elements). Nodes occur wherever elements intersect and are associated with the degrees of freedom. The nodes for the beam element each have six degrees of freedom, three in translation along each axis and three for rotation about each axis. Each individual beam element will have a corresponding stiffness matrix that relates the element forces with the nodal displacements. The stiffness of an individual beam element being used in this work is shown below:

$$K^e=\begin{bmatrix}
\frac{EA}{L} & 0 & 0 & 0 & 0 & 0 & \frac{-EA}{L} & 0 & 0 & 0 & 0 & 0 \\
0 & \frac{12EI_z}{L^3} & 0 & 0 & 0 & \frac{6EI_z}{L^2} & 0 & \frac{-12EI_z}{L^3} & 0 & 0 & 0 & \frac{6EI_z}{L^2} \\
0 & 0 & \frac{12EI_y}{L^3} & 0 & \frac{-6EI_y}{L^2} & 0 & 0 & 0 & \frac{-12EI_y}{L^3} & 0 & \frac{-6EI_y}{L^2} & 0 \\
0 & 0 & 0 & \frac{GJ}{L} & 0 & 0 & 0 & 0 & 0 & \frac{-GJ}{L} & 0 & 0 \\
0 & 0 & \frac{-6EI_y}{L^2} & 0 & \frac{4EI_y}{L} & 0 & 0 & 0 & \frac{6EI_y}{L^2} & 0 & \frac{2EI_y}{L} & 0 \\
0 & \frac{6EI_z}{L^2} & 0 & 0 & 0 & \frac{4EI_z}{L} & 0 & \frac{-6EI_z}{L^2} & 0 & 0 & 0 & \frac{2EI_z}{L} \\
\frac{-EA}{L} & 0 & 0 & 0 & 0 & 0 & \frac{EA}{L} & 0 & 0 & 0 & 0 & 0 \\
0 & \frac{-12EI_z}{L^3} & 0 & 0 & 0 & \frac{-6EI_z}{L^2} & 0 & \frac{12EI_z}{L^3} & 0 & 0 & 0 & \frac{-6EI_z}{L^2} \\
0 & 0 & \frac{-12EI_y}{L^3} & 0 & \frac{6EI_y}{L^2} & 0 & 0 & 0 & \frac{12EI_y}{L^3} & 0 & \frac{12EI_z}{L^3} & 0 \\
0 & 0 & 0 & \frac{-GJ}{L} & 0 & 0 & 0 & 0 & 0 & \frac{GJ}{L} & 0 & 0 \\
0 & 0 & \frac{-6EI_y}{L^2} & 0 & \frac{2EI_y}{L} & 0 & 0 & 0 & \frac{12EI_z}{L^3} & 0 & \frac{4EI_y}{L} & 0 \\
0 & \frac{6EI_z}{L^2} & 0 & 0 & 0 & \frac{2EI_z}{L} & 0 & \frac{-6EI_z}{L^2} & 0 & 0 & 0 & \frac{4EI_z}{L}
\end{bmatrix} \quad (1)$$

In the above equation A is the cross-sectional area, I_z and I_y are the moments of inertia about the local z and y axes respectively, J is the polar moment of inertia, E is Young's modulus and is equal to $206x10^9$Pa G is the shear modulus and is equal to $79.8x10^9$Pa. The material properties being used are most closely related to carbon steel.

The stiffness of a vehicle would be formed by assembling the individual element stiffness matrices into a global stiffness matrix using the direct stiffness method. The solution procedure is called the stiffness method where the displacements are unknown and related to the global forces by the stiffness matrix. The stiffness method is the most common solution method and is used in commercial finite element solvers. The FEM used here is a system of linear equations that can be solved using the developed computer program and implemented iteratively for the optimization process.

The objective of optimization is to improve the bending stiffness to weight ratio. The stiffness can be calculated based on the following equation.

$$K_B=\frac{F}{\delta}=\frac{F_d+F_p}{\left(\frac{\delta_d+\delta_p}{2}\right)} \quad (2)$$

Where F_d is the force on the driver side and F_p is the force on the passenger side being applied on the chassis, δ_d will be the vertical deflection of the driver side and similarly δ_p is the vertical deflection of the passenger side.

METHODOLOGY

The analysis and optimization of the beam-frame structure is a multi-step process. The first step is to determine appropriate loads to be applied to the structure. This is done by utilizing the existing analysis of a vehicle model based on the SSS method [6]. The SSB model is shown below, in Fig. 2, as it would appear in a commercial solver.

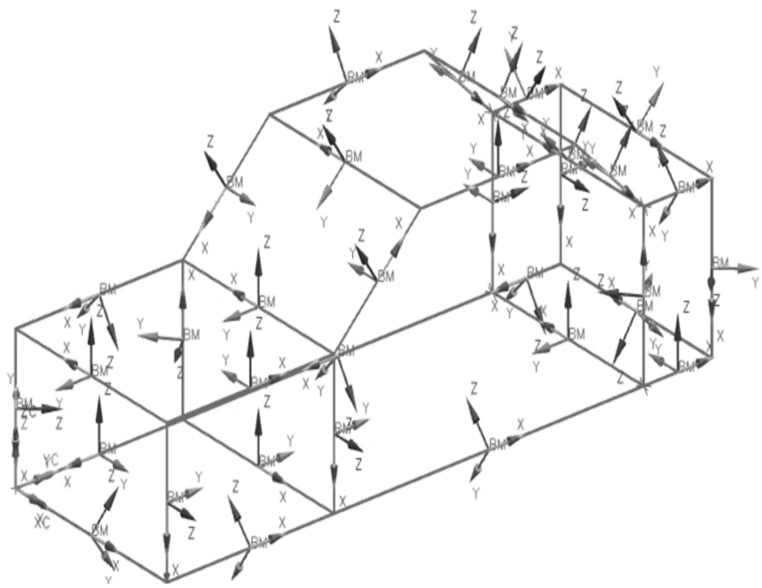

FIG. 3: BEAM ELEMENT MODEL

The loads that are applied are based on assumed weights for the vehicle components such as the drivetrain and passengers as well as the weight of the structure itself. The initial weight of the beam frame model is not known so the weight of the structure is based on the SSS model. Based on the initial applied loads and target bending stiffness the initial radiuses can be determined using the following equation.

$$K_{B_{Target}}=K_{B_{SSB}} \tag{3}$$

In the above equation K_B is the bending stiffness of the target value and the bending stiffness of the initial SSB model respectively. Using Equation 1, a set of radius values, $R_{Original}$ which is of the form of a vector shown below, will be found.

$$R_{Original}=[r_1 \quad r_2\dots \quad r_n] \tag{4}$$

In the above equation n is number of unique elements and r refers to radius of each of these elements. A unique element is any element that can potentially have a different radius from all other elements. For the initial analysis and estimation these values are assumed to be uniform for all elements. Before the optimization process the initial results are validated by comparing them with the results developed by commercial finite element software. The validation process is used to ensure the numerical finite element method employed here is correct and there are no mistakes in the code which was used. After developing the initial estimates and validation of results the developed numerical method is used to generate data for different combinations of radius values. The generated data is used to estimate an empirical model for stiffness and to estimate a suitable initial condition for the optimization process. The data generation is conducted based on a full factorial design of experiments in terms of radius and elements. There are m levels of radius that are determined based on the initial estimates for and n unique elements. The total number of trials is therefore $N=m^n$ trials.

The next step in the process is filtering the data to reduce the number of data points. Before conducting the filtering process, the data is sorted in ascending order based on the weight. The filtering process is a multistep process. The first filter excludes data based on the equation below.

$$[T']=[T_i \quad i\in[1\dots N] \;\wedge\; W^i_{SSB}<\alpha_1 W_{Original}] \tag{5}$$

In the above equation T_i represents the data associated with the i^{th} trial. If the weight of that trial is less than the acceptable weight the data is stored in the matrix T'. The acceptable weight can be considered as the original weight multiplied by a factor, α_1, which represents an increase or decrease over the original weight. This filter will reduce the amount of trials stored from N to N'. The next step in the filtering process is described by the following equation.

$$[T''] = [T_i' \;\; i \in [1 \ldots N'] \;\; \wedge \;\; K^i_{B_{SSB}} > \alpha_2 K_{T_{Original}}] \tag{6}$$

In the above equation T_i' represents the data associated with the i^{th} trial of the previously filtered date. If the bending stiffness of that trial is larger than the acceptable stiffness the data is stored in the matrix T". The acceptable target stiffness can be considered as the original stiffness multiplied by a factor, α_2, which represents an increase or decrease over the original stiffness. This filter will reduce the amount of trials stored from N' to N''. The next step in the filtering process is described by the following equation.

$$[T'''] = [T_i'' \;\; i \in [1 \ldots N''] \;\; \wedge \;\; \frac{K^i_{B_{SSB}}}{W^i_{SSB}} > \frac{\alpha_2 K^i_{B_{Original}}}{\alpha_1 W^i_{Original}}] \tag{7}$$

The final filter also sorts the data according to the ratio between the stiffness and weight of the i^{th} iteration to find the best trial as the initial condition for the optimization process

The filtered data is used to form a non-linear model in terms of stiffness and weight. The model selected for the stiffness is a quadratic form of the square of radiuses (fourth order). The model utilizes quadratic components, two factor interactions and forth order components since the elements of stiffness matrix in Equation 1 only include second and forth orders of r based on the following equations:

$$A = \pi r^2 \tag{8}$$

$$I_y = I_z = \frac{\pi r^4}{4} \tag{9}$$

$$J = I_y + I_z = \frac{\pi r^4}{2} \tag{10}$$

In the above equation r is the element radius, A is the area, I_z and I_y are the moments of inertia and J is the polar moment of inertia. The desired format for the non-linear model of the bending stiffness is shown below.

$$K_b = \beta_1 + \sum_{i=1}^{n} \beta_{i+1} r_i^2 + \sum_{i=1}^{n-1} \sum_{j=i+1}^{n} \beta_{\frac{(2n-i+1)i}{2}+j+1} r_i^2 r_j^2 + \sum_{i=1}^{n} \beta_{1+n+\frac{n(n-i)}{2}+i} r_i^4 \tag{11}$$

The coefficients, β, are the coefficients that fit the non-linear model for stiffness and n is the number of unique elements as described above. The weight is a function of square of the radius and an incomplete second order model is used for the weight. The format of the equation is shown below.

$$W = \gamma_1 + \sum_{i=1}^{n} \gamma_{i+1} r_i^2 \tag{12}$$

The coefficient, γ, is the coefficient that fits the non-linear model for weight and n is again the number of unique elements.

The optimization process is used to determine the radius values that will give the largest ratio between stiffness and weight. The optimization process uses a constrained multi-function process that utilizes four different algorithms. The algorithms used for the process are interior point, SQP, active set and trust region reflective [14-22]. The process is a constrained optimization that attempts to minimize a non-linear multivariable function. The variables that can be adjusted are the 'n' unique radius values. The initial step in the optimizer uses a set of initial radius values that are found to give the largest ratio between bending stiffness and structure weight. The optimization process can be summarized as follows.

$$\text{Objective} = Min_{[r_1, r_2 \ldots r_n]} \left\{ \frac{W^i_{SSB}}{K^i_{B_{SSB}}} \right\} \qquad i \in [1 \ldots N''] \tag{13}$$

The output of the optimization process is the radius values that will give the smallest ratio between the structure weight and bending stiffness. This is analogous to having the structure with the largest bending stiffness for a fixed limit of weight. Bounds are set for the radius values based on the initial analysis so that the values being chosen are reasonable. The process uses a Hessian to drive the direction of each step and the process ends when a set number of consecutive trials show no improvement to within a specified tolerance.

IMPLEMENTATION

The presented method is implemented for validation purpose. As stated in the Methodology Section, the first step in the process is preliminary analysis to determine initial radius values as well as the original stiffness and weight. For this process only solid circular cross-sections are considered. Circular cross sections were chosen as there is only one parameter available for optimization and a circle is comparable to actual beam cross sections found in a vehicle structure. A bending load is created by applying vertical forces on the front two points. Both forces will be in the positive vertical direction. A fixed boundary condition is applied at the rear of the structure. The load and boundary conditions are shown in the figure below. The figure also shows the labelled nodes and elements of the structure. As can be seen, a total of twenty nodes and thirty four elements are present in the model.

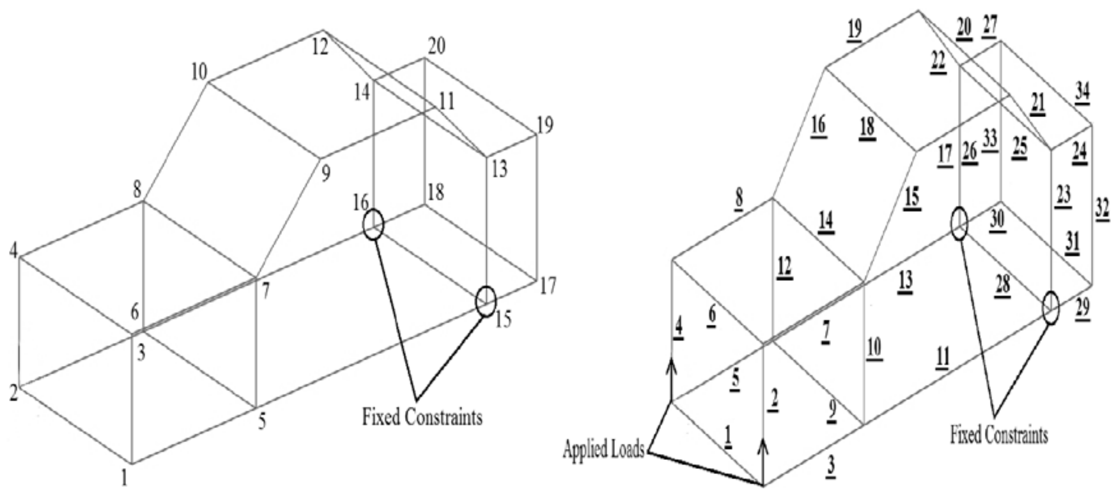

(a) (b)

FIG. 4: BEAM ELEMENT GEOMETRY WITH CONSTRAINTS AND LOADS: (a) ELEMENT NUMBERS (b) NODE NUMBERS

The first step of the process was to determine initial loads. These loads are based on assumed loads that are commonly found in a vehicle such as passengers, the power train and the other components. The structure loads are found based on existing analysis of the SSS method and can be found in the Tab. 1.

TAB. 1: COMPONENT WEIGHTS FOR ANALYSIS

Component	Weight (N)	Centre of Gravity Position (m)
Front Bumper	200	0
Powertrain	3000	0.65
Front Passengers & Seats	2000	2.2
Rear Passengers & Seats	2500	3
Fuel Tank	500	2.95
Luggage	950	4
Rear Bumper	300	4.4
Exhaust	350	2.5
Front Structure	2227.5	0.675
Passenger Compartment	3870	2.425
Rear Structure	1170	3.95

The initial analysis generates the loads that are applied. The next step is to determine uniform radius values for each of the elements that will yield sufficient bending stiffness (7000N/m) for the initial applied loads [23]. This uniform radius will be used to determine the levels of the radius, m, that are used as part of the process. The resulting uniform radius was found to be 15millimetres. This uniform radius is used to calculate the original bending stiffness and weight that are used for the filtering process later. The initial bending stiffness was found to be 8600Newton/metre and the initial weight was found to be 2532Newtons. As the weight of the structure changes the load applied to the structure will change and for this reason the load needs to be re-calculated for every iteration during the data generation step. The loads are recalculated for each iteration to reflect the static loading condition of those iterations geometric properties. This gives a ratio between the bending stiffness and structure weight of 3.397. A three level design was utilized, m=3, and the radius values used are 7.5millimetres which is half the initial value, 30millimetres which is twice the initial value, and finally 18.75millimetres which is halfway between the two extremes. Before proceeding with the data generation, the numerical finite element method is validated. This was done by comparing the numerical results with results obtained through the use of a commercial solver. The loads in both cases were kept fixed and the uniform radius was varied from 10millimetres to 25millimetres. By conducting variety of experiences it was seen that the difference of results using two methods is quite small which validates the numerical method being implemented here. A sample of the displacement result from the commercial solver is shown in Figure 5.

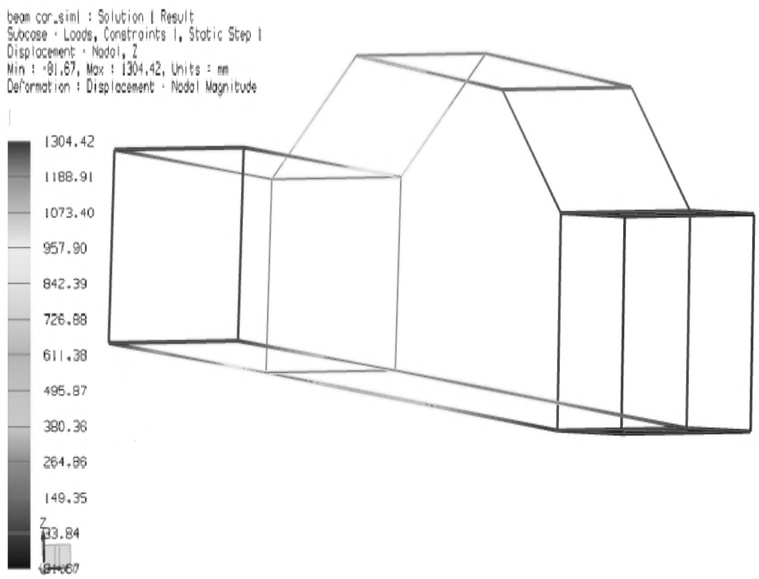

FIG. 5: BENDING DEFLECTION RESULT OF COMMERCIAL SOFTWARE

As shown in Fig. 1 there are a large number of elements and if each one was to be considered unique, where n is equal to 34, a total of $m^n=3^{34}$ trials would be required. This number of trials is computationally expensive and unnecessary. In order to reduce the number of trials to be completed symmetry was introduced. Any element on the driver side of the structure will have the same radius value as the corresponding element on the passenger side. Also all lateral elements that connect the two sides to each other will have a common radius. Using these simplifications the number of unique elements was reduced from 34 to 13 which results in 3^{13}=1549323 total trials. Tab. 2 shows the unique elements is based on the image shown in Fig. 1. The amount of time required for each simulation is 0.02s on average. As can be seen this is a relatively short computation time but given the number of trials required the total time would be substantial.

TAB. 2: NUMBER OF UNIQUE ELEMENTS

	Nodes	Element Number		Nodes	Element Number
Unique Element 1	1,2	1	Unique Element 6	5,15	11
	3,4	6		6,16	13
	5,6	9	Unique Element 7	7,9	15
	7,8	14		8,10	16

	9,10	18	Unique Element 8	9,11	17
	11,12	20		10,12	19
	13,14	25	Unique Element 9	11,13	21
	15,16	28		12,14	22
	17,18	31	Unique Element 10	13,15	23
	19,20	34		14,16	26
Unique Element 2	1,3	2	Unique Element 11	13,19	24
	2,4	4		14,20	27
Unique Element 3	1,5	3	Unique Element 12	15,17	29
	2,6	5		16,18	30
Unique Element 4	3,7	7	Unique Element 13	17,19	32
	4,8	8		18,20	33
Unique Element 5	5,7	10			
	6,8	12			

After the data was generated it was sorted according to weight. The results for all trials are shown below in order of increasing weight.

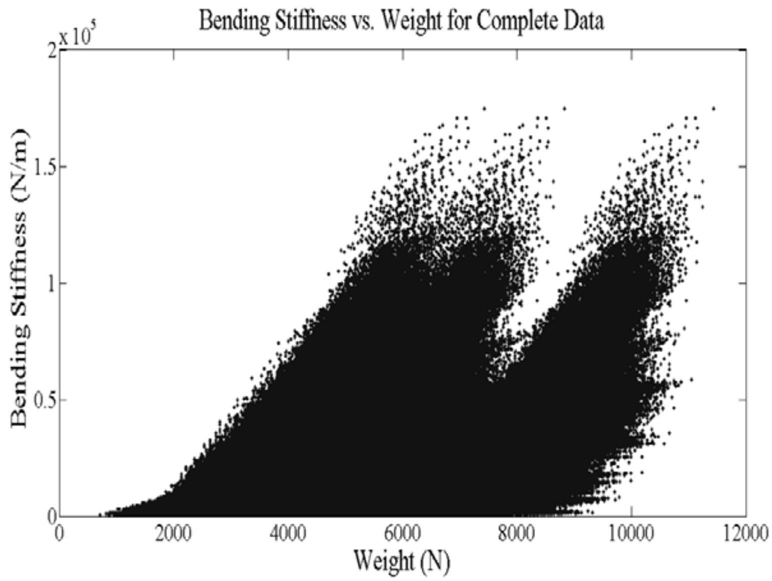

FIG 6: UNFILTERED DATA

The next step in the process is filtering the data in order to reduce the amount that is to be analyzed as part of the modeling process. The first filter is governed by Eqn. 6 where α_1 was selected as equal to 1.1. This alpha value ensures the weight can increase by only ten percent over the original weight. Filtering the initial data reduces the number of points to 15180. The result of this filter is shown in Figure 6.

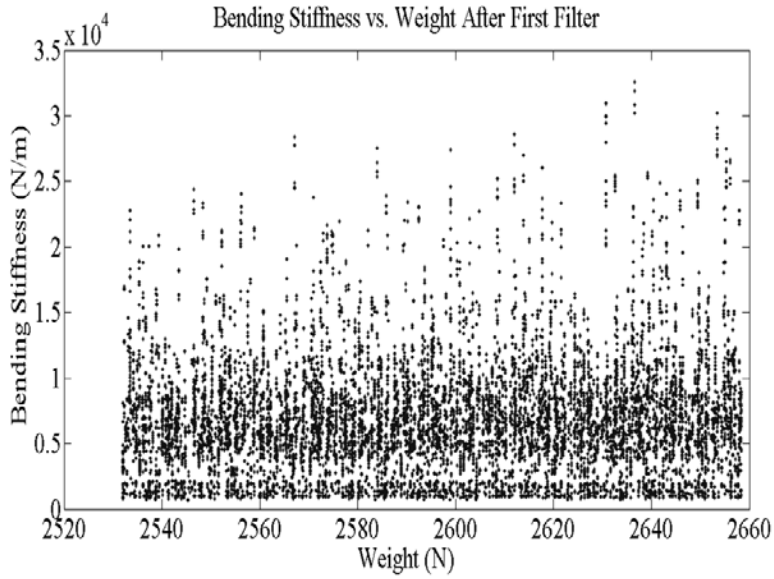

FIG. 7: DATA FILTERED BY WEIGHT

The first filtering process significantly reduced the amount of data however a further reduction is required. This filtering process was based on Eqn. 7 where α_2 value of 1 was chosen. This α_2 value ensures that only data points that have bending stiffness greater than the initial stiffness are stored. This filtering process reduced that amount of data to 1462 points. A figure showing the results is shown below.

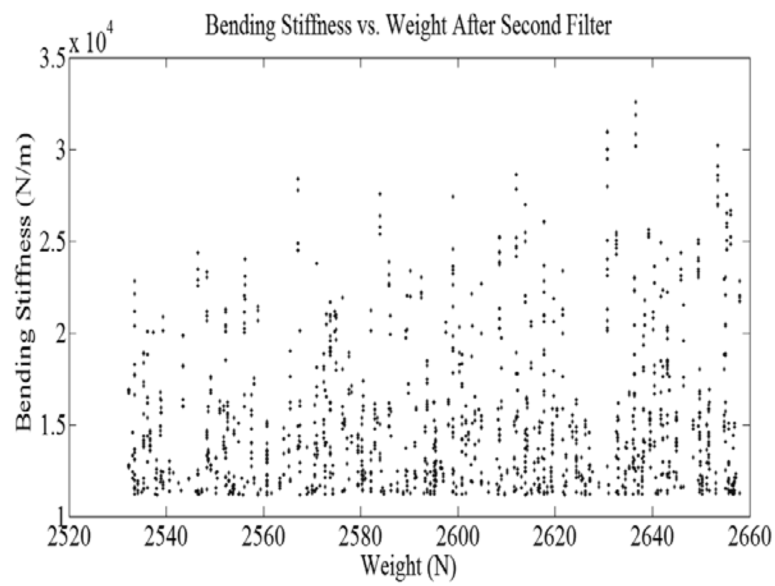

FIG. 8: DATA FILTERED BY WEIGHT AND BENDING STIFFNESS

The next process was modeling the data. As mentioned a non-linear model was used for both the stiffness and weight. A fourth order model in terms of radius was used for the stiffness while a second order model in terms of radius was used for the weight. A sample of the modeling is shown below.

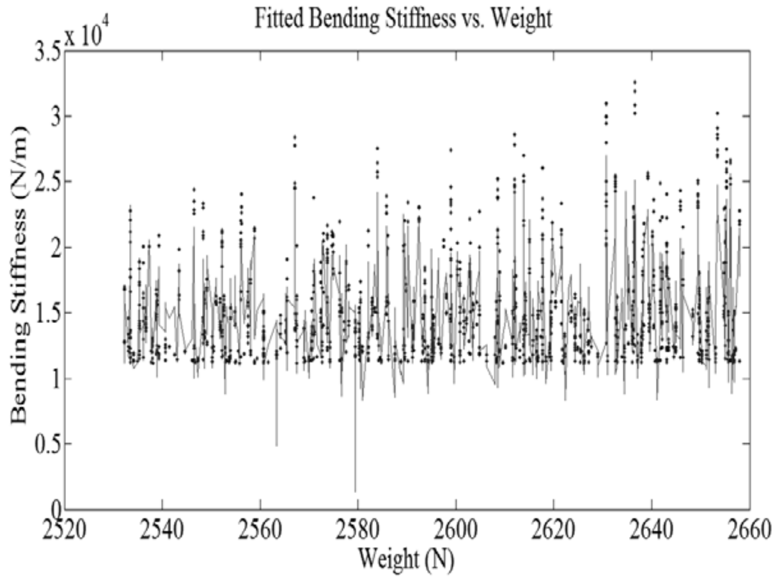

FIG. 9: FILTERED DATA WITH FITTED MODEL

The equation generated to model the stiffness also gave some indication of the sensitivity of the stiffness to each element based on the derivative.

The final step in the procedure is to perform the optimization. As stated the optimization is a non-linear constrained optimization that seeks to minimize the ratio between the weight and the stiffness. The initial condition for the optimization process was the radius values corresponding to the best observed data run, which is to say that the radius values chosen gave the largest ratio between stiffness and weight. After running the optimization process the following results were found.

TAB. 3: RESULTS OF OPTIMIZATION PROCESS

Property	Optimization Initial Condition	Optimization's Initial Condition	Optimized Model
Stiffness K_b (N/m)	8600	32580	41050
Weight W (N)	2532	2636	2579
Objective Ratio, K_b/W (1/m)	3.40	12.36	15.92

As can be seen the objective ratio for the optimum trial is almost twice that of the initial data. This represents a significant improvement over the initial values. The radius values, in millimeters, that produced this result are shown in Tab.4.

TAB. 4: OPTIMAL RADIUS VALUES IN MILLIMETRE (MM)

Radius	Original Condition	Optimization's Initial Condition	Optimum Result	
R_1	17	8.5	3.928	5.1393
R_2	17	21.25	20.1146	22.5165
R_3	17	8.5	10.5585	6.1199
R_4	17	21.25	20.5447	22.3214
R_5	17	21.25	17.2849	20.5145
R_6	17	8.5	3.3692	5.1414
R_7	17	8.5	13.7601	11.8538
R_8	17	21.25	25.2389	26.8812
R_9	17	34	36.805	36.9245
R_{10}	17	21.25	23.3085	22.6032
R_{11}	17	34	35.1165	36.6653
R_{12}	17	34	35.2001	37.2032
R_{13}	17	8.5	5.3903	8.4520

CONCLUSION

A new approach to model and analyse the vehicle's structure called Simple Structural Beam-frame (SSB) is introduced and is used to optimize the structural design based on bending stiffness requirements. The goal of the optimization is to determine the radius of each beam frame element that would give the largest ratio between stiffness and structure weight. The optimization process sought to determine the dimensions that minimize the introduced objective function. The optimization process maximizes the overall bending stiffness of the vehicle when its weight is remained in a constant range.

Implementing only solid circular cross-sections are considered in this work, however a number of other cross-sectional geometries can be introduced to the algorithm. The use of different cross-sectional shapes, specifically hollow shapes, would closer match the design of actual vehicles. The use of hollow shapes would also serve to reduce the weight. Implementation of the methodology and the conducted case-study successfully demonstrates 400% increase of the structural bending stiffness comparing to an initial design by optimum selection of the design parameter. This method can be efficiently employed for initial design of vehicle structure when reducing weight and enhance of structural stiffness are the major objectives.

ACKNOWLEDGMENTS

The research support provided by the Natural Science and Engineering Research Council of Canada (NSERC) is greatly appreciated.

REFERENCES

[1] Brown, J. C. Robertson, J. A. and Serpento, S. T., 2002 Motor Vehicle Structures, Butterworth Heinemann

[2] Barari, A. Platanitis, G. and Pop-Iliev, R., 2010 "Introducing Design Rigidity to Model Unexpected Disturbances In a DSM-Based Design Process," ASME 2010 IDETC-CIE

[3] George, A. R. and Riley, W. B., 2002, "Design, Analysis and Testing of a Formula SAE Car Chassis," SAE Motorsports Engineering Conference and Exhibition

[4] Law, E. H., Raju, S. Soni, P. H., and Thompson, L. L., 1998, "The Effects of Chassis Flexibility on Roll Stiffness of a Winston Cup Car," Motorsports Engineering Conference Proceedings

[5] Crocombe, A., Sampe, E. and Somiotti, A., 2010, "Chassis Torsional Stiffness: Analysis of the Influence on Vehicle Dynamics," SAE 2010 World Congress & Exhibition

[6] Barari, A., Esmailzadeh, E. and Tebby, S., 2011, "Methods to Determine Torsion Stiffness in an Automotive Chassis," Computer Aided Design and Applications, 1, pp. 66-75

[7] Ceglarek, D., Shi, J. and Shiu, B. W., 1997, "Flexible Beam-Based Modeling of Sheet Metal Assembly for Dimensional Control," Transactions of NAMRI, 25

[8] Donders, S., Mundo, D., Stigliano, G. and Tamarozzi, T., 2010, "Advanced Vehicle Body Concept Modeling Approach Using Reduced Models of Beams and Joints," Proceedings of ISMA2010 Including USD2010

[9] Ali, R., Hedges, J.L, and Mills, B., 1970, "Dynamic Analysis of an Automobile Chassis Frame," Proceedings of the Institution of Mechanical Engineers

[10] Happian-Smith, J., 2002, An Introduction to Modern Vehicle Design, Butterworth-Heinemann, United States of America

[11] Chon, C. T., El-Essawi, M. and Mohammadtorab, H., 1986, "Generic Stick Model of a Vehicular Structure, " Proceedings Society of Automotive Engineers, pp. 235-24

[12] Kamal, M. M. and Wolf Jr., J. A., 1977, "Finite Element Models for Autmotoive Vehicle Vibrations," Finite Element Applications in Vibration Problems, pp. 67-92

[13] Logan, D. L., 2007, A First Course in the Finite Element Method, Thomsen Canada Limited, Toronto, Canada

[14] Byrd, R.H., Gilbert, J. C. and Nocedal, J., 2000, "A Trust Region Method Based on Interior Point Techniques for Nonlinear Programming," Mathematical Programming, 89, pp. 149–185

[15] Byrd, R.H., Hribar, Mary E. and Nocedal, J., 1999, "An Interior Point Algorithm for Large-Scale Nonlinear Programming," in SIAM Journal on Optimization, 9, pp. 877–900

[16] Coleman, T.F., Li, Y., 1996, “An Interior, Trust Region Approach for Nonlinear Minimization Subject to Bounds,” SIAM Journal on Optimization, 6, pp. 418–445

[17] Coleman, T.F. and Li, Y., 1994, “On the Convergence of Reflective Newton Methods for Large-Scale Nonlinear Minimization Subject to Bounds,” Mathematical Programming, 67, pp. 189–224

[18] Gill, P.E. Murray, W. and Wright, M.H., 1981 Practical Optimization, London, Academic Press

[19] Han, S.P., 1977, “A Globally Convergent Method for Nonlinear Programming,” Journal of Optimization Theory and Applications, vol. 22, p. 297 http://dx.doi.org/10.1007/BF00932858

[20] Powell, M.J.D., 1978, “A Fast Algorithm for Nonlinearly Constrained Optimization Calculations,” Numerical Analysis, ed. G.A. Watson, Lecture Notes Mathematics, Springer Verlag, 630,

[21] Powell, M.J.D., 1978, “The Convergence of Variable Metric Methods For Nonlinearly Constrained Optimization Calculations,” Nonlinear Programming 3, Academic Press,

[22] Morales, J. L., Nocedal, Orban, J. D. and Waltz, R. A., 2006, “An interior algorithm for nonlinear optimization that combines line search and trust region steps,” Mathematical Programming, 107, pp. 391–408

[23] Malen, D. E., 2011, Fundamentals of Automobile Body Structure Design, SAE, Warrendale, United States of America

Appendix II- SSB Optimization for Torsion Stiffness using Circular Elements

Optimization of Vehicle Structure Considering Torsion Stiffness Using Simple Structural Beam Frame-Approach

Steven Tebby[1], Ahmad Barari[2] and Ebrahim Esmailzadeh[3]

[1]University of Ontario Institute of Technology, Steven.Tebby@uoit.ca
[2]Corresponding Author, University of Ontario Institute of Technology, Ahmad.Barari@uoit.ca
[3]University of Ontario Institute of Technology, Ebrahim.Esmailzadeh@uoit.ca

ABSTRACT

Vehicle structural design is an important component of automotive design since the structure of a vehicle plays complex interactions with the other vehicle components and has significant impact on the performance of the vehicle. Structural design is usually completed after many iterations and the design changes in the late design stages effect many other parameters in the design of vehicle. Therefore, it is highly valuable for designers to employ simple but effective analyses at the early design stages. One method of analysis is using Simple Structural Surfaces. This method utilizes planar sheets to model the vehicle structure and allows the determination of the forces in each sheet. The major drawback of this method is its inability to determine deflections in a structure. To overcome this drawback a method that uses beam elements to represent the vehicle structure has been developed. This method uses a numerical finite element method and is able to determine unknown deflections and reaction forces as well as the internal loading on each member. This method can also be readily adapted to allow for parametric optimization for torsion stiffness. The parameters associated with each beam element are the length, orientation and the beam characteristics of beams' cross-sectional area and moment of inertia. An automated process is developed that manipulates some of these parameters to develop a structure that will have the greatest torsional stiffness.

Keywords: Stiffness Matrix Method, Automotive Structure, Finite Element Analysis- Based Design, Beam-Frame Model

DOI: 10.3722/cadaps.2012.xxx-yyy

INTRODUCTION

The design of an automotive structure is critical to the overall performance of a vehicle. The structure of the vehicle is important to ensure it can satisfactorily carry the applied loads that occur [1]. The structure of a vehicle interacts with all other vehicle sub-components and it has complex influence one their functionality. Due to its design complexity, the structural design process is traditionally conducted by trial and errors and is subject to too many changes even till the latest stages of vehicle design. However, some of the changes in the design of structure may cause significant re-design of the other vehicle components and this may become very costly. Typically, it is much more desired to maximize design changes during the early design stages and particularly before the detail design activities [2]. However, employing a very comprehensive and detailed process of analyses at the conceptual design stage, when there are long ranges of design choices still available, may become very time consuming and computationally expensive. Therefore, it is very valuable for designers to employ simple but effective analyses at the early design stages. The objective of this paper is to present a method of analyzing a vehicle structural model and implement an optimization process to improve the structural design. A simplified model is used to test the analysis and optimization processes which reduces the accuracy but can be used to test the implemented methods.

One of the most important criteria in automotive structural design is structural stiffness. The chassis stiffness, both in bending and torsion, has significant impacts on the ride and comfort characteristics as well as the overall dynamic vehicle performance [3], [4], [5]. For this reason the stiffness values are used as design parameters to be optimized. Increasing the structural stiffness is highly demanding to enhance the vehicle performance. However, due to economical constrains increasing vehicle stiffness by increasing the structural weight is not recommended. An optimised solution is desired that maximizes structural stiffness while it keep the structural weight as low as possible.

Being able to efficiently analyze the body structure during the conceptual design stages is important to determining the performance characteristics. A primary method used to analyze the structure is the Simple Structural Surfaces (SSS) [1], [6]. This method utilizes planar sheets to model the body structure. SSS method can be used to determine the load-paths present in a body structure, but it is not able to analyze indeterminate static conditions. Alternatively, the method utilized in this work, uses beam-frame elements to represent the structure as an equivalent space frame. The approach of using beam elements has the advantage of being able to determine displacements due to these forces by using the Finite Element Method (FEM). The use of the beam-frame finite element model can be used for basic analysis of a vehicle structure and as an initial estimate of some important vehicle parameters such as bending and torsion stiffness as well as some vibration characteristics. Using analogy of names, this method is referred in this paper as Simple Structural Beam-Frames (SSB) method. This paper presents an approach to optimize design parameters of a SSB model to optimize the torsion stiffness of a conceptual model. The optimization of the model will improve the stiffness to weight ratio compared with an initial model that has been used in previous analysis.

An SSS model has been previously analyzed using commercial finite element software [6]. A diagram of this geometry is shown below in Fig. 1(a). The deflection results that were produced using this model are shown in Fig. 1(b).

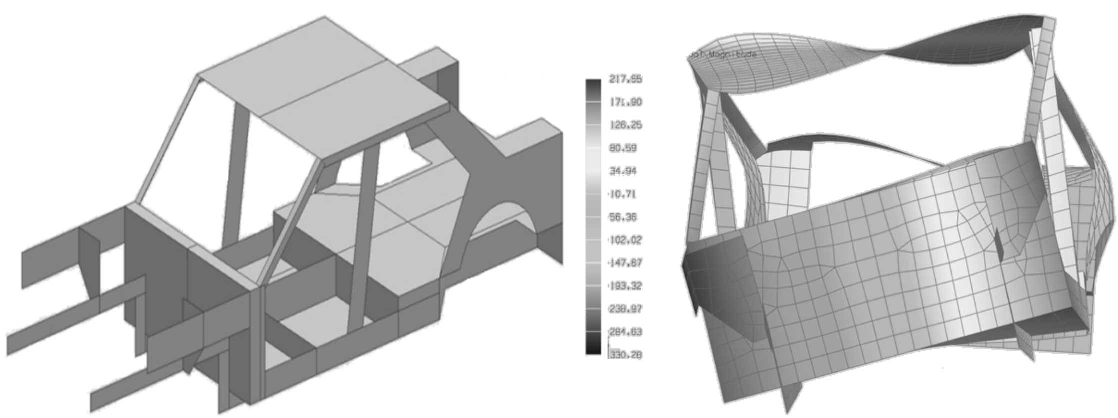

(a) **(b)**

Fig. 1: (a) SSS Model (b) Deflection Result of SSS Model [6]

Background

A simpler model is often utilized since the finite element method can be computationally intense with a trade-off between accuracy and computation time [7]. Both SSS and SSB methods can be used to determine forces that are present throughout the structure and assist with preliminary design decisions.

These methods are still used, despite their limitations, as they can provide insight into how the initial geometry of the structure interacts for different loading conditions. A brief explanation of both of these analysis methods is presented here as background information. Another important aspect of this structural analysis is the utilized finite element method that is also briefly presented here. Finally a short introduction about optimization is presented here.

The Simple Structural Surface method uses planar surfaces to model a structure. It was developed initially to analyze the load path of a vehicle [1]. The surfaces are able to react in plane loads only and transfer the forces from one surface to another via edge shear loads. The original intent of this method is to analyze the structure and determine a suitable load path. This method of analysis has a few limitations which restrict the benefits however as an initial estimation before the development of improved techniques it is sufficient. One of the major limitations of this method is that it cannot analyze structures with redundancy which occurs regularly in automotive vehicles. This requires that the structure to be statically determinant throughout. This may not be able to fully represent the structure and simplifications may be required. The second major limitation is this method does not have the capacity to determine deflections that will occur due to different loading conditions. This disadvantage prevents the method from significantly contributing to the design process since it doesn't allow an initial analytical estimation of some important design parameters such as stiffness. Overall the SSS method is only of interest as part of early automotive structural design and has been replaced by improved models that allow for a greater range of analysis such as the SSB method presented here.

In order to overcome some of the limitations of the SSS method the SSB method is employed in this work. A beam-frame uses beam elements to model the structure of the vehicle [8]. An example of simple beam frame model is shown in Fig. 2. The beam frame model was developed primarily because it can be easily implemented in the Finite Element Method. This method allows the determination of the deflection of the vehicle based on applied loading conditions. Once the deflections have been found, it is possible to determine torsion stiffness of the chassis. This method neglects the sheet components that occur in a structure however where necessary an extra beam element is implemented in the model to account for missing sheets [9]. The beam frame model also has the added flexibility of allowing for optimization of the design by improving the cross-section type and dimensions [10]. Finally the beam element model allows for the determination of the vibration characteristics [11].

More complete models have been developed that utilize plate and shell elements to more accurately model the vehicle structure [9]. However, their application may become computationally too expensive for an optimization process when there are too many design variables. And typically this is the case during the early stages of the design process. It is more appropriate to use a simplified conceptual model during the early optimization process to roughly select values for majority of the structural design parameters and then use the more accurate models for a few more important parameters and the final tuning during detail design. The SSB method presented here is a trade-off between accuracy and time, and is sufficient for the purposes of preliminary design estimation of majority of the design parameters.

The finite element solver developed for the SSB method uses typical beam elements with linear shape functions and Galerkin's Method is used for deriving the beam element equations [12]. The method divides the structure into nodes and beams (elements). Nodes occur wherever elements intersect and are associated with the degrees of freedom. The nodes for the beam element each have six degrees of freedom, three in translation along each axis and three for rotation about each axis. Each individual beam element will have a corresponding stiffness matrix that relates the element forces with the nodal displacements. The beam element's stiffness matrix employed in this work is as follows:

$$K^e=\begin{bmatrix}
\frac{EA}{L} & 0 & 0 & 0 & 0 & 0 & \frac{-EA}{L} & 0 & 0 & 0 & 0 & 0 \\
0 & \frac{12EI_z}{L^3} & 0 & 0 & 0 & \frac{6EI_z}{L^2} & 0 & \frac{-12EI_z}{L^3} & 0 & 0 & 0 & \frac{6EI_z}{L^2} \\
0 & 0 & \frac{12EI_y}{L^3} & 0 & \frac{-6EI_y}{L^2} & 0 & 0 & 0 & \frac{-12EI_y}{L^3} & 0 & \frac{-6EI_y}{L^2} & 0 \\
0 & 0 & 0 & \frac{GJ}{L} & 0 & 0 & 0 & 0 & 0 & \frac{-GJ}{L} & 0 & 0 \\
0 & 0 & \frac{-6EI_y}{L^2} & 0 & \frac{4EI_y}{L} & 0 & 0 & 0 & \frac{6EI_y}{L^2} & 0 & \frac{2EI_y}{L} & 0 \\
0 & \frac{6EI_z}{L^2} & 0 & 0 & 0 & \frac{4EI_z}{L} & 0 & \frac{-6EI_z}{L^2} & 0 & 0 & 0 & \frac{2EI_z}{L} \\
\frac{-EA}{L} & 0 & 0 & 0 & 0 & 0 & \frac{EA}{L} & 0 & 0 & 0 & 0 & 0 \\
0 & \frac{-12EI_z}{L^3} & 0 & 0 & 0 & \frac{-6EI_z}{L^2} & 0 & \frac{12EI_z}{L^3} & 0 & 0 & 0 & \frac{-6EI_z}{L^2} \\
0 & 0 & \frac{-12EI_y}{L^3} & 0 & \frac{6EI_y}{L^2} & 0 & 0 & 0 & \frac{12EI_y}{L^3} & 0 & \frac{12EI_z}{L^3} & 0 \\
0 & 0 & 0 & \frac{-GJ}{L} & 0 & 0 & 0 & 0 & 0 & \frac{GJ}{L} & 0 & 0 \\
0 & 0 & \frac{-6EI_y}{L^2} & 0 & \frac{2EI_y}{L} & 0 & 0 & 0 & \frac{12EI_z}{L^3} & 0 & \frac{4EI_y}{L} & 0 \\
0 & \frac{6EI_z}{L^2} & 0 & 0 & 0 & \frac{2EI_z}{L} & 0 & \frac{-6EI_z}{L^2} & 0 & 0 & 0 & \frac{4EI_z}{L}
\end{bmatrix} \qquad \text{Eqn. 1}$$

In the above equation A is the cross-sectional area, I_z and I_y are the moments of inertia about the local z and y axes respectively, J is the polar moment of inertia, E is Young's modulus and is equal to $206x10^9$Pa G is the shear modulus and is equal to $79.8x10^9$Pa. As Eqn. 1 is standard for the beam element analysis the equations to calculate the element stress and strain are also standard for this element type and thus not shown here [12].

The overall structure will have a global stiffness matrix that is a combination of individual stiffness matrices. The solution procedure is called the stiffness method where the displacements are unknown and related to the global forces by the stiffness matrix. The stiffness method is the most common solution method and is used in commercial finite element solvers. The FEM used here is a system of linear equations that can be solved using the developed computer program and implemented iteratively for the optimization process.

Optimization is one of the oldest fields in mathematics and has found modern application in a variety of scientific and engineering disciplines [13]. Most optimization methods are based on principles from calculus and have a strong connection to inequalities. A number of algorithms can be applied depending on the objective of optimization and what constraints exist. Generally an optimization program requires the definition of an objective function to be optimized by varying the parameters associated with the objective [14]. The constraints are applied to the optimization parameters since the parameters can be interrelated by physical laws or must be constrained to ensure physical compatibility, or to simplify the model. A problem that has no inequality constraints is said to be unconstrained, however there will still be bounds on the parameter values. Some examples of available optimization algorithms are simplex method, sequential quadratic programming and interior point methods. Optimization is applied to the design of the SSB model in order to improve the torsion stiffness to weight ratio. The stiffness can be calculated based on the following equation.

$$K_T=\frac{T}{\varphi}=\frac{FB}{(\varphi_d+\varphi_p)} \qquad \text{Eqn. 2}$$

Where T is the torque being applied on the chassis, the force applied at the front nodes is represented by F, and B represents the track width of the structure, the angle of rotation of the passenger side is given by φ_p while the driver side angle of rotation is given by φ_d. These values are calculated using the following equations where δ_d will be the vertical deflection of the driver side and similarly δ_p is the vertical deflection of the passenger side:

$$\varphi_d=\tan^{-1}\left(\frac{\delta_d}{B/2}\right) \qquad \text{Eqn. 3}$$

$$\varphi_p=\tan^{-1}\left(\frac{\delta_p}{B/2}\right) \qquad \text{Eqn. 4}$$

Methodology

The analysis and optimization of the beam-frame structure is a multi-step process. The first step is to determine appropriate loads to be applied to the structure. This is done by utilizing the existing analysis of a vehicle model based on the SSS method [6]. The SSB model is shown below, in Fig. 2, as it would appear in a commercial solver.

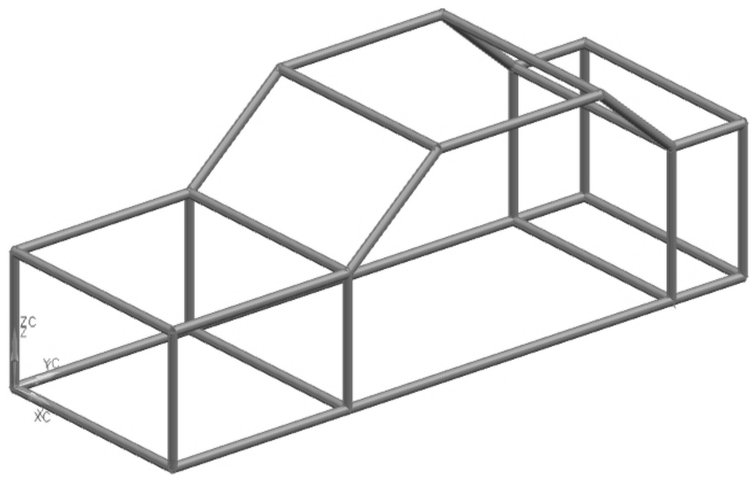

Fig. 2: Beam Element Model

The loads that are applied are based on assumed weights for the vehicle components such as the drivetrain and passengers as well as the weight of the structure itself. The initial weight of the beam frame model is not known so the weight of the structure is based on the SSS model. Based on the initial applied loads and target torsion stiffness the initial radiuses can be determined using the following equation.

$$K_{T_{Target}} = K_{T_{SSB}} \qquad \text{Eqn. 5}$$

In the above equation K_T is the torsion stiffness of the target value and the torsion stiffness of the initial SSB model respectively. Using Equation 1, a set of radius values, $R_{Original}$ which is of the form of a vector shown below, will be found. Only solid circular cross-sections are considered throughout the process.

$$R_{Original} = [r_1 \quad r_2 \ldots \quad r_n] \qquad \text{Eqn. 6}$$

In the above equation n is number of unique elements and r refers to radius of each of these elements. A unique element is any element that can potentially have a different radius from all other elements. For the initial analysis and estimation these values are assumed to be uniform for all elements. Before the optimization process the initial results are validated by comparing them with the results developed by commercial finite element software. After developing the initial estimates and validation of results the developed numerical method is used to generate data for different combinations of radius values. The generated data is used to estimate an empirical model for stiffness and to estimate a suitable initial condition for the optimization process. The data generation is conducted based on a full factorial design of experiments in terms of radius and elements. There are m levels of radius that are determined based on the initial estimates and n unique elements. The total number of trials is therefore $N=m^n$ trials.

The next step in the process is filtering the data to reduce the number of data points to be utilized in the model generation process. Before conducting the filtering process, the data is sorted in ascending order based on the weight. The filtering process is a multistep process. The first filter excludes data based on the equation below.

$$[T'] = [T_i \quad i \in [1 \ldots N] \ \wedge \ W^i_{SSB} < \alpha_1 W_{Original}] \qquad \text{Eqn. 7}$$

In the above equation T_i represents the data associated with the i^{th} trial. If the weight of that trial is less than the acceptable weight the data is stored in the matrix T'. The acceptable weight can be considered as the original weight multiplied by a factor, α_1, which represents an increase or decrease over the original weight. This filter will reduce the amount of trials stored from N to N'. The next step in the filtering process is described by the following equation.

$$[T''] = [T_i' \; i \in [1...N'] \;\wedge\; K^i_{T_{SSB}} > \alpha_2 K_{T_{Original}}] \qquad \text{Eqn. 8}$$

In the above equation T_i' represents the data associated with the i^{th} trial of the previously filtered date. If the torsion stiffness of that trial is larger than the acceptable stiffness the data is stored in the matrix T". The acceptable target stiffness can be considered as the original stiffness multiplied by a factor, α_2, which represents an increase or decrease over the original stiffness. This filter will reduce the amount of trials stored from N' to N''. The next step in the filtering process is described by the following equation.

$$[T'''] = [T_i'' \; i \in [1...N''] \;\wedge\; \frac{K^i_{T_{SSB}}}{W^i_{SSB}} > \frac{\alpha_2 K^i_{T_{Original}}}{\alpha_1 W^i_{Original}}] \qquad \text{Eqn. 9}$$

The final filter also sorts the data according to the ratio between the stiffness and weight of the i^{th} iteration to find the best trial as the initial condition for the optimization process. The filtering process can be illustrated graphically with the following flow chart.

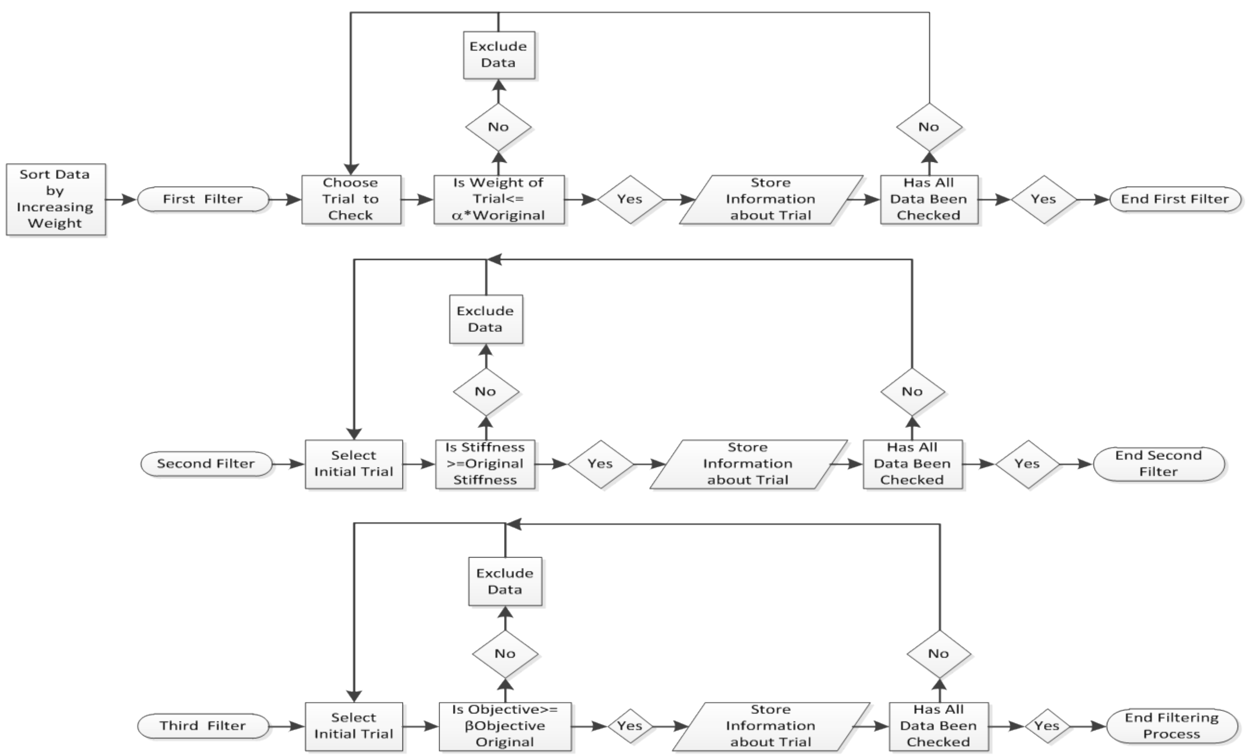

Fig. 3: Flow Chart of Filtering Process

The filtered data is used to form a non-linear model in terms of stiffness and weight. The model selected for the stiffness is a quadratic form of the square of radiuses (fourth order). The model contains quadratic components, their interactions, and forth order components since the elements of stiffness matrix in Equation 1 only include second and forth orders of r based on the following equations:

$$A = \pi r^2 \quad \text{Eqn. 10}$$

$$I_y = I_z = \frac{\pi r^4}{4} \quad \text{Eqn. 11}$$

$$J = I_y + I_z = \frac{\pi r^4}{2} \quad \text{Eqn. 12}$$

In the above equation r is the element radius, A is the area, I_z and I_y are the moments of inertia and J is the polar moment of inertia. The desired format for the non-linear model of the torsion stiffness is shown below.

$$K_T = \beta_1 + \sum_{i=1}^{n} \beta_{i+1} r_i^2 + \sum_{i=1}^{n-1} \sum_{j=i+1}^{n} \beta_{\frac{(2n-i+1)i}{2}+j+1} r_i^2 r_j^2 + \sum_{i=1}^{n} \beta_{1+n+\frac{n(n-i)}{2}+i} r_i^4 \quad \text{Eqn. 13}$$

The coefficients, β, are the coefficients that fit the non-linear model for stiffness and n is the number of unique elements as described above. The weight is a function of square of the radius and an incomplete second order model is used for the weight. The format of the equation is shown below.

$$W = \gamma_1 + \sum_{i=1}^{n} \gamma_{i+1} r_i^2 \quad \text{Eqn. 14}$$

The coefficient, γ, is the coefficient that fits the non-linear model for weight and n is again the number of unique elements.

The optimization process is used to determine the radius values that will give the largest ratio between stiffness and weight. The optimization process uses a constrained multi-function process that utilizes four different algorithms. The algorithms used for the process are interior point, SQP, active set and trust region reflective [15-23]. The process is a constrained optimization that attempts to minimize a non-linear multivariable function. The variables that can be adjusted are the 'n' unique solid radius values. The initial step in the optimization uses the set of radius values that were found to give the largest ratio between torsion stiffness and structure weight based on the data that was generated and filtered. The radius values are restricted based on the results of the data generation and filtering process. The restrictions provide an upper bound and lower bound for the radius of each unique element. These restrictions ensure that the radius values being tested are feasible and that the design will have good compatibility between different element members. The optimization process can be summarized as follows.

$$Objective = Min_{[r_1, r_2 \ldots r_n]} \left\{ \frac{W_{SSB}^i}{K_{T_{SSB}}^i} \right\} \quad i \in [1 \ldots N''] \quad \text{Eqn. 15}$$

The output of the optimization process is the element radius values that will give the smallest ratio between the structure weight and torsion stiffness. This is analogous to having the structure with the largest torsion stiffness for a fixed limit of weight. Bounds are set for the radius values based on the initial analysis so that the values being chosen are reasonable. The process uses a Hessian to drive the direction of each step and the process ends when a set number of consecutive trials show no improvement to within a specified tolerance.

Implementation

The presented method is implemented for validation purpose. As stated in the Methodology Section, the first step in the process is preliminary analysis to determine initial radius values as well as the original stiffness and weight. A torsion load is created by applying vertical forces on the front two points. One force will be in the positive vertical direction and the other load will be in the negative vertical direction. A fixed boundary condition is applied at the rear of the structure. The load and boundary conditions can be seen in Fig. 3 which is shown below. The figure also shows the labelled nodes and elements of the structure. As can be seen, a total of twenty nodes and thirty four elements are present in the model. Each element utilizes a solid circular cross-section with the radius as a design parameter.

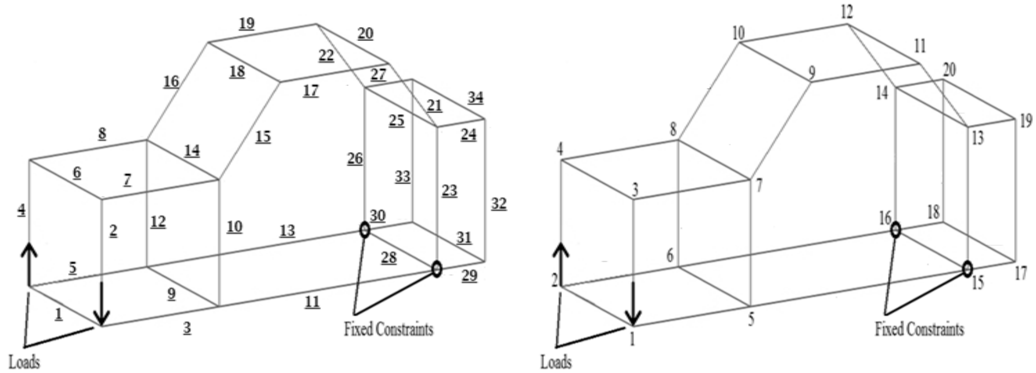

(a) (b)

Fig.3: Beam Element Geometry with Constraints and Loads: (a) elements' numbers (b) nodes' numbers

The first step of the process was to determine initial loads. These loads are based on assumed loads that are commonly found in a vehicle such as passengers, the power train and the other components. The structure loads are found based on existing analysis of the SSS method and can be found in the Table 1.

Component	Weight (N)	Centre of Gravity Position (m)
Front Bumper	200	0
Powertrain	3000	0.65
Front Passengers & Seats	2000	2.2
Rear Passengers & Seats	2500	3
Fuel Tank	500	2.95
Luggage	950	4
Rear Bumper	300	4.4
Exhaust	350	2.5
Front Structure	2227.5	0.675
Passenger Compartment	3870	2.425
Rear Structure	1170	3.95

Tab. 1: Component Weights for Initial Analysis

The initial analysis generates the loads that are applied. The next step is to determine uniform radius values for each of the elements that will yield sufficient torsion stiffness (12000Nm/ radian) for the initial applied loads [24]. This uniform radius will be used to determine the levels of the radius, m, that are used as part of the process. The resulting uniform radius was found to be 15mm. This uniform radius is used to calculate the original torsion stiffness and weight that are used for the filtering process later. The initial torsion stiffness was found to be 12475Nm/radian and the initial weight was found to be 2225N. As the weight of the structure changes the load applied to the structure will change and for this reason the load needs to be re-calculated for every iteration during the data generation step. This gives a ratio between the torsion stiffness and structure weight of 5.77. A three level design was utilized, m=3, and the radius values used are 7.5mm which is half the initial value, 30mm which is twice the initial value, and finally 18.75millimetres which is halfway between the two extremes. The performance of the numeric method was evaluated by comparing the results with an analytical approach where possible as well as commercial FEA software. A sample of the displacement result from the commercial solver is shown below.

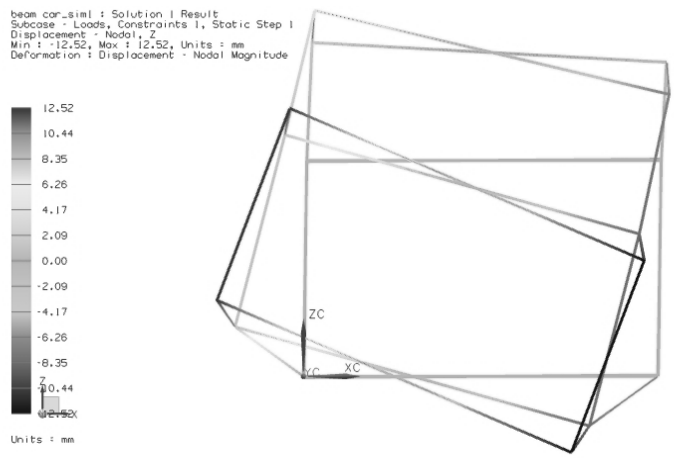

Fig. 4: Torsion Deflection of NX Model

As shown in Fig. 1 there are a large number of elements and if each one was to be considered unique, where n is equal to 34, a total of $m^n=3^{34}$ trials would be required. This number of trials is computationally expensive and unnecessary. In order to reduce the number of trials to be completed symmetry was introduced. Any element on the driver side of the structure will have the same radius value as the corresponding element on the passenger side. Also all lateral elements that connect the two sides to each other will have a common radius. Using these simplifications the number of unique elements was reduced from 34 to 13 which results in 3^{13}=1549323 total trials. A table showing the unique elements is shown below based on the image shown in Fig. 1.

	Nodes	Element Number		Nodes	Element Number
Unique Element 1	1,2	1	Unique Element 6	5,15	11
	3,4	6		6,16	13
	5,6	9	Unique Element 7	7,9	15
	7,8	14		8,10	16
	9,10	18	Unique Element 8	9,11	17
	11,12	20		10,12	19
	13,14	25	Unique Element 9	11,13	21
	15,16	28		12,14	22
	17,18	31	Unique Element 10	13,15	23
	19,20	34		14,16	26
Unique Element 2	1,3	2	Unique Element 11	13,19	24
	2,4	4		14,20	27
Unique Element 3	1,5	3	Unique Element 12	15,17	29
	2,6	5		16,18	30
Unique Element 4	3,7	7	Unique Element 13	17,19	32
	4,8	8		18,20	33
Unique Element 5	5,7	10			
	6,8	12			

Tab. 3: Number of Unique Elements

After the data was generated it was sorted according to weight. The results for all trials are shown below in order of increasing weight.

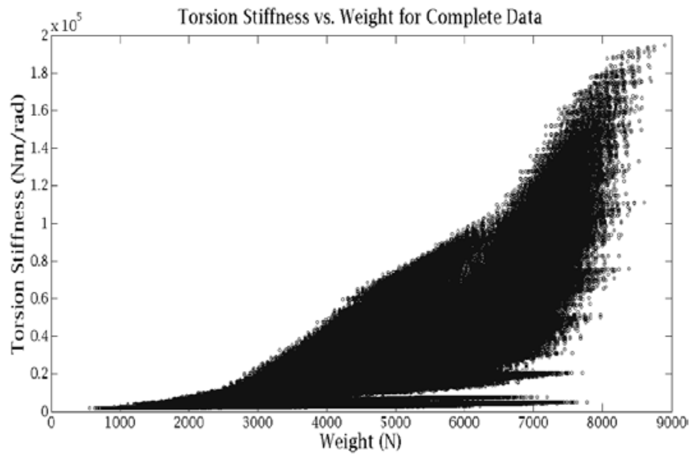

Fig. 5: Unfiltered Data

As can be seen there are a large number of data points that are in the high weight range. These points represent the structure where most elements have larger radiuses. The larger radiuses will drastically increase weight, but will also improve the torsion stiffness. The next step in the process is filtering the data in order to reduce the amount that is to be analyzed as part of the modelling process. The first filter is governed by Eqn. 6 where α_1 was selected as equal to 1.1. This alpha value ensures the weight can increase by only ten percent over the original weight. Filtering the initial data reduces the number of points to 83882. The result of this filter is shown in Figure 6.

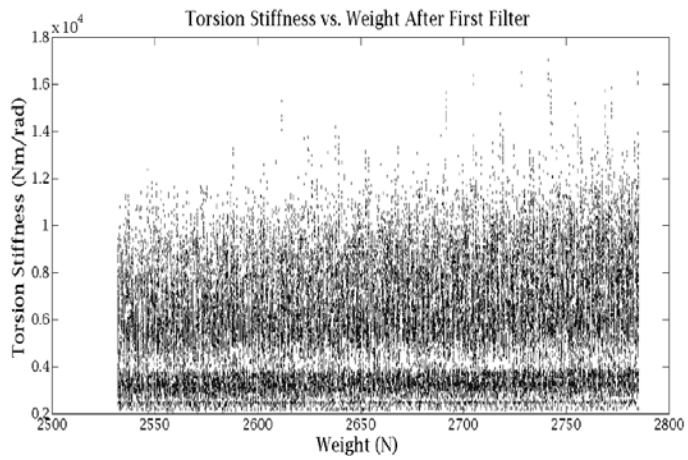

Fig. 6: Data Filtered by Weight

The first filtering process significantly reduced the amount of data however a further reduction is required. This filtering process was based on Eqn. 7 where α_2 was chosen to be 1. This α_2 value ensures that only data points that have torsion stiffness greater than the initial stiffness are stored. This filtering process reduced that amount of data to 176 points. A figure showing the results is shown below.

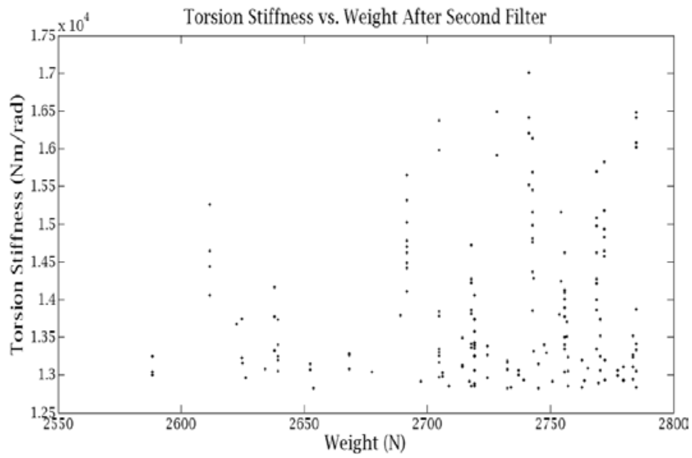

Fig. 7: Data Filtered by Weight and Torsion Stiffness

The next process was modelling the data. As mentioned a non-linear model was used for both the stiffness and weight. A fourth order model in terms of radius was used for the stiffness while a second order model in terms of radius was used for the weight. A sample of the modelling is shown below.

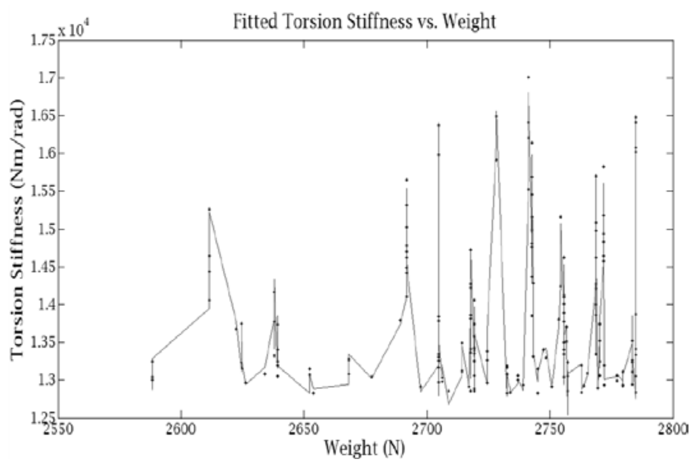

Fig. 8: Filtered Data with Fitted Model

The equation generated to model the stiffness also gave some indication of the sensitivity of the stiffness to each element based on the derivative.

The final step in the procedure is to perform the optimization. As stated the optimization is a non-linear constrained optimization that seeks to minimize the ratio between the weight and the stiffness. The initial condition for the optimization process was the radius values corresponding to the best observed data run, which is to say that the radius values chosen gave the largest ratio between stiffness and weight. After running the optimization process the following results were found.

Property	Optimization Initial Condition	Optimization's Initial Condition	Optimized Model
Stiffness K_T (Nm/rad)	12475	17008	27163
Weight W (N)	2225	2741	3035
Objective Ratio, K_T/W (m/rad)	5.607	6.205	8.947

Table 4: Results of Optimization Process

As can be seen the objective ratio for the optimum trial is almost twice that of the initial data. This represents a significant improvement over the initial values. The radius values, in millimetres, that produced this result are shown in Table 5.

Radius	R_1	R_2	R_3	R_4	R_5	R_6	R_7	R_8	R_9	R_{10}	R_{11}	R_{12}	R_{13}
Original Condition	15	15	15	15	15	15	15	15	15	15	15	15	15
Optimization's Initial Condition	18.8	7.5	7.5	18.8	18.8	18.8	18.8	18.8	18.8	7.5	7.5	7.5	7.5
Optimum Result	15.7	9.2	24.78	12.8	14.1	30.7	12.8	12.9	12.8	1.9	12.8	10.9	5.9

Table 5: Optimal Radius Values in millimeter (mm)

Conclusion

A new approach to model and FEA-based selection of the structural design parameters of a vehicle called Simple Structural Beam-frame (SSB) is introduced and is used to optimize the design based on Torsion stiffness of the structure. The optimization objective is to determine the radius of each beam frame element that would give the largest ratio between stiffness and structure weight. The optimization process sought to determine the dimensions that minimize the introduced objective function by maximizing the overall torsion stiffness of the vehicle when its weight is remained in a constant range.

Implementation of the methodology and the conducted case-study successfully demonstrates more than 60% increase of the structural torsion stiffness to weight ratio when comparing an initial design to a design with optimum selection of the design parameter. Implementing only solid circular cross-sections are considered in this work, however a number of other cross-sectional geometries can be introduced to the algorithm. The use of different cross-sectional shapes, specifically hollow shapes, would closer match the design of actual vehicles. The use of hollow shapes would also serve to reduce the weight. This method can be efficiently employed for initial design of vehicle structure when weight reduction and enhance of structural stiffness are the major objectives.

ACKNOWLEDGMENT

The research support provided by the Natural Science and Engineering Research Council of Canada (NSERC) is greatly appreciated.

References

[1] Brown, Jason C.; Robertson, John A.; Serpento, Stan T.: Motor Vehicle Structures, Butterworth Heinemann 2002

[2] Barari, A.; Platanitis, G.; Pop-Iliev, R.: Introducing Design Rigidity to Model Unexpected Disturbances In a DSM-Based Design Process, ASME 2010 IDETC-CIE, 2010

[3] George, A. R.; Riley W. B.: Design, Analysis and Testing of a Formula SAE Car Chassis, SAE Motorsports Engineering Conference and Exhibition, 2002

[4] Law, E. H.; Raju, S.; Soni, P. H.; Thompson, L. L.: The Effects of Chassis Flexibility on Roll Stiffness of a Winston Cup Car, Motorsports Engineering Conference Proceedings, 1998

[5] Crocombe, A.; Sampe, E.; Somiotti, A.: Chassis Torsional Stiffness: Analysis of the Influence on Vehicle Dynamics, SAE 2010 World Congress & Exhibition, 2010

[6] Barari, A.; Esmailzadeh, E.; Tebby, S.: Methods to Determine Torsion Stiffness in an Automotive Chassis, Computer Aided Design and Applications, vol. 1, 2011, pp. 66-75

[7] Le, Thuy T.: Approcimate Element Computational Time for Domain Decomposition in Parallel Finite Element Code, Computer and Information Science, 2007, pp. 633-639

[8] Ceglarek, D.; Shi, J.; Shiu, B. W.: Flexible Beam-Based Modeling of Sheet Metal Assembly for Dimensional Control, Transactions of NAMRI, vol. 25, 1997

[9] Happian-Smith, Julian: An Introduction to Modern Vehicle Design, Butterworth-Heinemann, United States of America 2002

[10] Chon, Choon T.; El-Essawi, Mohamed; Mohammadtorab, Homa: Generic Stick Model of a Vehicular Structure, Proceedings Society of Automotive Engineers, 1986, pp. 235-241 http://dx.doi.org/10.4271/860825

[11] Kamal, Mounir M.; Wolf Jr., Joseph A.: Finite Element Models for Autmotoive Vehicle Vibrations, Finite Element Applications in Vibration Problems, 1977, pp. 67-92

[12] Logan, Daryl L.: A First Course in the Finite Element Method, Thomsen Canada Limited, Toronto, Canada 2007

[13] Lange, Kenneth: Optimization, Springer-Verlag, Los Angeles, United States of America, 2004

[14] Antoniou, Andreas and Lu, Wu-Sheng: Practical Optimization Algorithms and Engineering Applications, Springer Science, Victoria, Canada, 2007

[15] Byrd, R.H.; Gilbert, J. C.; Nocedal, J.: A Trust Region Method Based on Interior Point Techniques for Nonlinear Programming, Mathematical Programming, vol. 89, 2000, pp. 149–185 http://dx.doi.org/10.1007/PL00011391

[16] Byrd, R.H., Hribar, Mary E.; Nocedal, Jorge: An Interior Point Algorithm for Large-Scale Nonlinear Programming, SIAM Journal on Optimization, SIAM Journal on Optimization, vol. 9, 1999, pp. 877–900 http://dx.doi.org/10.1137/S1052623497325107

[17] Coleman, T.F.; Li, Y.: An Interior, Trust Region Approach for Nonlinear Minimization Subject to Bounds, SIAM Journal on Optimization, vol. 6, 1996, pp. 418–445 http://dx.doi.org/10.1137/0806023

[18] Coleman, T.F.; Li, Y.: On the Convergence of Reflective Newton Methods for Large-Scale Nonlinear Minimization Subject to Bounds, Mathematical Programming, vol. 67, 1994, pp. 189–224 http://dx.doi.org/10.1007/BF01582221

[19] Gill, P.E., Murray W.; Wright, M.H.: Practical Optimization, London, Academic Press, 1981

[20] Han, S.P.: A Globally Convergent Method for Nonlinear Programming, Journal of Optimization Theory and Applications, vol. 22, 1977, p. 297 http://dx.doi.org/10.1007/BF00932858

[21] Powell, M.J.D.: A Fast Algorithm for Nonlinearly Constrained Optimization Calculations, Numerical Analysis, ed. G.A. Watson, Lectures in Mathematics, Springer Verlag, Vol. 630, 1978

[22] Powell, M.J.D.: The Convergence of Variable Metric Methods For Nonlinearly Constrained Optimization Calculations, Nonlinear Programming 3, Academic Press, 1978

[23] Morales, J. L.; Nocedal, J.; Orban, D. Waltz, R. A.: An interior algorithm for nonlinear optimization that combines line search and trust region steps, Mathematical Programming, Vol 107, 2006, pp. 391–408 http://dx.doi.org/10.1007/s10107-004-0560-5

[24] Malen, Donald E.: Fundamentals of Automobile Body Structure Design, SAE, Warrendale, United States of America 2011 http://dx.doi.org/10.4271/R-394

Appendix III- Selection of Suitable Number of Plate Elements in Substructure Analysis

As mentioned the number of plate elements was chosen to be the minimum number of elements that provided an accurate result when compared with similar analysis using the commercial software. Only vertical loads were used for the first test and once an initial decision has been made deflection in the other directions are analyzed. A summary of the results for vertical bending loads is shown below in Table 19.

Load (N)	Length x Width (m)	MATLAB Elements	MATLAB Displacement (mm)	NX Displacement (mm)	% Difference
500	1x1	1	58	74.51	22.15809958
500	2x1	1	464	596	22.14765101
1500	1x3	1	58	74.4	22.04301075
3000	1x3	1	116	148.9	22.09536602
3000	3x1	1	9396	12070	22.15410108
1000	1x1	4	149.6	144.6	3.457814661
2000	1x1	4	299.3	289.1	3.528190937
3000	1x1	4	448.9	433.7	3.50472677
4000	1x1	4	598.5	578.3	3.492996715
5000	1x1	4	748.2	722.8	3.514111787
500	1x1	9	70.6	73.37	3.775385035
500	2x1	9	574	592.6	3.138710766
1500	1x3	9	72.2	72.5	0.413793103
3000	1x3	9	144.5	144.9	0.27605245
3000	3x1	9	11700	12130	3.544929926

Table 19: Estimation of number of plate elements

As can be seen using a single plate element results in unacceptable error, but increasing the number of elements to four and nine substantially reduced the error between the two programs. Ultimately nine elements were chosen as the errors present were equal to or smaller than the error present when four elements were used. The selection of nine elements represents an element distribution of three along the x-axis and three along the y-axis. With the selection of the number of elements complete further analysis was conducted to estimate the error present for a more general loading condition. The results of this process are shown below in Table 20.

Test 1	NX	MATLAB	% Error
u (m)	0.0133	0.013397448	-0.73269456
v (m)	0.0007697	0.000845513	-9.84974332
w (m)	0.209	0.204655508	2.078704196
Test 2	NX	MATLAB	% Error
u (m)	0.025	0.025188832	-0.755327
v (m)	0.0009529	0.001031775	-8.27741104
w (m)	0.824	0.816249071	0.940646746
Test 3	NX	MATLAB	% Error
u (m)	0.025	0.025188832	-0.755326998
v (m)	0.0009529	0.001031775	-8.277411045
w (m)	3.296	3.264996283	0.940646746
Test 4	NX	MATLAB	% Error
u (m)	0.01059	0.010622668	-0.308478186
v (m)	0.00004472	4.44171E-05	0.677250089
w (m)	2.1	2.065262501	1.65416662

Table 20: Plate analysis comparison

As can be seen the results of the two programs are similar and the percent error is within the acceptable error inherent in FEM. In the above table u, v and w represent the deformation in along the x, y and z axes respectively. The above analysis justifies the selection of nine elements for the plate element when conducting the substructure analysis. It should be noted that the selection of nine elements requires using three elements for each bordering beam of the substructure.

Appendix IV- Extended Validation of Developed FEA Program

The presented validation of the developed FEA program illustrates how the results compare with a typical commercial program, in this case NX NASTRAN. Further validation is required however to ensure the developed program produces results for a wide variety of analysis. To perform this validation an array of structures were tested under different loading conditions and the results between the developed program and the commercial software are compared. The first step of the validation was for a single cantilevered beam element as shown below in Figure 52. The loads are applied at node two and node one is held fixed

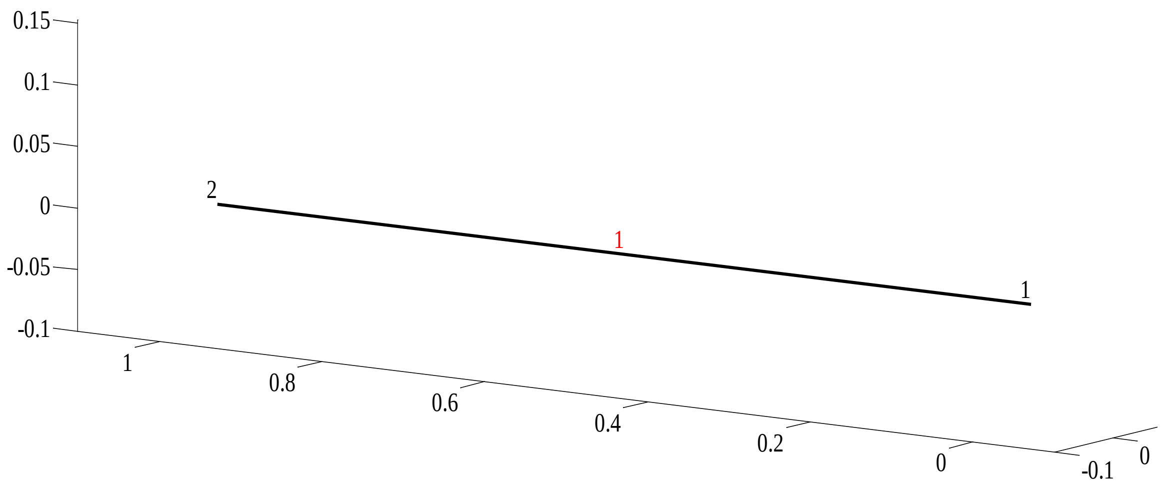

Figure 52: Cantilevered beam

The beam properties and applied loads are shown below in Table 21.

Length (mm)	1000
Section Shape	Hollow Square
Side Length (mm)	50
Thickness (mm)	5
F_x (N)	10000
F_y (N)	10000
F_z (N)	10000

Table 21: Cantilevered beam properties

The displacement results are summarized below in Table 22.

	MATLAB	NX NASTRAN	% Difference
d_x (mm)	0.05394	0.05398	0.0741
d_y (mm)	52.62	52.69	0.1329
d_z (mm)	52.62	52.69	0.1329

Table 22: Results summary for cantilevered beam

As can be seen the difference between the results of the two programs are minimal, therefore verifying the FEA program that has been developed. The next step of the validation will be to analyze a simple cantilevered structure. This structure is used to validate the results when multiple beam elements are present and arranged arbitrarily. The structure that was tested is shown below in Figure 53. In the structure below nodes one, four, five and six are fixed with the loads applied at nodes two and three.

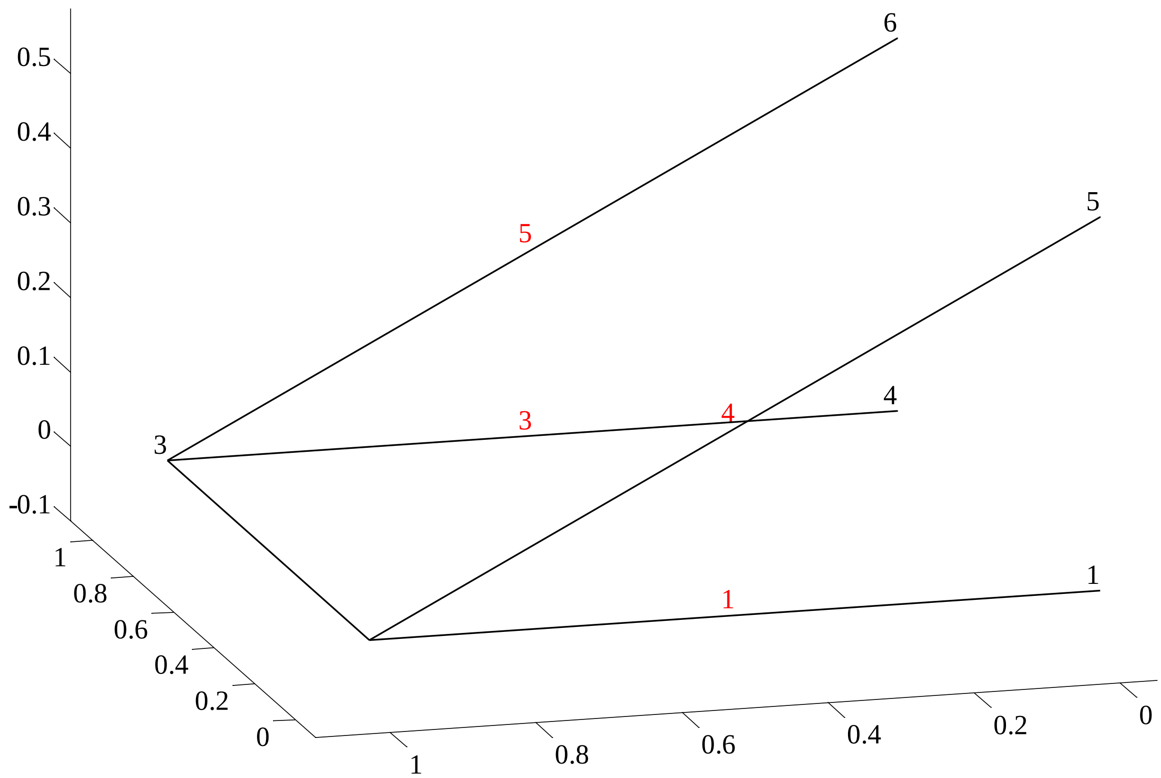

Figure 53: Simple beam structure

The beam section properties and loading condition are described below in Table 23.

Section Shape	Hollow Square

Side Length (mm)	30
Thickness (mm)	5
F_x (N)	10000
F_y (N)	1000
F_z (N)	1000000

Table 23: Beam structure properties

The total applied load can be considered as double the applied loads since they are applied equally at nodes two and three. All beam elements have uniform section properties. A summary of the displacements at the two free nodes is below in Table 24.

	MATLAB		NX NASTRAN		% Difference	
	Node 2	Node 3	Node 2	Node 3	Node 2	Node 3
Dx (mm)	2.03	2.03	2.02	2.02	-0.4950	-0.4950
Dy (mm)	7.33	7.33	7.34	7.34	0.1362	0.1362
Dz (mm)	9.46	9.46	9.41	9.41	-0.5313	-0.5313

Table 24: Simple structure displacement results

As can be seen the difference in deflections between the two programs is small. These results in combination with the results of the comparison between the programs for the full vehicle model provide verification of the developed programs accuracy. The errors that are present are acceptable given the inherent inaccuracies of FEM.

Appendix V- Comparison of Optimization Penalty Functions and Scaling Factors

As discussed penalty functions have been utilized as part of numerous optimization processes. The process used in this work is based on a differential value between the values for the current iteration and the initial values. The calculation of the penalty value uses a scaling factor to determine a suitable magnitude. The selection of a suitable scaling factor however is presented here based. The same optimization process is conducted for the vehicle model used throughout this work with different scaling factors. A summary of the results is shown below.

	Initial	α=0	% Change
Number of Iterations	-	21	
Weight	12567.9174912751	7754.439345	-38.2997
Bending Stiffness	738024.932514391	985922.4329	33.58931
Torsion Stiffness	1511743.86253544	1051623.846	-30.4364

Table 25: Results without penalty function

	Initial	α=10	% Change
Number of Iterations	-	24	
Weight	12567.9174912751	8702.85193447340	-30.7534
Bending Stiffness	738024.932514391	767037.348029814	3.931089
Torsion Stiffness	1511743.86253544	1671002.90243399	10.53479

Table 26: Results with scaling factor of 10

	Initial	α=100	% Change
Number of Iterations	-	24	
Weight	12567.9174912751	8702.854932	-30.7534
Bending Stiffness	738024.932514391	767035.4126	3.930827
Torsion Stiffness	1511743.86253544	1671003.478	10.53483

Table 27: Results with scaling factor of 100

	Initial	α=1000	% Change
Number of Iterations	-	38	
Weight	12567.9174912751	8702.692765	-30.7547
Bending Stiffness	738024.932514391	766995.3341	3.925396
Torsion Stiffness	1511743.86253544	1670972.344	10.53277

Table 28: Results with scaling factor of 1000

As can be seen the inclusion of a penalty function improves the results of the optimization process. While the test without a penalty function had the greatest reduction in weight, which is a fundamental objective of this work, the decrease in torsion stiffness would be unacceptable for an automotive structure. The results of the tests using various scaling factors shows how penalty functions can be used to improve the results of the optimization process. The choice of the scaling factor is arbitrary as there is a minimal difference between the different values tested; however the use of a value of 1000 required a substantially greater number of iterations for convergence which reduces the desirability of that value for scaling factor. For the work presented here a scale factor of ten was chosen for each penalty calculation.